Griffith School of Engineering

Griffith University

6002ENG – Industry Affiliates Program

Footfall Analysis of Residential Floor Structure Using Cold-Formed Steel C-Shaped Floor Joists

Xu Zhao, s5216867

13/06/2022 Trimester 1

Xstructe Consulting

Dr. Bin (Ben) Wang

Professor Hong Guan

A report submitted in partial fulfillment of the degree of Bachelor of Engineering (Honours)

Griffith UNIVERSITY

EXECUTIVE SUMMARY

As a representative of lightweight materials, cold-formed steel (CFS) is widely used as a building material due to its many advantages over traditional building materials, such as its light weight and strength. However, floor vibrations caused by human activities have always been a significant challenge for CFS floors, which severely impact occupant comfort. Furthermore, the study of floor vibration is complex and influenced by various factors. This thesis focuses on the study and analysis of floor vibration in residential floor structures with different CFS c-shaped floor joists using finite element analysis (FEA).

The project began with modelling a residential floor slab with three CFS c-slab joists using strand7 computer software. The model was then solved using the strand7 software's finite element solver, after which the vibration parameters of the model, both static and dynamic, could be obtained. These floor vibration parameters are fixed displacement, natural frequency, and harmonic response. In particular, the harmonic response requires curves to be plotted using Excel. These data and curves are the basis for analysing the strengths and weaknesses of the three scenarios for this project.

Based on the results of this thesis, it was concluded that the conventional joist floor has the lowest static displacement. For both new joist types, the "C" joist is better than the "dumbbell" in terms of natural frequency range and harmonic response results. In general, the type of CFS c-joist influences floor vibrations, but which case is good or bad cannot be evaluated based on one parameter.

ACKNOWLEDGEMENT

Firstly, I would like to express my gratitude to Professor Guan Hong and Dr. Ben Wang for accompanying me throughout my thesis and research and for the technical support and advice they gave me throughout the thesis. They met with me every week without fail and used their expertise and experience to provide me with guidance and answer my questions. I would also like to thank Dr. Ben Wang for taking me to an accurate construction site to give me a more concrete understanding of what I am researching. Without them, this thesis would not have been completed successfully.

I would also like to thank Dr. Ivan Gratchev, who explained the format, layout, and requirements of the dissertation in the 6002ENG IAP course. Without Dr. Ivan Gratchev, the formatting of my dissertation would have been very confusing, and I would not have been able to submit it in the correct format and requirements.

Also, I would like to thank Amanda Sutherland of the EnglishHELP consultation at Griffith University. She checked and corrected the grammar and sentences of my thesis. This was very helpful for me as I am not a native English speaker.

Finally, I would like to thank my classmates and friends. I would like to thank them for being there for me to encourage and help me to complete this thesis.

TABLE OF CONTENTS

LIST OF FIGURES

LIST OF TABLES

1 INTRODUCTION

1.1 Background

1.1.1 Cold-formed steel

Cold-formed steel (CFS), also known as light steel, is a type of cold-formed employing joints at room temperature. Structural elements in CFS are usually made from steel sheets, lamellas, or strips. The manufacturing process involves extrusion or cold rolling, forming the material to achieve the desired shape. Compared to conventional construction materials, CFS has the advantages of high strength, lightweight, relatively simple manufacturing process, high flexibility in obtaining various cross-sectional shapes, ease of transport, and speed of construction (Dhanavade et al., 2021). Therefore, CFS has good social, economic, and environmental benefits and is widely used in the construction sector, such as apartment buildings, office buildings, and warehouses. As shown in the site plan in Figure1, where the grey component is the joist studied in this project, this case is also the most common type of CFS joist.

Figure 1. Site view of CFS joists

1.1.2 Strand7 software

Strand7 software (Sreand7, 1996) was developed jointly by the University of Sydney and the University of New South Wales. It is a general-purpose finite element analysis (FEA) system for structural and heat transfer analysis and has applications in a wide range of fields, including aerospace, mining, and marine. It contains a variety of solvers (see Figure2) , such as linear statics, natural frequency, and harmonic response, providing a reliable computational solution for engineering.

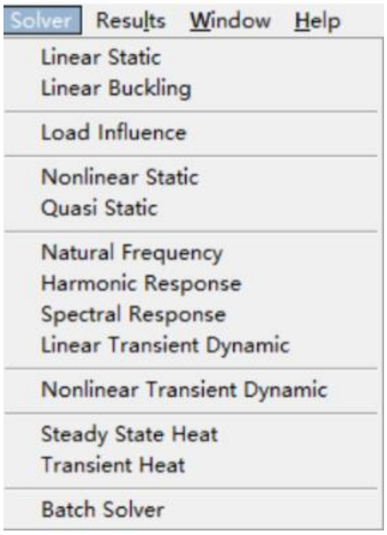

Figure 2. Solver for Strand7

(Resources from：Strand7, 1996)

1.2 Aims and Objectives

The purpose of this project is to compare the vibration parameters of CFS floor slabs with different joist types and compare them to the current Australian Standard Vibration Guidelines to analyse and assess the effect of joist types on the vibration of CFS floor slabs. If the appropriate joist type is selected, the vibration response of the CFS floor slab can be reduced, thereby improving occupant comfort.

In order to achieve the aims of this project, the following specific objectives have been identified:

- Using CAD software, draw up dimensioned drawings of the three joists section types and details of the project.
- The 3D models of the three joists were correctly modelled using Strand7 from the CAD dimensional drawings.
- The Strand7 solver was used to measure linear static, intrinsic frequency, and harmonic response parameters for three types of the joist.
- The parameters are calculated and compared for different conditions, and the vibration of the CFS floor is discussed and evaluated.

2 LITERATURE REVIEW

This literature is centered on CFS floor systems and focuses on the changes and challenges in the market for CFS and the issues related to vibration in CFS floor systems. The second half of this section focuses on the experimental methods, some influencing factors, and relevant parameters used by previous researchers for floor vibrations. This literature reflects the importance and needs to study vibration in CFS flooring systems today, both in terms of market demand and the large body of previous research. The gap in this literature is that the stability of joists has not been analysed using the functionality of Strand7 software modelling to make the characteristic parameters of floor vibrations more straightforward. In addition, this project focuses on using the Strand7 solver to study the effects of floor vibrations in joists; therefore, these papers do not expand on this in detail.

2.1 Markets and challenges for cold-formed steel

2.1.1 Markets of cold-formed steel

Changes in the market for CFS can expose the shortcomings of CFS construction, but they can also lead to technological innovation.

Hancock's article points out that CFS has been developed for over a century and that its market has grown significantly over conventional hot-rolled steel due to its high strength and wide range of applications (Hancock, 2003). Furthermore, as Hancock (2003) mentions, as the market for CFS expands, this will lead to significant developments in CFS construction and design. Today, CFS is available in various cross-sections to meet different working requirements, the most common being 'Cee,' 'Zed,' and 'Sigma,' as shown in Figure 3 (Tahir, Siang, & Ngian, 2006). Furthermore, at the end of the 20th century, Laine and Tuomala (1999) studied the effect of internal bracing and sheeting on purlins under gravity with different CFS sections. However, this report did not mention the effect of joists on floor stability.

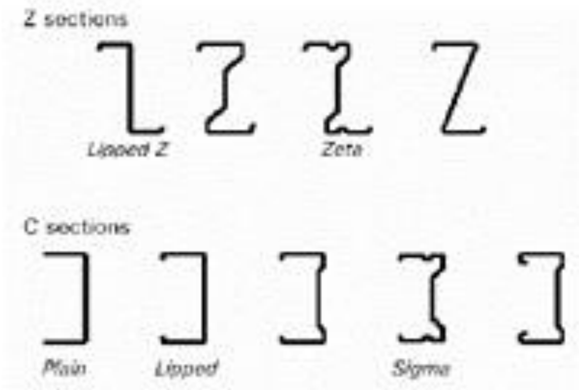

Figure 3. Cold-formed steel section type

（Resources from：Tahir，Siang & Ngian，2006）

2.1.2 Challenges of cold-formed steel

Indeed, the development of CFS comes with problems associated with its outcome, which can affect the market for CFS on the one hand. As Hagberg, Persson & Hook (2009) point out, if the sensitive details of lightweight steel are not well-considered, this could slow down the growth of the potential market for lightweight housing.

On the other hand, higher demands are also placed on the stability of CFS structures. As the quality of CFS is reduced, its strength is also affected to a certain extent. The wrong structural design of CFS may affect the comfort of the occupants in mild cases; in severe cases, it may endanger lives. One of the causes of accidents with CFS is defective design (Qi, Zhao & He, 2015), as shown in Figure 4 for a disaster caused by incorrectly designed light steel.

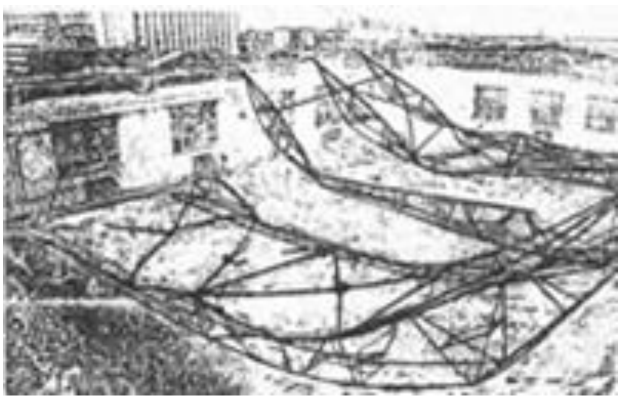

Figure 4. Serious disaster

（Resources from： Qi, Zhao & He，2015）

2.2 Floor vibrations

Floor vibrations constitute a significant cause of occupant comfort. Floor vibrations affect occupant comfort and test the stability of CFS structures. Moreover, these floor vibrations affect people's comfort and are very expensive to maintain after completion (Xu, 2011). This section explains the generation of floor vibrations, human perception, and floor loading.

2.2.1 Generation of floor vibrations

Floor vibrations constitute a significant cause of occupant comfort. CFS is typically a high-strength-to-weight material. The high strength-to-weight ratio is an advantage of CFS, but it also brings with it the problem of floor vibrations (Davis, Parnell & Xu, 2008). Dynamic loads usually cause floor vibration applied directly to the floor by people or machines. The most common source of vibration is human walking. Occupants generate loads and behave as a dynamic system interacting with the structure, called human-structure interaction (HIS) (Shahabpoor et al., 2017).

Wyatt (1989) first introduced high-frequency and low-frequency floors, and he specified that a floor with an intrinsic frequency exceeding the third harmonic of the walking speed is a high-frequency floor. Furthermore, he argued that the response of a low-frequency floor is harmonic, i.e., a resonant response; the response of a high-frequency floor is impulsive, i.e., a transient response. In detail, the low-frequency floor is most likely to resonate with one of the harmonics, and the footsteps will maintain the resonance; on the other hand, high-frequency floor plates will always reduce to a small value due to the damping of the surrounding area due to the individual footfall. Therefore, resonance is unlikely to occur, whereas transient responses are likely to cause vibrations.

2.2.2 Perception of floor vibrations

Human perception of floor vibration is through a combination of floor motion, physical perception, and mental perception. Specifically, the frequency, duration, and timing of floor vibrations, and Xu (2011) notes that research into the perception of vibration strength is problematic because vibration perception is a subjective awareness influenced by various factors. Reiher and Meister (1931) first investigated people's vibration perception and found that the sensitivity to floor vibration decreases as the excitation frequency increases. The Figure5 shows that as the frequency increases, the displacement due to vibration decreases. Furthermore, when the fundamental frequency of the floor is close to the stride frequency, the human footsteps may produce a more significant response (Zhang & Xu, 2020).

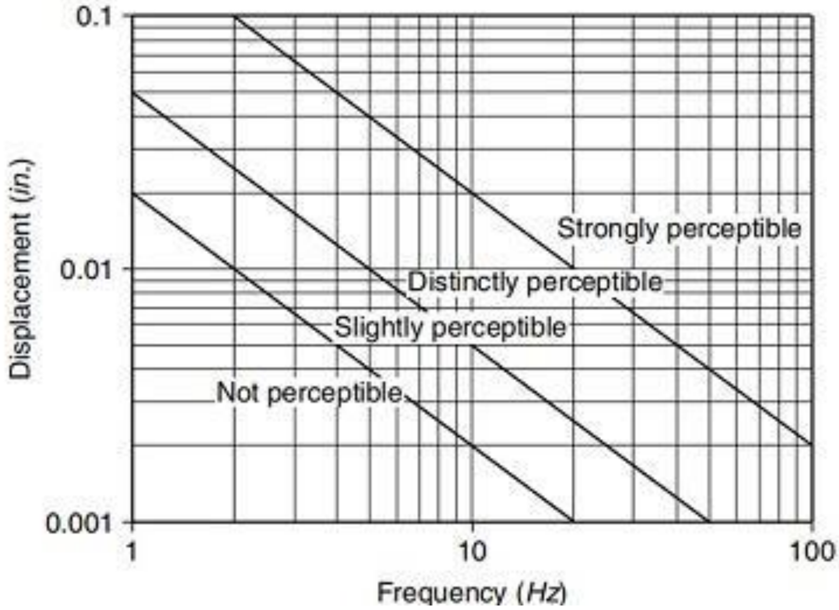

Figure 5. Modified Reiher-Meister scale

(Resources from：Lenzen 1966)

Alternatively, floor vibrations can be reflected in the root mean square (RMS), which the International Standards Organisation (ISO) uses as part of its standard for mechanical vibration and shock, based on ISO 2631, Assessment of human exposure to whole-body vibration (ISO, 1989). Furthermore, it has developed the current floor vibration standard, which specifies the limits applicable to floor vibrations generated at fundamental frequencies. RMS curve (Figure6), the vertical coordinate of the picture, is the RMS acceleration. Image 4 shows that the minimum allowable acceleration corresponds to frequencies in the range 4Hz-8Hz for different environments and modes of movement, which is in line with Grether's (1971) study that humans are physiologically more sensitive to the 4Hz-8Hz range.

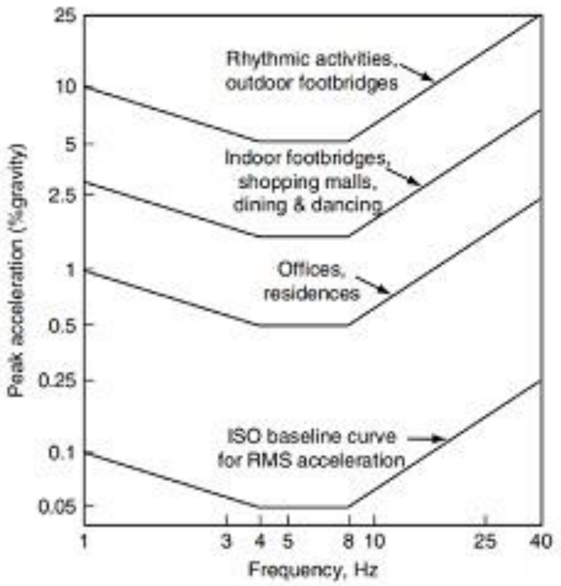

Figure 6. ISO acceleration limits

(Resources from：ISO 1989)

2.2.3 The loading of floor vibrations

The general situation is that human activity generates load loading on the floor, which causes the floor response. According to the damped plate - oscillator model of Zhang et al. (2017), three loading methods can be classified: moving force, moving damped-oscillator, and moving and stationary damped-oscillators.

Moving force (MF)

Typically, the footsteps are modelled by loading with a single foot force on the position the foot is in (Zhang & Xu, 2020), as shown in Figure 7.

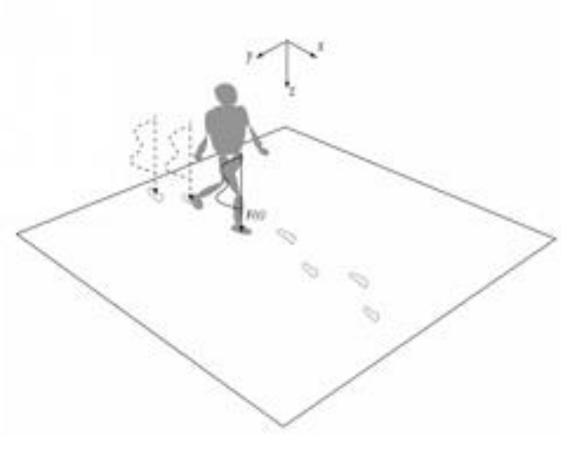

Figure 7. Moving force loading
(Resources from：Zhang & Xu, 2020)

The expressions established (Zhang & Xu, 2020):

$$f\ (x, y, t) = F(t)\delta(x\ \ \xi_i)\delta(y\ \ \eta_i) \qquad (1)$$

The F(t) in the expression is the force of a single footstep, based on the Young equation (Young, 2001), a single foot force model (Li, Fan & Nie, 2010).

$$F(t) = G\sum_{n=1}^{+\infty} A_n \sin(\frac{n\pi}{t_e}t), t_e = \frac{1}{0.76 f_s}, 0 \le t \le t_e \qquad (2)$$

Therefore, Zhang and Xu (2020) simulated a single-leg force map for a 2Hz walking frequency, as shown in Figure 8.

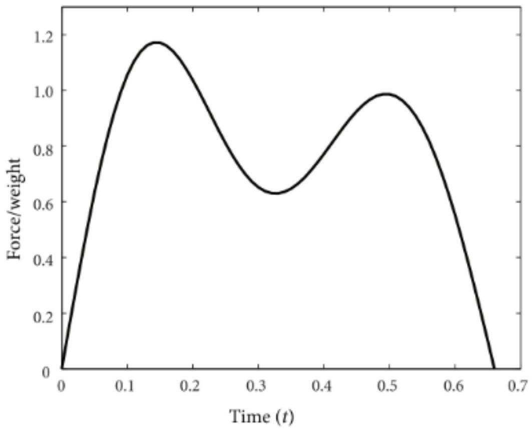

Figure 8. Single-footfall force

(Resources from：Zhang & Xu, 2020)

However, the actual situation is that the two will touch the floor one after another, and there is an overlap. Therefore, Zhang and Xu (2020) proposed a new loading scheme, as shown in Figure 9.

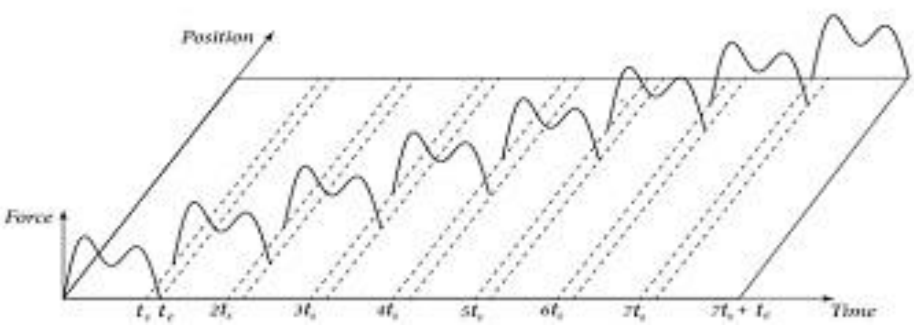

Figure 9. Loading scheme of single-footfall force

(Resources from：Zhang & Xu, 2020)

Moving damped-oscillator (MDO)

When human-structure interaction (HIS) is considered, the human body can be compared to a strongly damped oscillator (Zhang & Xu, 2020), as in Figure 10. Combining the human impact with the footprint gives a floor response for each footprint. In addition, the loading is similar to that in Figure 8. This method of predicting floor vibrations is the Moving damped-oscillator (MDO).

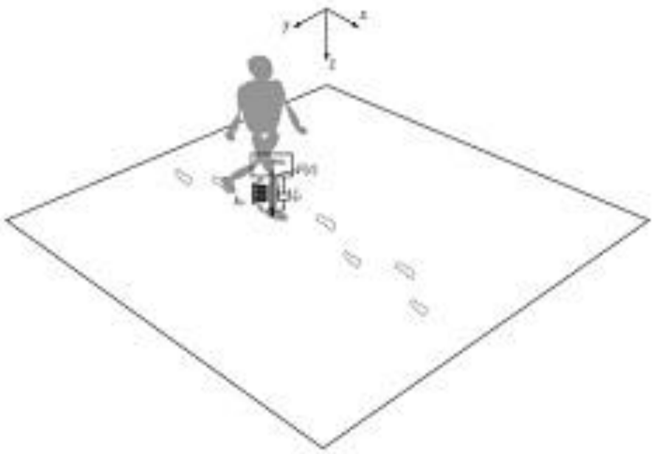

Figure 10. Moving damped-oscillator loading

(Resources from：Zhang & Xu,2020)

Moving and stationary damped-oscillators (MSDO)

In addition to the loads generated by moving occupants on the floor, loads are also generated by seated people. Therefore, Pedersen (2011) introduced the concept of moving (active) occupants and stationary occupants. Compared to stationary occupants, moving occupants can receive more excellent floor vibrations (Ohlsson, 1986). Therefore, the maximum floor vibration should be determined by seated rather than standing or moving occupants (Onysko et al., 2000). Therefore, when conducting floor vibration studies, both stationary and active occupants should be modelled to measure floor vibrations for all occupants.

Moving and stationary damped-oscillators (MSDO) models can be used to predict the dynamic response of floors to moving and stationary people (Zhang & Xu, 2020). As shown in Figure 11, moving people are modelled as moving damped oscillators, and stationary people are modelled as oscillators with fixed positions. In addition, this model is loaded similarly to the previous two models.

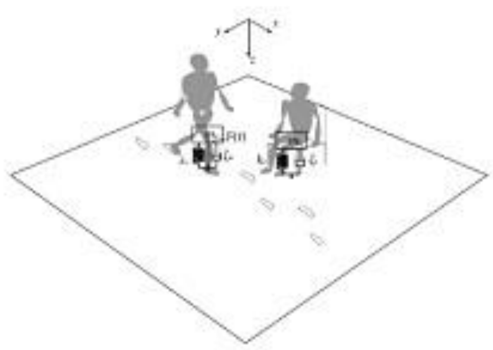

Figure 11. Model of moving and stationary damped-oscillators

(Resources from：Zhang & Xu,2020)

2.3 Related content of floor vibration experiment

2.3.1 Experimental protocols

Davis and Parnell et al. (2008) and Xu (2011) describe both methods in detail. As shown in Table 1, laboratory testing uses laboratory instrumentation to measure the performance of CFS flooring under various configurations of floor vibration by varying the conditions of the experiment, such as span, material, and thickness. In addition, the responses obtained in the laboratory can be used to verify the feasibility of the design (Xu, 2011).

Name	Joist Type	Joist Thickness	Floor Span	Subfloor	Topping Thickness	Ceiling	Strongback
LF14.5A	C-shape	54 mil	14.5'	OSB	-	-	-
LF14.5B	C-shape	54 mil	14.5'	FC	-	-	-
LF14.5B$_{i}$	C-shape	54 mil	14.5'	FC	-	-	-
LF14.5C	TDW	54 mil	14.5'	OSB	-	-	-
LF14.5D	TDW	54 mil	14.5'	FC	-	Type X	-
LF14.5D$_{i}$	TDW	54 mil	14.5'	FC	-	-	-
LF14.5E	TDW	54 mil	14.5'	FC	3/4"	Type X	-
LF14.5F	TDW	54 mil	14.5'	MD	1.5"	Type X	-
LF17.0A	TDW	68 mil	17'	FC	3/4"	Type C	-
LF17.0C	TDW	68 mil	17'	MD	1.5"	Type C	-
LF19.5A	TDW	68 mil	19.5'	FC	3/4"	Type C	-
LF19.5A$_{i}$	TDW	68 mil	19.5'	FC	3/4"	-	-
LF19.5A$_{ii}$	TDW	68 mil	19.5'	FC	3/4"	-	Yes
LF19.5A$_{iii}$	TDW	68 mil	19.5'	FC	3/4"	Type C	Yes
LF19.5A$_{iv}$	TDW	68 mil	19.5'	FC	3/4"	Type C	-
LF19.5B	TDW	68 mil	19.5'	MD	1.5"	Type C	-
LF19.5B$_{i}$	TDW	68 mil	19.5'	MD	1.5"	-	-
LF19.5B$_{ii}$	TDW	68 mil	19.5'	MD	1.5"	-	Yes
LF19.5B$_{iii}$	TDW	68 mil	19.5'	MD	1.5"	Type C	Yes
LF19.5B$_{iv}$	TDW	68 mil	19.5'	MD	1.5"	Type C	-
LF21.8A	(2)TDW	54 mil	21.83'	MD	1.5"	Type C	-

Table 1. Floor Construction Configurations

(Resources from:Davis, Parnell & Xu, 2008)

In situ investigation is carried out on the construction site and is more reflective of the performance of floor vibrations after the building has been used. On the one hand, in situ investigation validates the laboratory test results; on the other hand, in situ investigation also quantifies the errors associated with on-site construction (Davis, Parnell & Xu, 2008).

Based on the differences between laboratory testing and in-situ survey testing, Xu (2011) concluded that in almost all cases, there is a slight central disturbance in the in-situ survey as the laboratory testing is supported on both the in-situ survey is supported on all sides. Secondly, other factors such as plasterboard and wall surfaces can influence site survey floors. The result is that Situ Investigation has a higher fundamental frequency and damping ratio, so Laboratory Testing has a worse vibration performance than Situ Investigation. In other words, the results of Laboratory Testing are more conservative.

2.3.2 Testing methods

This section is based on literature from Virginia Tech (Kraus & Murray, 1997) and the University of Waterloo (Davis et al., 2008; Xu & Tangorra, 2007).

Static tests - deflection tests

Static tests quantify the maximum disturbance of a floor under external loading. A concentrated force of 1KN is usually applied to the center of the test object (Xu, 2011), as shown in Figure 12. A concentrated force of 1KN was chosen for the external load because the central disturbance generated by 1KN can be used as a basis (Ohlsson, 1988; CWC, 1996; Allen et al., 1999). In addition, this also allows the perturbations to be corresponded to and compared with those of other design codes (Davis, Parnell & Xu, 2008).

Figure 12. Static tests

(Resources from：Xu, 2011)

Dynamic tests

Dynamic tests are divided into three specific types of tests: heel drop, sandbag, and walking tests. The walking test measures the root mean squared (RMS) acceleration response (Davis, Parnell & Xu, 2008).

- Heel Drop Test

The heel drop test is performed by striking the floor with the heel in the center of the floor. Williams et al. (2003) concluded that the heel drop test adequately characterizes the dynamics of floor vibrations.

- Sandbag Test

The sandbag test is in which a sandbag is struck vertically against the center of the floor from a certain height. This test also validates the results of the heel drop test. This test uses a sandbag so that human factors do not influence the results (Davis, Parnell & Xu, 2008).

- Walking Tests

The walking test is a test where the researcher walks along the edge of the floor from one end to the other in the direction of the joists and perpendicular to the joists, respectively. The test quantifies and compares the conditions of the actual situation (containing the occupants) of the activity.

Both the heel drop and sandbag experiments were assumed to be impulsive loads; in addition, the sandbag test was the same for the sandbag impact in comparison to the heel drop experiment as it avoided the massing of the heel drop experimenter (Parnell, Davis & Xu, 2008).

2.3.3 Characteristic parameters

In order to determine and study the influence of floor vibrations on occupant comfort, representative characteristic parameters should be selected to reflect floor vibrations. The parameters should be measurable, calculable, and interpretable (Zhang & Xu, 2020).

For example, the Step frequency, Mass ratio, and Walking path parameters mentioned by Zhang and Xu (2020) are also important. However, this section focuses on the quantitative parameters in dynamic and static tests. These parameters are determined using acceleration response and time (Davis, Parnell & Xu, 2008).

Natural Frequencies

The fixed frequency can be determined from the first two peaks of the power spectrum. The first peak corresponds to the fundamental frequency, which is related to the first bending mode; moreover, the fundamental frequency has the most significant effect on the floor response (Davis, Parnell & Xu, 2008). Because of the impulsive loading, the resulting higher-order multipliers and torsional modes have little effect on the slab system (Johnson, 1994).

Damping Ratio

The damping ratio is divided into two cases: in the frequency domain and in the time domain. For the frequency domain, the half-power bandwidth method is used to calculate the damping ratio; for the time domain, the logarithmic decrement is used to calculate the damping ratio (Davis, Parnell & Xu, 2008).

If both the wheel drop test and the sandbag test are shock pulses, the half-power bandwidth method is valid for both tests since the half-power bandwidth method can solve the damping ratio under pulse loading (Davis, Parnell & Xu, 2008).

The half-power bandwidth method is not very applicable to floor systems with small natural frequency intervals, as the damping ratio cannot be shown in this case. Furthermore, the logarithmic decrement can only find the damping ratio for single-degree-of-freedom systems, as it produces incorrect results in other cases (Parnell, Davis & Xu,).

RMS Acceleration

Using ISO 2631 (1997) calculation procedure, the root means the square value of acceleration for walking tests is calculated. This parameter is weighted without the effect of frequency（Parnell, Davis & Xu, 2008).

Deflection

This parameter is a characteristic parameter of the static response. It reflects and assesses the static flexural stiffness of the floor system. It is measured by placing the diameter gauges underneath the joists (Parnell, Davis & Xu, 2008). This parameter is the most intuitive parameter of the floor response and is better understood by engineers.

2.3.4 Influence of Construction Details

This section focuses on the changes in the details of the floor system, resulting in changes in the relevant parameters for dynamic and static tests. By changing the details of the conditions of the floor system, the main factors affecting the stability of the floor system can be explored. Although many different details affect the floor system, this section focuses on some of the main details: The effect of floor framing, the effect of span length, the effect of the connection method, and the effect of the strongback. Table2, Table3, and Table4 illustrate the effects of these details.

Floor Name	f_1 (Hz)	f_2 (Hz)	ζ (%)	Δ_{center} (in)
LF14.5A	25.3	32.7	4.3*	0.020
LF14.5B	22.5	25.1	3.2*	0.017
LF14.5C	26.3	33.2	2.1*	0.023
LF14.5D	19.7	24.2	4.7	0.013
LF14.5E	17.7	22.5	3.1	0.009
LF14.5F	16.1	22.5	3.8	0.007
LF17.0A	14.9	19.1	4.4	0.012
LF17.0C	14.9	19.7	3.9	0.011
LF19.5A	14.3	18.3	3.6	0.010
LF19.5A$_{rr}$	13.2	24.0	4.5	0.014
LF19.5B	13.0	23.0	4.5	0.012
LF21.8A	12.5	23.4	4.0	0.010

Table 2. Balloon Framing

(Resources from:Davis, Parnell & Xu, 2008)

Floor Name	f_1 (Hz)	f_2 (Hz)	ζ (%)	Δ_{center} (in)
LF14.5A	17.9	29.8	3.7*	0.026
LF14.5B	17.2	18.8	3.8*	0.019
LF14.5C	16.4	27.8	3.7*	0.024
LF14.5D	16.9	22.0	7.0	0.015
LF14.5E	16.2	22.2	5.3	0.009
LF14.5F	14.8	22.0	3.4	0.007
LF17.0A	13.6	19.4	4.0	0.013
LF17.0C	13.3	19.3	5.7	0.011
LF19.5A	13.4	18.8	4.0	0.010
LF19.5A$_{rr}$	13.4	20.2	4.1	0.009
LF19.5B	11.8	17.3	3.8	0.013
LF21.8A	10.6	15.3	2.5	0.013

Table 3. Platform Framing

(Resources from:Davis, Parnell & Xu, 2008)

Floor Name	f_1 (Hz)	f_2 (Hz)	ζ (%)	Δ_{center} (in)
LF14.5A	19.1	27.4	5.5*	0.022
LF14.5B	17.2	21.4	2.9*	0.021
LF14.5C	17.7	26.0	2.3*	0.028
LF14.5D	16.2	22.4	7.7	0.016
LF14.5E	15.7	21.1	5.7	0.010
LF14.5F	14.6	21.2	3.2	0.008
LF17.0A	13.5	17.9	4.8	0.013
LF17.0C	13.3	18.1	4.4	0.013
LF19.5A	12.8	18.4	3.2	0.010
LF19.5A$_{rr}$	13.2	18.6	4.5	0.009
LF19.5B	11.4	16.4	4.9	0.014
LF21.8A	10.1	14.7	3.5	0.014

Table 4. Simple Support

(Resources from:Davis, Parnell & Xu, 2008)

Effect of Floor Framing

The common types of framing are platform framing, balloon framing, and simple support. According to Davis et al. (2008) and Xu et al. (2018), the type of floor framing significantly affects the fundamental frequency, damping ratio, and central deflection of the floor. Balloon framing has the most significant fundamental frequency, but its central deflection is the smallest; the platform framing has the minor fundamental frequency, but its central deflection is the largest. Davis et al. (2008) conclude that the reason for this difference is due to the restraint at the support. When the restraint at the support is reduced, the damping ratio of the structure increases. When the rotation at the support is limited, the flexural stiffness of the structure increases, resulting in an increase in the fundamental frequency and a decrease in the central deflection. In addition, as shown in Figure 13, all other things being equal, balloon framing has the minor transverse deflection, and simple support has the slightest transverse deflection.

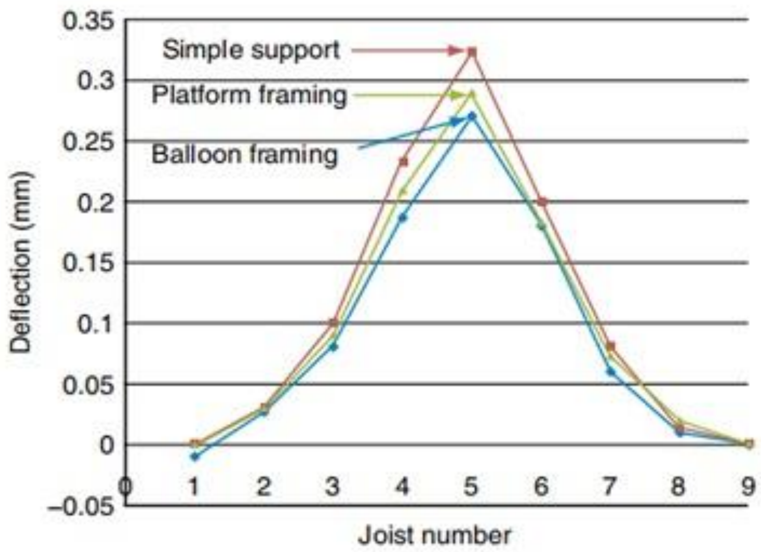

Figure 13. Distribution of floor transverse deflection

（Resources from:Xu，2011）

Effect of Span Length

When the other conditions of the floor system are kept constant and the span is changed, the stability of the floor system is affected. On the one hand this is because the bending strength is inversely proportional to the span length, the longer the span length the less the bending strength of the material, which leads to a greater central disturbance with longer spans; on the other hand, increasing the length of the span increases the mass but not the stiffness, which leads to a reduction in the fundamental frequency of the system as the span increases (Davis, Parnell & Xu, 2008).

Effect of the shear transfer type

As shown in Figure 14, these are common types of shear transfer in joists, including Pre-drilled holes, Pre-fabricated bent-up tabs, and Self-drilling screws, which can enhance the shear transfer of joists. A detailed study of the shear transfer of joists by Lakkavalli & Liu (2006) found that: the enhancement effect of bent-up tabs was the best, drilled holes were the second-best and self-drilling screws were the least effective; furthermore, the shear enhancement spacing varied from 200mm to 150mm, bent-up tabs performed, and self-drilling screws were the least effective. The ultimate load capacity of both bent-up tabs and self-drilling screws decreased as the shear enhancement spacing changed from 200 mm to 150 mm. Only the ultimate load capacity of circular holes increased.

Figure 14. Three kinds of shear transfer
(Resources from: Lakkavalli & Liu, 2006)

Effect of Strongback

Strongback is a strengthening configuration added to the floor system, oriented perpendicular to the joists and mainly divided into the restrained end and a free end. Parnell et al. (2010) state that a restrained strongback simulates a long, narrow floor. It is fixed to the webs of the joists, and the ends are screwed to the supports. It adds a constraint to the system with the reduced centre deflection but increases the fundamental frequency of the floor system. In addition, the damping ratio is increased due to the friction of the attachment screws.

The free-end strongback simulates a short and wide floor, which is unrestrained at the end compared to the restrained strongback. This configuration has a negligible effect on the bending stiffness, and therefore it has a negligible effect on the floor system's fundamental frequency and damping ratio. In addition, the strongback increases the lateral stiffness, reducing the center deflection.

2.4 Literature Review: Conclusion

The above literature covers the development and problems of CFS and the theoretical aspects of floor vibrations, as well as laboratory and field-specific experimental operations to calculate and analyse the characteristic parameters and stability of floor systems using relevant equations. The stability of floor systems is a complex issue that several researchers have investigated, and the study of floor systems is constantly evolving. This literature provides the basis for this project. This thesis also fills a gap in this literature. These studies require complex physical manipulation, and there is no guarantee that the experiments will give the desired results, which can be costly in terms of human resources and money. This project uses the Srand7 computer software to model different joist types of flooring systems and uses solvers to investigate the stability of flooring systems and assess occupant comfort. Using a computer instead of tedious physical operations and formulae simplifies the calculations and reduces the time taken to perform them. By simulating the stability of joists' floor systems under three scenarios in advance, the project avoids the failures and wastage of resources that would result from rash experimentation and provides preliminary data and predictions of results for subsequent physical experiments.

The project can provide new research and prediction ideas for subsequent studies. The use of computer software to solve engineering problems is now commonplace, e.g., CAD. In the future, with the development and advancement of computers and the internet, using computer software such as this to analyse engineering problems is sure to become increasingly important.

3 RESEARCH METHODOLOGY

This project is based on the knowledge of structural mechanics, modelling, and FEA through Stran7 software. In addition to the method based on FEA, the experimental method of controlled variable method and method validation has been adopted to make this experiment more objective and effective.

3.1 Theoretical methods

3.1.1 Finite element analysis (FEA)

Finite Element Analysis (FEA) is the primary method for performing structural engineering analysis, and the Finite Element Method (FEM) is a numerical technique. This method is computer-based and based on a numerical segmental polynomial interpolation applied to control the fundamental equations to simulate physical behavior, allowing the analysis of engineering structures and continua. FEA results can reflect structural stress and strain distributions and save time compared to traditional analysis methods (Shaikh, 2012).

Furthermore, FEA is closely related to the underlying theory and requires a rigorous theoretical basis for the engineer. The assumptions and limitations of FEA have to be fully understood during operation so that a more objective structure can be modelled. Furthermore, according to Rencis et al. (2007), undergraduate students' understanding of FEA is generally one-sided as it requires complete knowledge of engineering theory as a foundation. However, Strand7's well-established FEA program can effectively simplify this problem. Instructions for Students Enrolled in Software or Electronics Engineering.

3.1.2 The Controlled Variable Method

The controlled variable method is an essential method of thought in scientific inquiry and is widely used in various scientific inquiries and experimental scientific research. This method allows the influence of other factors on the experiment to be controlled. Only by controlling the variables other than the experimental variables can the influence of the experimental variables on the experimental results be better verified and assessed. In this project, the three types of joists are the experimental variables. At the same time, all other factors are irrelevant variables, such as span, material, and type of support, and it should be ensured that these irrelevant variables remain unchanged.

3.1.3 Validation method

In order to verify that the simulated bolts meet the structural mechanics, two parallel plates are created, as shown in Figure 15, connected by rigid at points 7 and 10, and an external force of 3N is applied in the X-axis direction at points 1, 2, 3, 4, 5, 6, 8 and 9, respectively, and the X-axis support reactions of the other plate (points 12, 14, 17 and 18) are shown in Table 5.

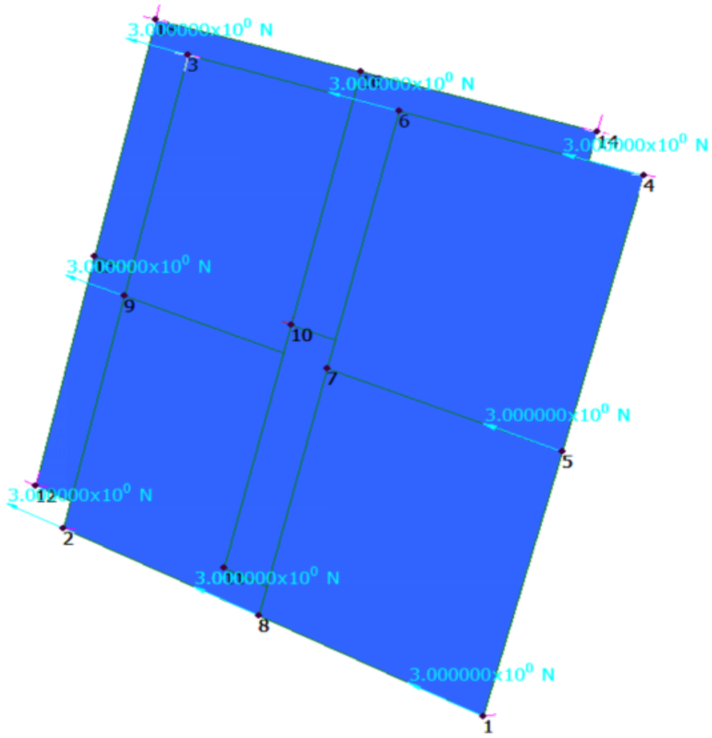

Figure 15. Validation of simulated bolts

	FX (N)
Node 14	-6.000000×10^{0}
Node 12	-6.000000×10^{0}
Node 17	-6.000000×10^{0}
Node 18	-6.000000×10^{0}

Table 5. Value of the support reaction force in the X-axis

The external force is 3*8=24N, which is relative to the total absolute value of the support reaction force in the X-axis, so the use of "Rigid" for modelling the bolt follows the structural mechanics and the actual situation.

In addition, to ensure the feasibility of this project, this section validates the modelling and analysis of the Strand7 software using simple physical models and knowledge of structural mechanics. For example, in the floor structure in Figure 16, a 2Kpa face force is applied to the floor slab. If the support reaction force in the Y direction is equal to the sum of the external forces applied in the Y direction, then the model created by the Strand7 software is more objective. Otherwise, it is incorrect. This verifies that the modelling approach and the analysis using the Strand7 software are feasible.

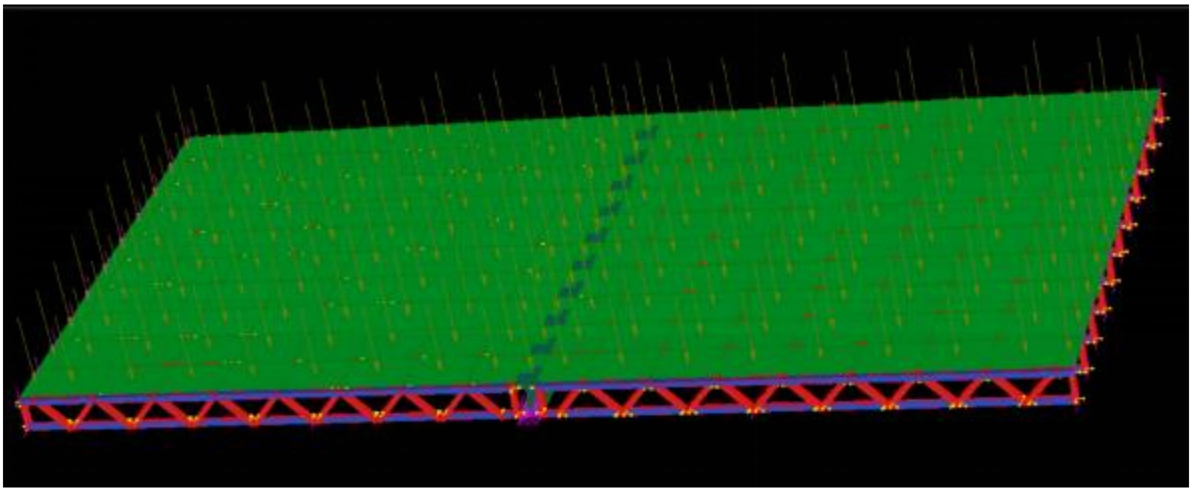

Figure 16. Model of the floor

Table 6 shows the values of the bearing reaction forces, which when summed using the Excel table are approximately 88KN.

The area of the floor slab: $(4.8*2+0.096*2+0.002*3)*4.5=44.091\text{m}^2$;

External forces: 44.091*2 ≈ 88KN.

The sum of the external forces in the Y-axis is equal to the support reaction force in the Y-axis, so the modelling approach and analysis method for this project is feasible.

	FY (kN)
Node 3	7.942837×10^{-1}
Node 4	2.330965×10^{0}
Node 5	-6.223457×10^{-1}
Node 6	1.572684×10^{-1}
Node 7	-9.140234×10^{0}
Node 22	7.942837×10^{-1}
Node 23	2.330965×10^{0}
Node 24	-6.223457×10^{-1}
Node 25	1.572684×10^{-1}
Node 26	-9.140234×10^{0}
Node 68	1.094945×10^{0}
Node 78	2.016092×10^{0}
Node 88	-5.396078×10^{-1}
Node 98	1.363880×10^{-1}
Node 108	-1.065685×10^{1}
Node 258	1.094945×10^{0}
Node 268	2.016092×10^{0}
Node 278	-5.396078×10^{-1}
Node 288	1.363880×10^{-1}
Node 298	-1.065685×10^{1}
Node 421	1.817837×10^{0}
Node 422	-4.181425×10^{-1}
Node 425	1.817837×10^{0}
Node 426	-4.181425×10^{-1}
Node 430	0.000000×10^{0}
Node 446	0.000000×10^{0}
Node 459	-2.499389×10^{-1}
Node 460	-2.608119×10^{-1}
Node 461	-2.555033×10^{-1}
Node 462	-2.496153×10^{-1}
Node 463	-2.463491×10^{-1}
Node 464	-2.448985×10^{-1}
Node 465	-2.465319×10^{-1}
Node 466	-2.486203×10^{-1}
Node 467	-2.361064×10^{-1}
Node 468	-3.950817×10^{-1}
Node 559	2.145137×10^{0}
Node 560	2.197151×10^{0}
Node 561	2.190435×10^{0}
Node 562	2.186673×10^{0}
Node 563	2.183377×10^{0}
Node 564	2.182605×10^{0}
Node 565	2.186681×10^{0}
Node 566	2.203041×10^{0}
Node 567	2.174004×10^{0}
Node 568	1.888750×10^{0}
Node 749	2.145137×10^{0}
Node 750	2.197151×10^{0}
Node 751	2.190435×10^{0}
Node 752	2.186673×10^{0}
Node 753	2.183377×10^{0}
Node 754	2.182605×10^{0}
Node 755	2.186681×10^{0}
Node 756	2.203041×10^{0}
Node 757	2.174004×10^{0}
Node 758	1.888750×10^{0}
Node 759	-2.499389×10^{-1}
Node 760	-2.608119×10^{-1}
Node 761	-2.555033×10^{-1}
Node 762	-2.496153×10^{-1}
Node 763	-2.463491×10^{-1}
Node 764	-2.448985×10^{-1}
Node 765	-2.465319×10^{-1}
Node 766	-2.486203×10^{-1}
Node 767	-2.361064×10^{-1}
Node 768	-3.950817×10^{-1}
Node 939	2.554547×10^{0}
Node 978	2.336587×10^{0}
Node 979	1.691108×10^{-1}
Node 1018	1.418007×10^{-1}
Node 1019	-5.228005×10^{-2}
Node 1058	-4.249724×10^{-2}
Node 1059	3.322741×10^{-2}
Node 1098	3.016514×10^{-2}
Node 1099	1.611237×10^{1}
Node 1138	1.692217×10^{1}
Node 1699	2.554547×10^{0}
Node 1738	2.336587×10^{0}
Node 1739	1.691108×10^{-1}
Node 1778	1.418007×10^{-1}
Node 1779	-5.228005×10^{-2}
Node 1818	-4.249724×10^{-2}
Node 1819	3.322741×10^{-2}
Node 1858	3.016514×10^{-2}
Node 1859	1.611237×10^{1}
Node 1898	1.692217×10^{1}

Table 6. Values of the bearing reaction forces

3.2 Strand7 modelling process

Rigorous and appropriate experimental steps are the key to the project's success. The practical steps of this project are mainly the use of Strand7 software to model the experimental project. The difficulty of the model established is: both to model as simple as possible, but more important is to meet the actual situation, reflect the entire floor system vibration problems, attention to details such as bolts, production conditions, and external loads. Only by being close to the actual situation will the project results be more realistic, and the experiment's conclusions will be meaningful. The specific practical steps are as follows：

- ***Determining the size of the module:*** According to the project's requirements, use CAD to determine the dimensional drawing of the project's structure. In Figure17, the length of the floor is divided into joists and back-to-back beams; joists are 4.8m long and have two sections, and beams are 0.096m long. Based on the actual situation, there is a gap between the beam and the joist. With a spacing of 0.002m, the total length of the floor is 9.798m, and the total width is 4.5m. The beam cross-section is shown in Figure 18, and the model number is C30024, the details of which are shown in Figure 19.

Figure 17. Dimensional drawing of the floor slab (mm)

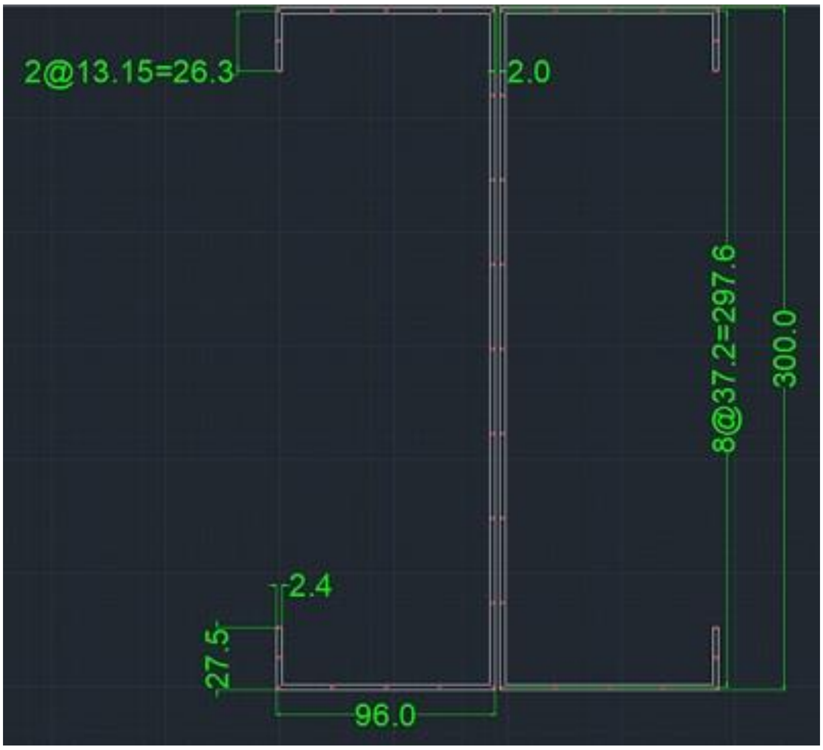

Figure 18. Beam cross section and dimensions (mm)

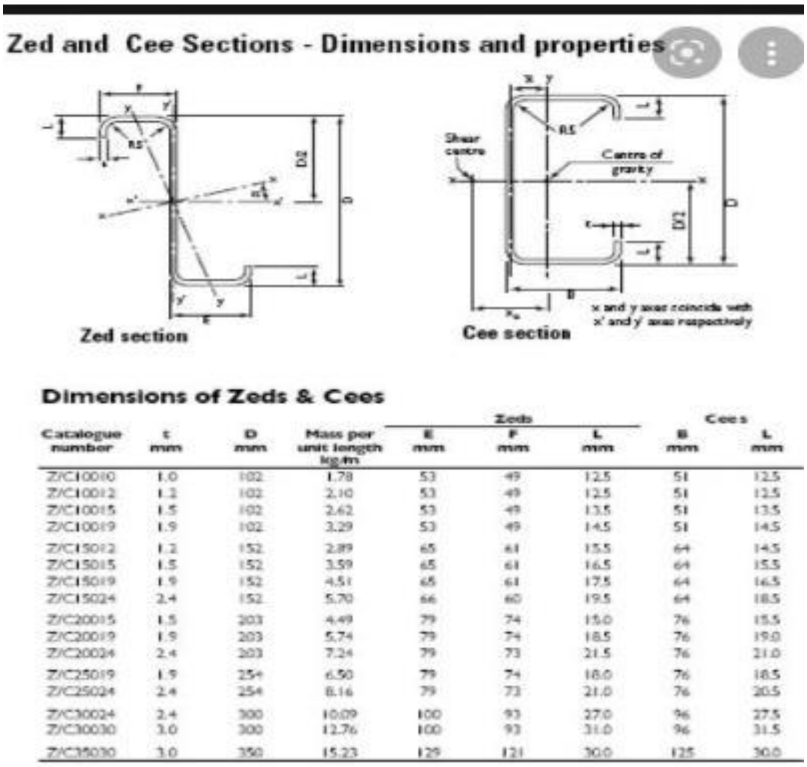

Dimensions of Zeds & Cees

Catalogue number	t mm	D mm	Mass per unit length kg/m	Zeds E mm	Zeds F mm	Zeds L mm	Cees B mm	Cees L mm
Z/C10010	1.0	102	1.78	53	49	12.5	51	12.5
Z/C10012	1.2	102	2.10	53	49	12.5	51	12.5
Z/C10015	1.5	102	2.62	53	49	13.5	51	13.5
Z/C10019	1.9	102	3.29	53	49	14.5	51	14.5
Z/C15012	1.2	152	2.89	65	61	15.5	64	14.5
Z/C15015	1.5	152	3.59	65	61	16.5	64	15.5
Z/C15019	1.9	152	4.51	65	61	17.5	64	16.5
Z/C15024	2.4	152	5.70	66	60	19.5	64	18.5
Z/C20015	1.5	203	4.49	79	74	15.0	76	15.5
Z/C20019	1.9	203	5.74	79	74	18.5	76	19.0
Z/C20024	2.4	203	7.24	79	73	21.5	76	21.0
Z/C25019	1.9	254	6.50	79	74	18.0	76	18.5
Z/C25024	2.4	254	8.16	79	73	21.0	76	20.5
Z/C30024	2.4	300	10.09	100	93	27.0	96	27.5
Z/C30030	3.0	300	12.76	100	93	31.0	96	31.5
Z/C35030	3.0	350	15.23	129	121	30.0	125	30.0

Figure 19. C30024

- ***Determining the type and size of joists for this project:*** This project focuses on three types of joists, divided into three experimental groups: case1, case2, and case3. Case1 is used as the control group for this project and is modelled in Strand7 using 'line units.' This is the most common type of joist in use, as shown in Figure 20, which has a complex structure and is difficult to install in the field; Figure 21 shows joists with a 'C' section; Figure 22 is a new type of joist with a 'dumbbell' cross-section. The latter two cases are modelled using 'plate units' and are simple to install on-site.

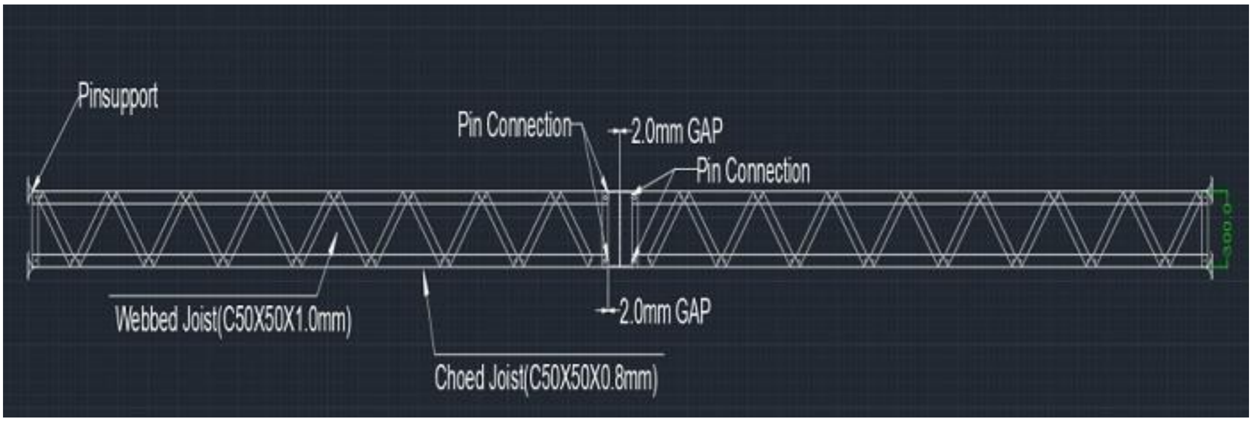

Figure 20. Common joist types（Case1）

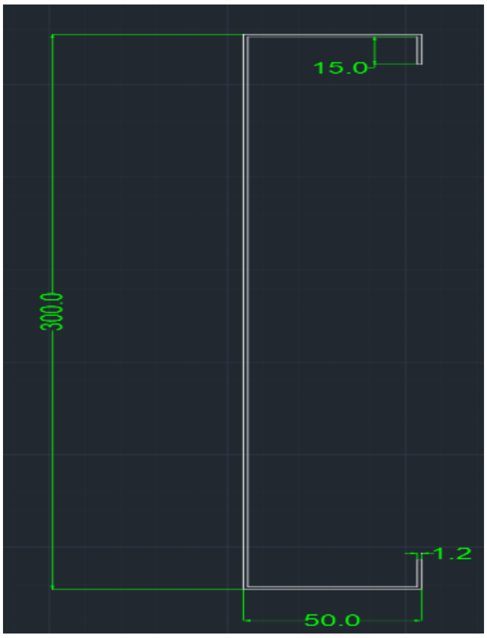

Figure 21.The "C" joist type(Case2)

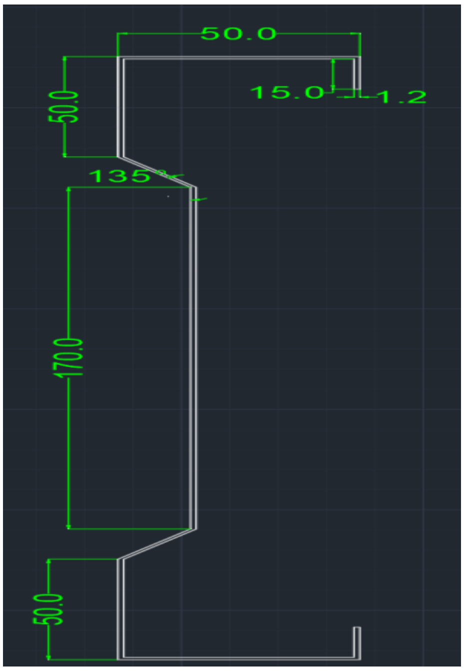

Figure 22.Cross-section of a "dumbbell" joist(Case3)

- ***Writing and modelling the coordinate values of points:*** The coordinates of the model points were determined from the CAD drawing of the dimensions, as shown in Table 7. In addition, these points are located on the central axis of the section. The accuracy of the point coordinates is the basis for the later modelling, including the connection of the points to the different structural components of the floor system.

Coordinates of beam																					
Point	1	2	3	4	5	6	7	8	9	10	11	12	13	14	15	16	17	18	19	20	21
X	0	0	0	0	0	0	0	0	0	0	0	0	0	0	0	0	0	0	0	0	0
Y	-122.5	-135.65	-148.8	-148.8	-148.8	-148.8	-148.8	-111.6	-74.4	-37.2	0	37.2	74.4	111.6	148.8	148.8	148.8	148.8	148.8	135.65	122.5
Z	-93.6	-93.6	-93.6	-70.2	-46.8	-23.4	0	0	0	0	0	0	0	0	0	-23.4	-46.8	-70.2	-93.6	-93.6	-93.6
	22	23	24	25	26	27	28	29	30	31	32	33	34	35	36	37	38	39	40	41	42
X	0	0	0	0	0	0	0	0	0	0	0	0	0	0	0	0	0	0	0	0	0
Y	-122.5	-135.65	-148.8	-148.8	-148.8	-148.8	-148.8	-111.6	-74.4	-37.2	0	37.2	74.4	111.6	148.8	148.8	148.8	148.8	148.8	135.65	122.5
Z	98	98	98	74.6	51.2	27.8	4.4	4.4	4.4	4.4	4.4	4.4	4.4	4.4	4.4	27.8	51.2	74.6	98	98	98
Coordinates of case1																					
	467	468	469	470	471	472	473	474	475	476	477	478	479	480	481	482					
X	0	0	0	0	0	0	0	0	0	0	0	0	0	0	0	0					
Y	-150	-150	-150	-150	-150	-150	-150	-150	150	150	150	150	150	150	150	150					
Z	251.2	851.2	1451.2	2051.2	2651.2	3251.2	3851.2	4451.2	551.2	1151.2	1751.2	2351.2	2951.2	3551.2	4151.2	4751.2					
	483	484	485	486	487	488	489	490	491	492	493	494	495	496	497	498					
X	0	0	0	0	0	0	0	0	0	0	0	0	0	0	0	0					
Y	-150	-150	-150	-150	-150	-150	-150	-150	150	150	150	150	150	150	150	150					
Z	-246.8	-846.8	-1446.8	-2046.8	-2646.8	-3246.8	-3846.8	-4446.8	-546.8	-1146.8	-1746.8	-2346.8	-2946.8	-3546.8	-4146.8	-4746.8					
Coordinates of case2																					
	463	464	465	466	467	468	469	470	471	472	473	474	475	476	477	478	479				
X	48.8	48.8	48.8	24.4	0	0	0	0	0	0	0	0	0	24.4	48.8	48.8	48.8				
Y	-133.8	-141.6	-149.4	-149.4	-149.4	-112.05	-74.7	-37.35	0	37.35	74.7	112.05	149.4	149.4	149.4	141.6	133.8				
Z	4901.2	4901.2	4901.2	4901.2	4901.2	4901.2	4901.2	4901.2	4901.2	4901.2	4901.2	4901.2	4901.2	4901.2	4901.2	4901.2	4901.2				
	650	651	652	653	654	655	656	657	658	659	660	661	662	663	664	665	666				
X	48.8	48.8	48.8	24.4	0	0	0	0	0	0	0	0	0	24.4	48.8	48.8	48.8				
Y	-133.8	-141.6	-149.4	-149.4	-149.4	-112.05	-74.7	-37.35	0	37.35	74.7	112.05	149.4	149.4	149.4	141.6	133.8				
Z	-4896.8	-4896.8	-4896.8	-4896.8	-4896.8	-4896.8	-4896.8	-4896.8	-4896.8	-4896.8	-4896.8	-4896.8	-4896.8	-4896.8	-4896.8	-4896.8	-4896.8				
Coordinates of case3																					
X	48.8	48.8	48.8	24.4	0	0	15	15	15	0	0	24.4	48.8	48.8	48.8						
Y	-133.8	-141.6	-149.4	-149.4	-149.4	-100	-85	0	85	100	149.4	149.4	149.4	141.6	133.8						
Z	4901.2	4901.2	4901.2	4901.2	4901.2	4901.2	4901.2	4901.2	4901.2	4901.2	4901.2	4901.2	4901.2	4901.2	4901.2						
X	48.8	48.8	48.8	24.4	0	0	15	15	15	0	0	24.4	48.8	48.8	48.8						
Y	-133.8	-141.6	-149.4	-149.4	-149.4	-100	-85	0	85	100	149.4	149.4	149.4	141.6	133.8						
Z	-4896.8	-4896.8	-4896.8	-4896.8	-4896.8	-4896.8	-4896.8	-4896.8	-4896.8	-4896.8	-4896.8	-4896.8	-4896.8	-4896.8	-4896.8						

Table 7. Coordinate value of the point

- ***Using 'Tools' to complete the model:*** Only a set of point coordinates is required, and the model can be refined using the tools of the Strand7 software, which simplifies the modelling process and shortens the modelling time. The main tools are Copy, Extrude and Subdivide. "Copy" (e.g., Figure23) is used to copy the first joists created to other locations. "Extrude" (e.g., Figure24) can turn a "line element" into a "plate element," mainly in case2 and case3. "Subdivide" (e.g., Figure25) splits the elements into the correct number of elements to ensure both accuracy and simulation time. The effect of element distribution (e.g., Figure26) on the central deflection and simulation time of the three cases is also explored later in this project.

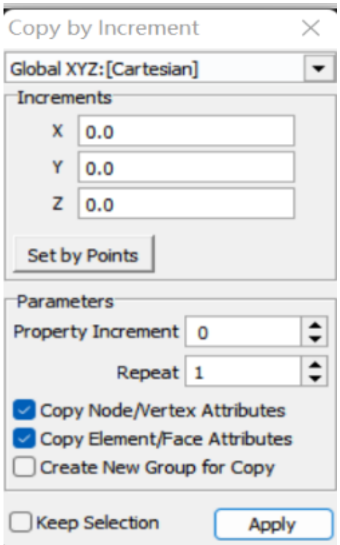

Figure 23. "Copy" tool

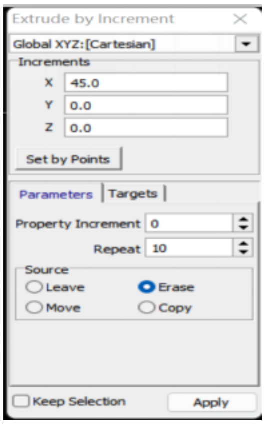

Figure 24. "Extrude" tool

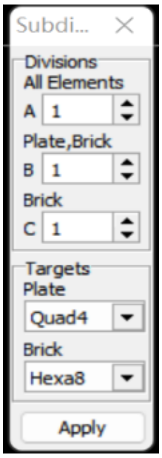

Figure 25. "Subdivide" tool

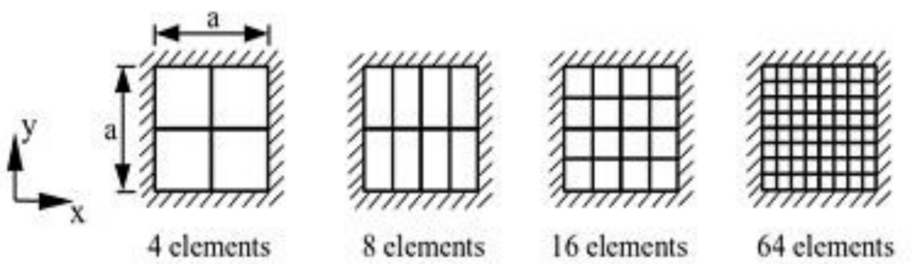

Figure 26. Number of elements

- ***Simulation of bolts:*** The Joists and beams are connected using bolts, and the "Rigid" is used to simulate the bolts in order to better match the construction conditions on-site. The simulator is shown in Figure27, and the appropriate parameters are set according to the section conditions. In addition, the "back-to-back" beams are independent and not connected in any way.

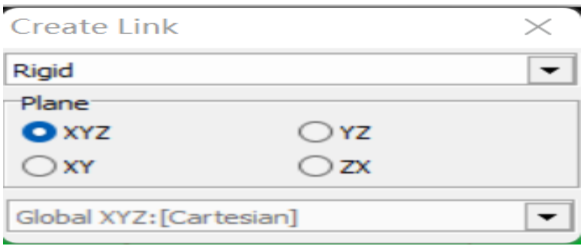

Figure 27. The simulators of bolts

In addition, as shown by the blue circle in Figure 28, "Rigid" has also been added to the joists' span to increase the system's stability in order to fit the actual situation.

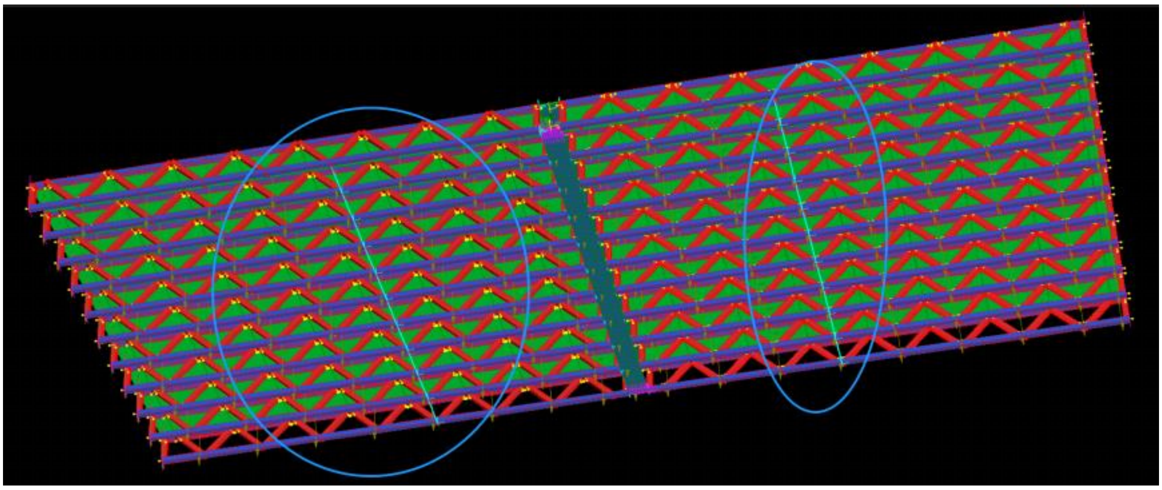

Figure 28. Cross-centre reinforcement of "Joists"

- ***Determining the restraint of the support:*** Setting up the bearings was to meet the realistic situation and minimize the restrictions on the floor system to amplify the effects of floor vibrations on parameters such as span and to facilitate the comparison of pulses in different joists. The support simulator for the point is shown in Figure 29. Depending on the setting of the axes shown in Figure 30 and the natural floor system situation, the floor system is free to rotate in all directions. The joists' support restraint restricts X-axis and y-axis displacement, preventing the floor system from moving left, right, and upwarp. Secondly, one end of the beam is simply-supported, and displacement is restricted in all directions; at the other end, displacement is restricted in the Y and Z axes.

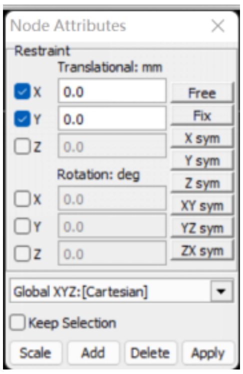

Figure 29. The simulators of restraint

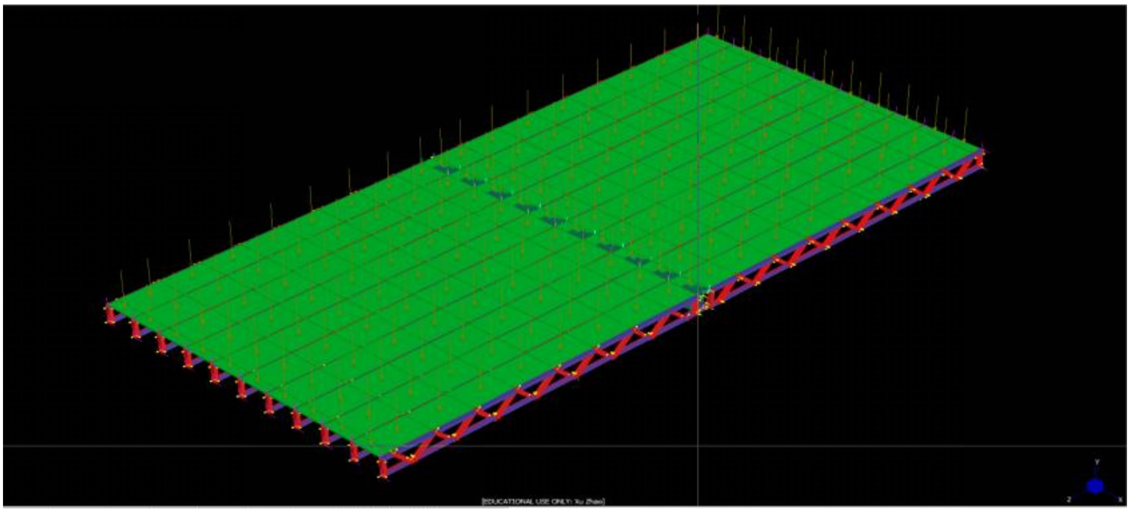

Figure 30. Axis settings for flooring systems

- ***Modelling of the plate:*** The floor is an essential part of the flooring system, and it affects the stability of the flooring system to a certain extent, so it is necessary to select the correct elements (e.g., Figure 31) to build the plates. In addition, as the built-up points are generally located on the axis, half of the built-up plate model will be inside the joists, and the plate's position will need to be adjusted.

Figure 31. Modelling of flooring

- ***Setting the characteristics of the elements:*** For Case 1, the joists are divided into two parts, web and chord, both of which are 300 mm high and have the characteristics shown in Figure 32. the web is C50*50*0.8, and the chord is C50*50*1.0. For case2 and case3, the characteristics of their elements are the same(e.g., Figure33). The CFS thickness in both cases is 1.2 mm. The characteristics of the floor are shown in Figure 34, the thickness of the floor is 15mm, and the material is timber.

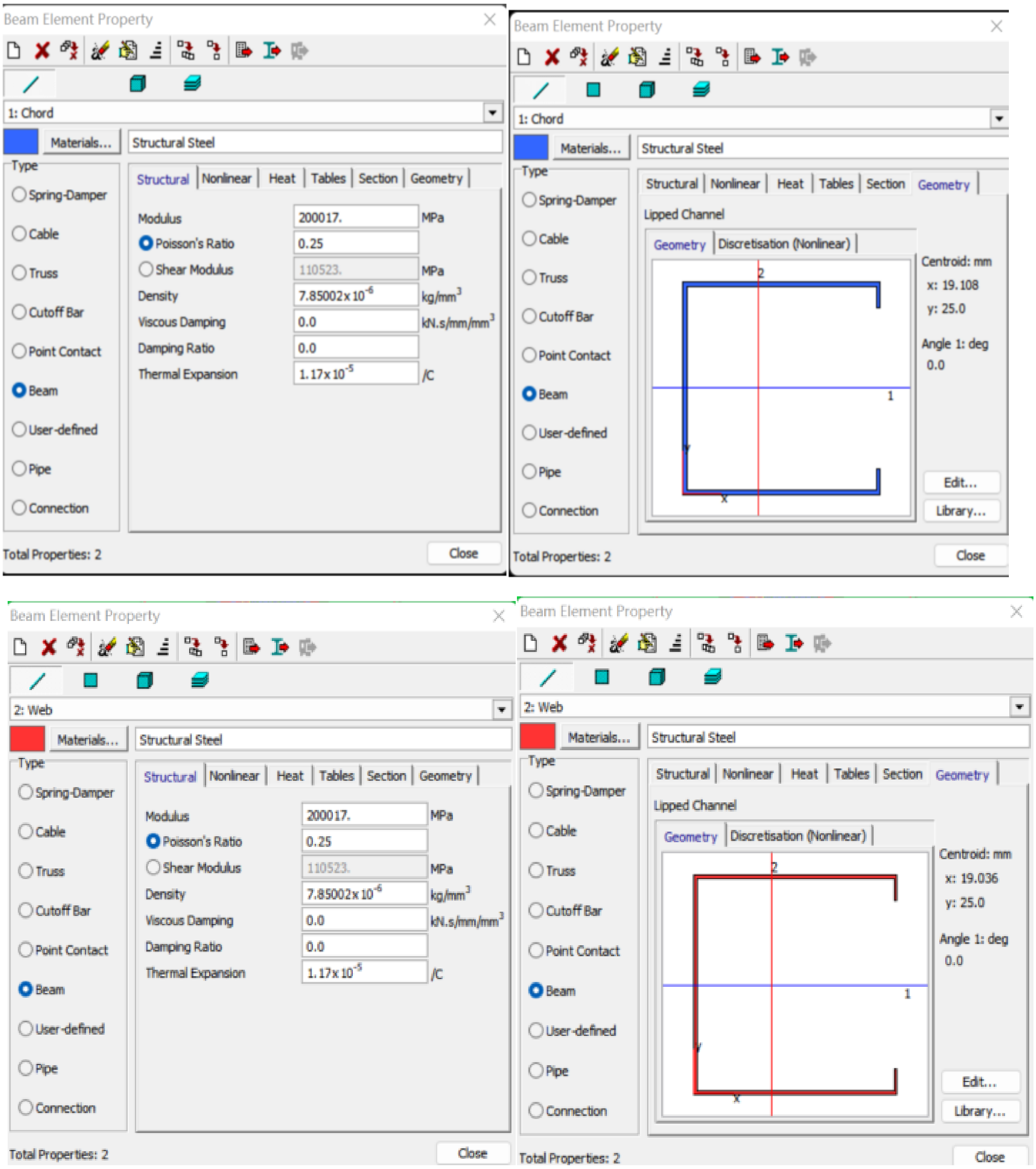

Figure 32. Case1 properties of "Web" and "Chord

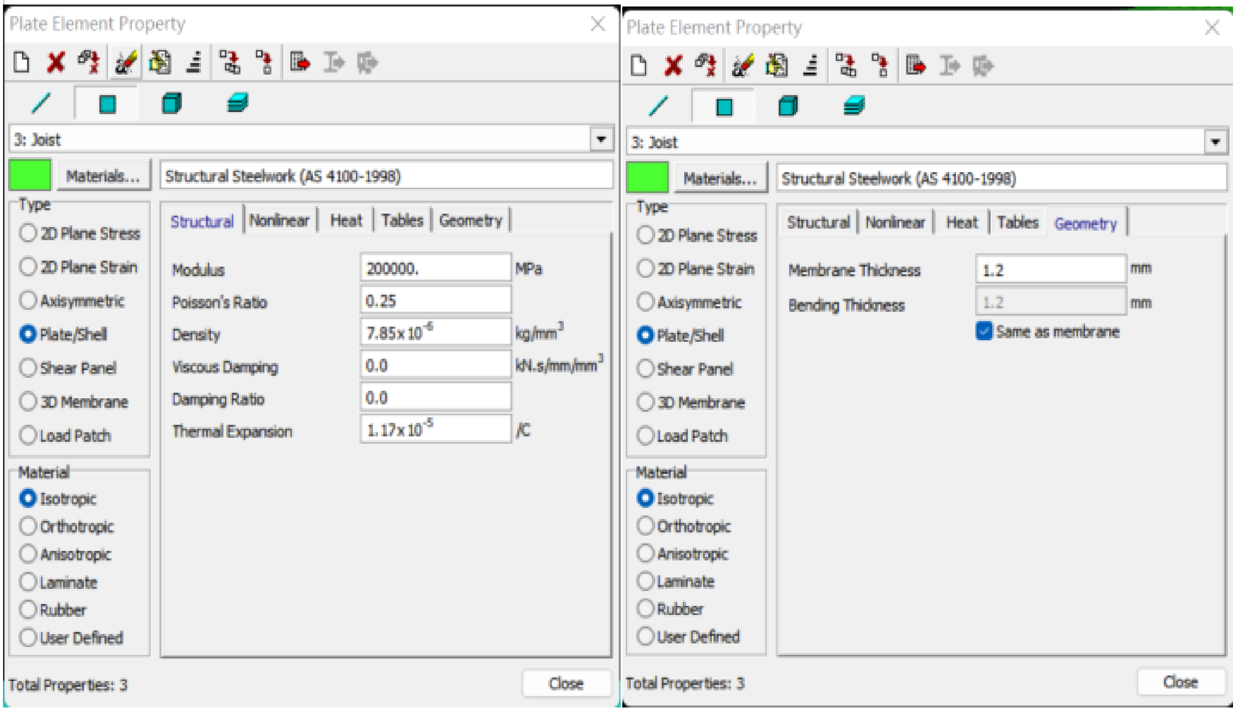

Figure 33. Properties of case2 and case3

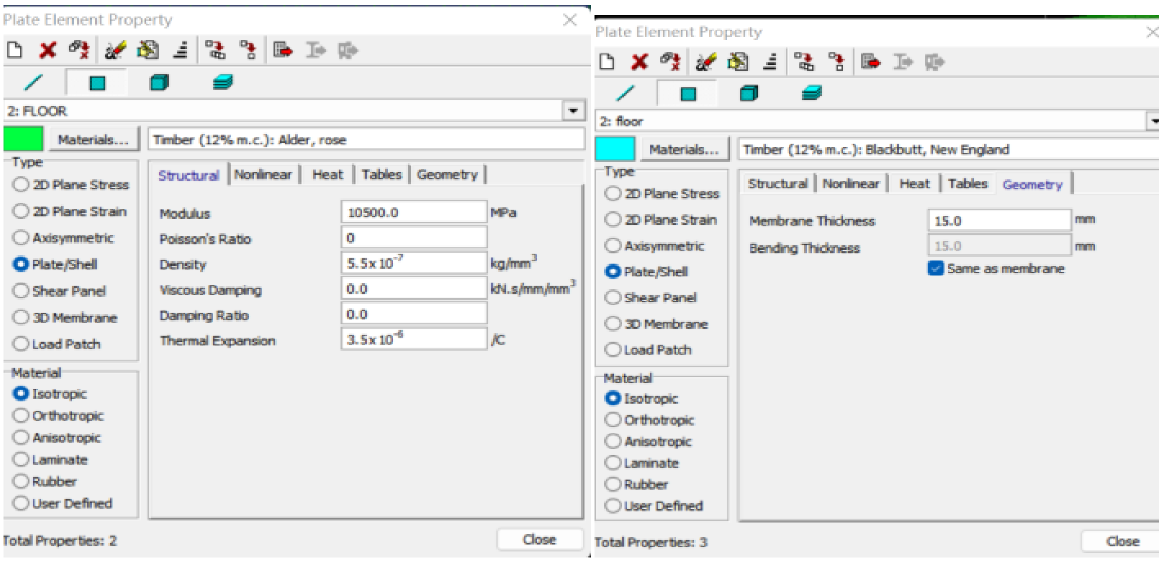

Figure 34. Properties of floor

- ***Adjustment of the plate position:*** Use the "Offset" function in the "Board Properties," as shown in Figure 35. Adjust the board's position to the thickness of the board so that it is close to the joists and beams and more in line with the actual construction operation of filling the gap between the floor and the beams with a specific glue. The before and after adjustments are shown in Figure 36.

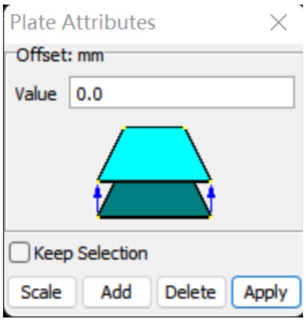

Figure 35. Attribute Tool - "Offset"

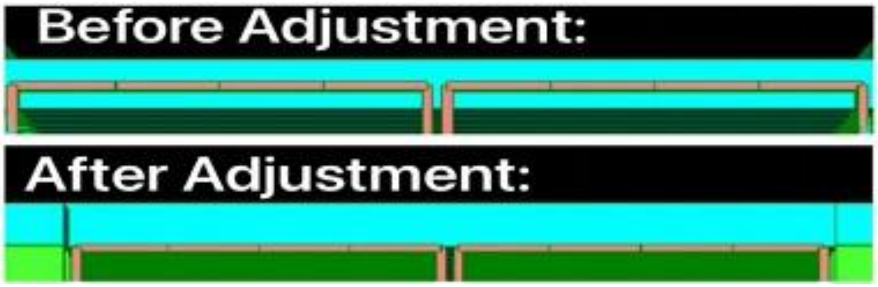

Figure 36. Comparison of before and after floor adjustment

- ***Modelling of the gravity of the structure:*** It would be more realistic to consider the structure's self-weight when modelling. The self-weight of the structure is therefore modelled (simulator as in Figure 37) with a gravitational acceleration of g = 9.8 m/s^2 = 9800 mm/s^2. The direction of gravity is along the negative direction of the Y-axis.

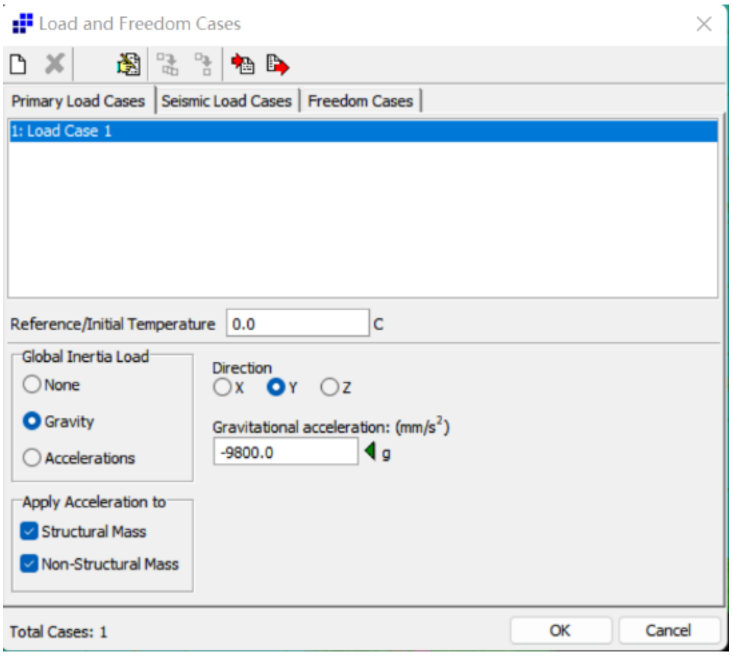

Figure 37. Simulation of gravity

4 FINITE ELEMENT ANALYSIS RESULTS

After analysis and calculation by Strand7 software, the parameters of static displacement, natural frequency, and the harmonic response of the project were obtained, and these indicators include both static and dynamic parameters. These results objectively reflect the vibration of the floor system. In addition, this section includes the experimental results and analysis of the number of elements.

4.1 Static displacement

4.1.1 Results

The floor was analysed statically using Strand7's 'Linear Static' solver (e.g., Figure 38), as detailed in Appendix A. The external force tested was a 2Kpa surface force.

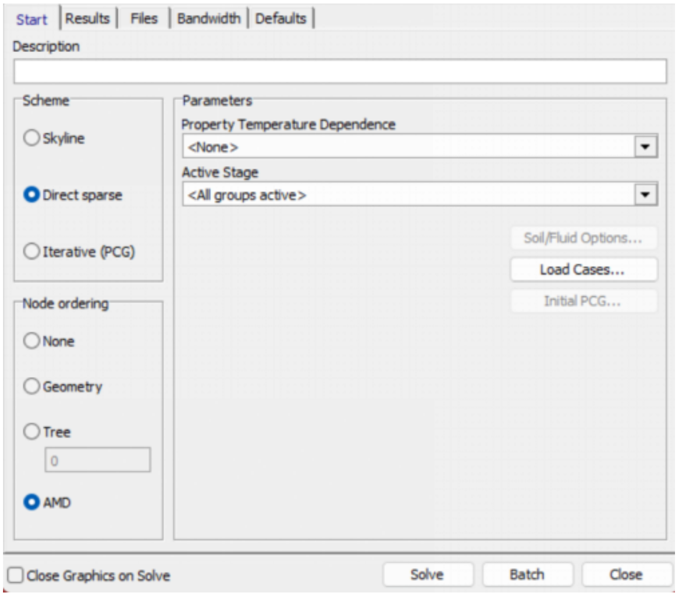

Figure 38. "Linear Static" solver

Case 1

The most important result of the static analysis is the static displacement. This project focuses on the displacement of the floor beams as an indicator of static displacement. Figure 39 shows the deformation of the floor; in addition, different colours are used to reflect the displacement. Figure 40 shows a numerical plot of the displacement, with the positive and negative signs representing the direction of displacement. The magnitude of the displacement should be compared to the absolute magnitude, so the maximum value of the floor displacement in case1 is 5.194mm.

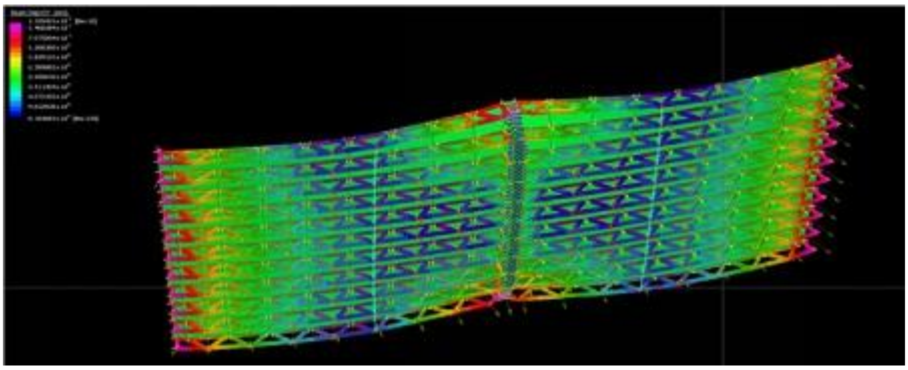

Figure 39. Colour chart for Beams displacement(Case1)

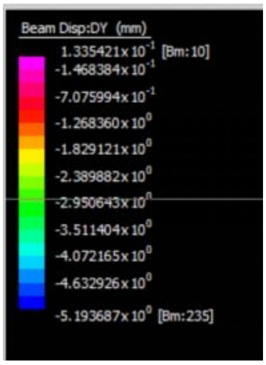

Figure 40. Value of Beams displacement (Case1)

Case 2

In this case (Case 2), the joists are modelled employing 'plate elements'. As shown in Figure 41, the displacements of each part of the floor are shown in different colours, and Figure 42 shows a graph of the numerical values of the displacements, with the positive and negative signs representing the direction of the displacements. The magnitude of the displacement should be compared to the magnitude of the absolute value, so the maximum value of the floor displacement in case2 is 8.3938 mm.

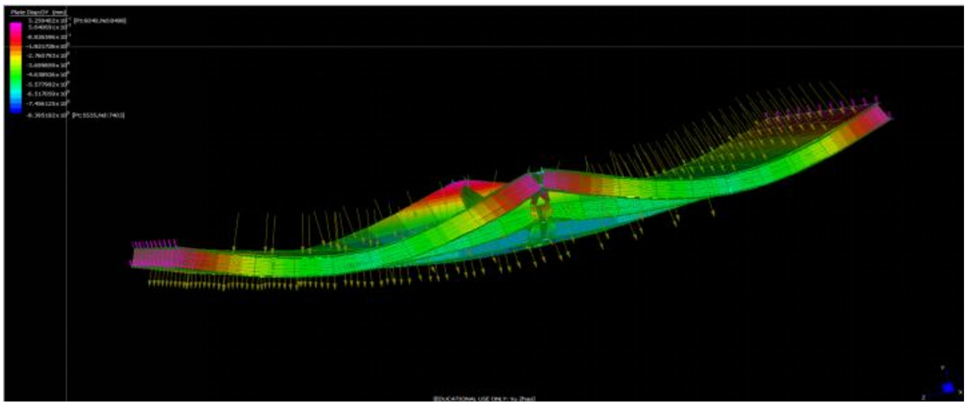

Figure 41.Colour chart for Beams displacement(Case2)

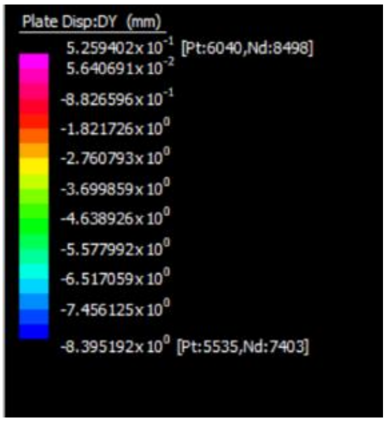

Figure 42. Value of Beams displacement (Case2)

Case 3

The displacement of each part of the floor is shown in different colours, as shown in Figure 43. Figure 44 shows a graph of the numerical values of the displacement, with the positive and negative signs representing the direction of displacement. The magnitude of the displacement should be compared to the magnitude of the absolute value, so the maximum value of the floor displacement in case3 is 13.66 mm.

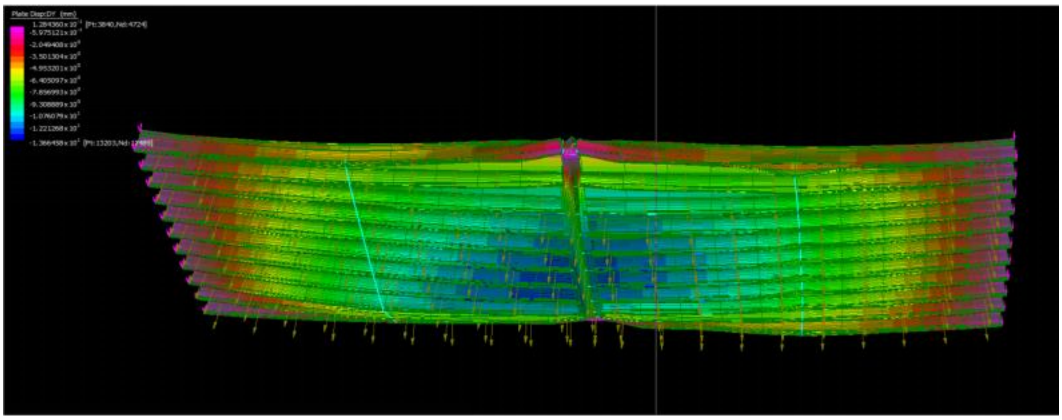

Figure 43.Colour chart for Beams displacement(Case3)

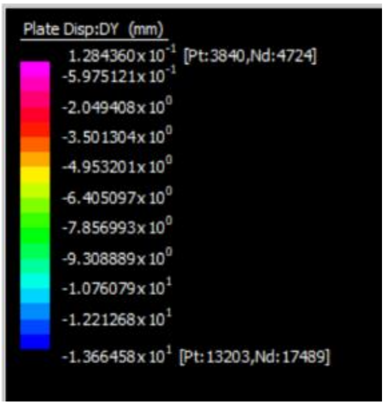

Figure 44. Value of Beams displacement (Case3)

4.1.2 Discussion

Experimental tests show that case1 has the minor static displacement and case3 has the most significant static displacement. Furthermore, only case3 was greater than the Australian Standard L/480. Indicating that case 1 was the most stable and case3 the least stable. Analysis of the results shows that the static displacements in case1 are smaller than in the other two cases because the engineered structure in case1 is more complete and efficient, with multiple triangles in its joist structure. Therefore it is more effective and efficient in resisting bending. In contrast, the static displacement of case2 is approximately 3mm more extraordinary than case1 under ideal conditions, but case2 is a more straightforward structure. It can be an alternative where static displacement is not required.

Also, in the actual case, the web and chord of case1 are bolted together; when simulated using the software, a rigid connection is used, resulting in a smaller static displacement in the simulated case1 than in the actual case. Therefore, the difference between the static displacements of case1 and case3 in the actual case will be reduced, and it may even be the case that the static displacement of case2 will be smaller than the static displacement of case1.

4.2 Natural frequency

4.2.1 Results

The solution parameters and eigenvalue settings for the Strand7 software's intrinsic frequency solver are shown in Figure 45. The software calculation and analysis process is detailed in Appendix B.

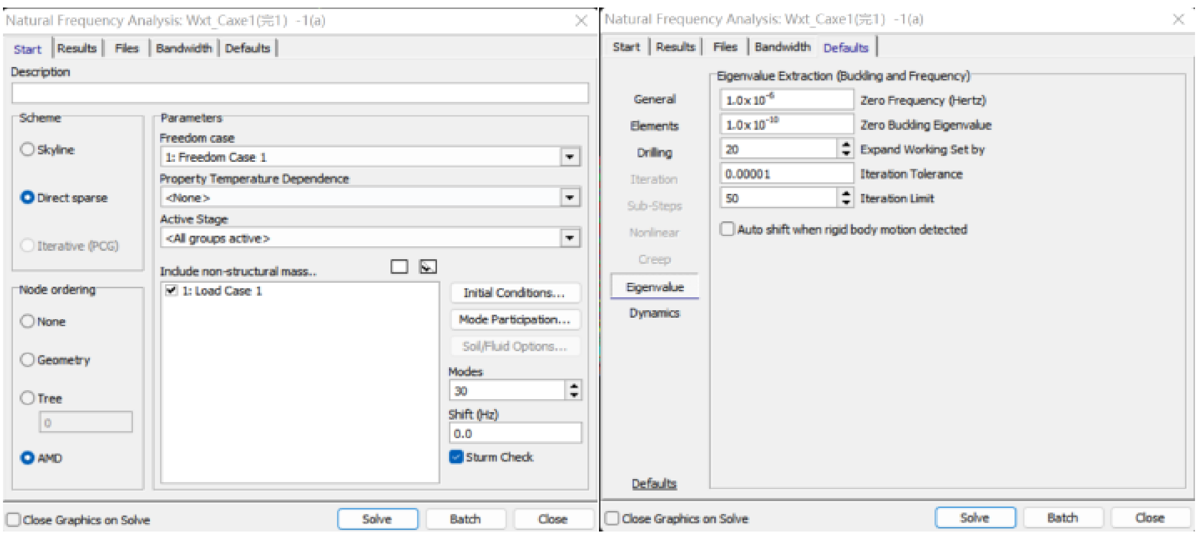

Figure 45. Eigenvalue settings for natural frequency solving

Case1

The natural frequencies of the floor were found to be in the range of 7.1784Hz-15.26Hz. For the 30 mod frequencies solved, mods with natural frequencies of 7.63039Hz, 8.97635Hz, 12.7273Hz, and 14.9864Hz were selected for display in Figure 46.

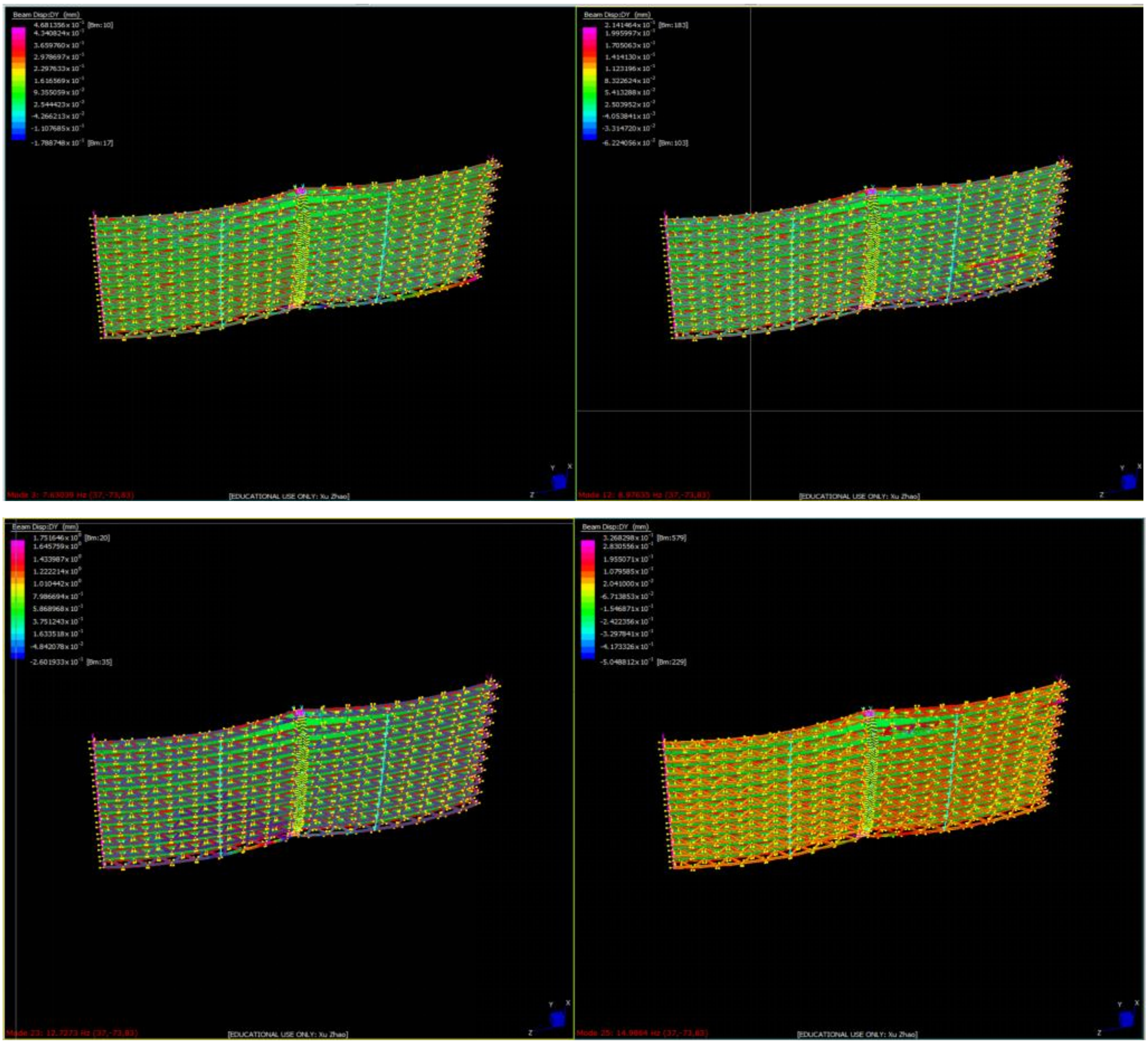

Figure 46. Presentation of four natural frequencies(Case1)

The natural frequencies of case1 are partly greater than 10Hz and partly less than 10Hz, which indicates that the natural frequencies of the floor in case1 are likely to be within the sensitive frequencies of 4-8Hz that humans are sensitive to causing discomfort to the occupants.

Case2

The intrinsic frequency range of case2 is 20.1164 ~ 36.4089 Hz. Modes with natural frequencies of 20.1153 Hz, 27.038 Hz, 27.7884 Hz, and 36.1966 Hz were displayed in Figure47.

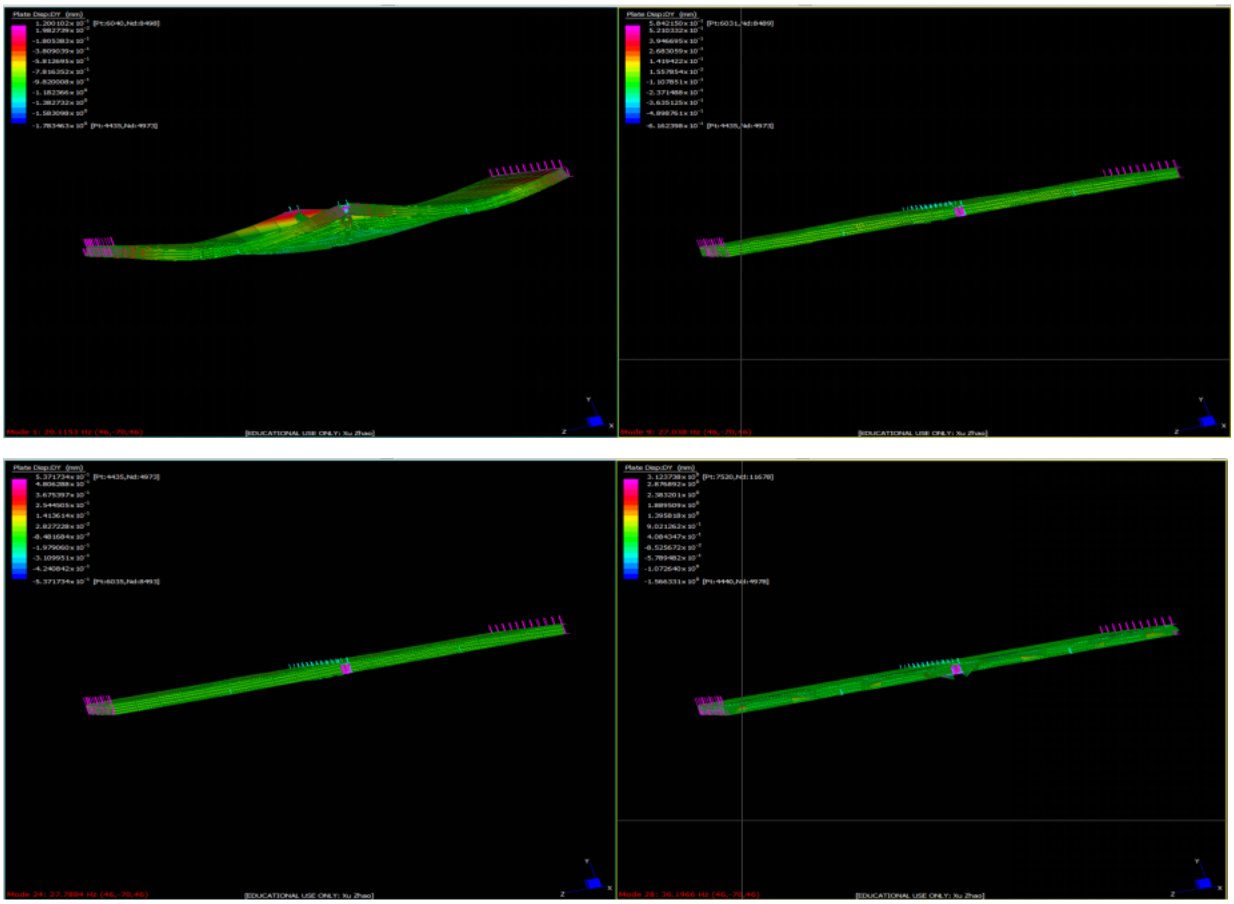

Figure 47. Presentation of four natural frequencies(Case2)

Case2 has a sizeable natural frequency range, all greater than 10Hz, which is far from humans' 4-8Hz sensitive frequency range. Too many boundary constraints may cause this, but these boundary constraints are consistent with reality.

Case3

The range of natural frequencies for the case3 is 10.3313-29.4908 Hz. Figure 48 shows the modes with natural frequencies of 10.3313 Hz, 23.5158 Hz, 25.2076 Hz, and 28.1909. The natural frequency range for case3 is just outside the human-sensitive frequency of 4- 8hz.

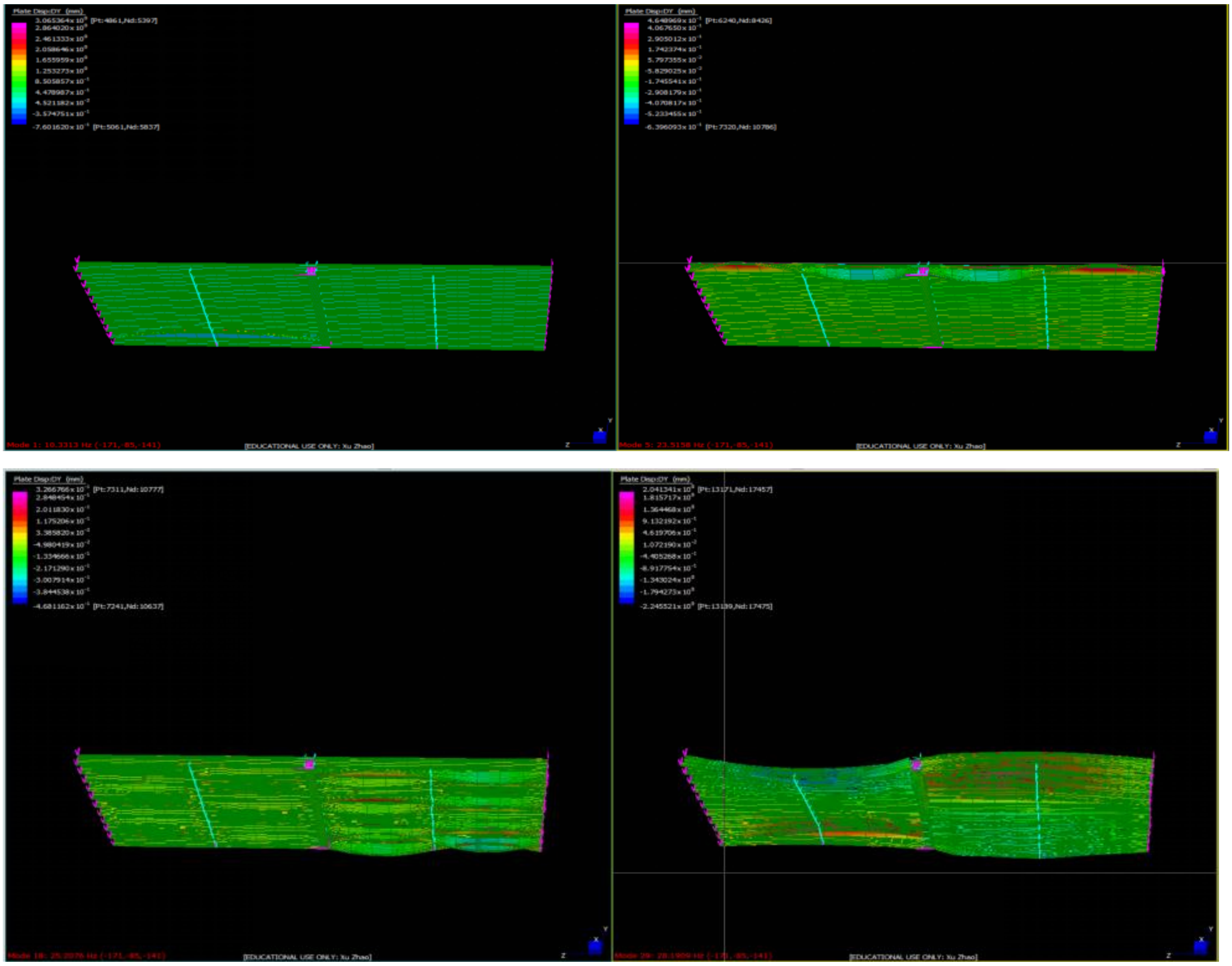

Figure 48. Presentation of four natural frequencies(Case3)

4.2.2 Discussion

Case 1 is modelled by the 'line element,' case 2 and case 3 are modelled by the 'plate element,' and the natural frequencies are dynamic parameters. In order to make the discussion of intrinsic frequencies meaningful, this section only compares and discusses the differences between case2 and case3 for the 'plate cell' modelling. The first peak of the natural frequency is also referred to as the fundamental frequency.

The analysis of natural frequencies and reference vibration criteria revealed that the most significant natural frequencies were found in cases 2 and 3, exceeding 10 Hz. Zhang and Xu (2020) also concluded that the fundamental frequencies of light steel floor slabs are typically greater than 10 Hz. This reflects that case 2 and case 3 are far from the sensitive frequency range of 4-8 Hz for humans, which would ensure that occupants in both cases would have a weaker perception of the floor, especially in case 2. This may be because case 2 has a greater bending stiffness than case 3, resulting in case 2 having a better bending resistance than case 3.

4.3 Results and analysis of harmonic response

4.3.1 Results

The analysis of the harmonic response is based on the results of the natural frequency analysis. The solver for the harmonic response is shown in Figure 49. Damping ratios are all set to 0.01. After the harmonic response has been solved using Strand7, the response factor, peak acceleration, and peak displacement are also calculated from the data. Following the formulae, the parameters are calculated and plotted for each case using Excel. In addition, the following equation is taken from a paper by Strand7(n.d.)

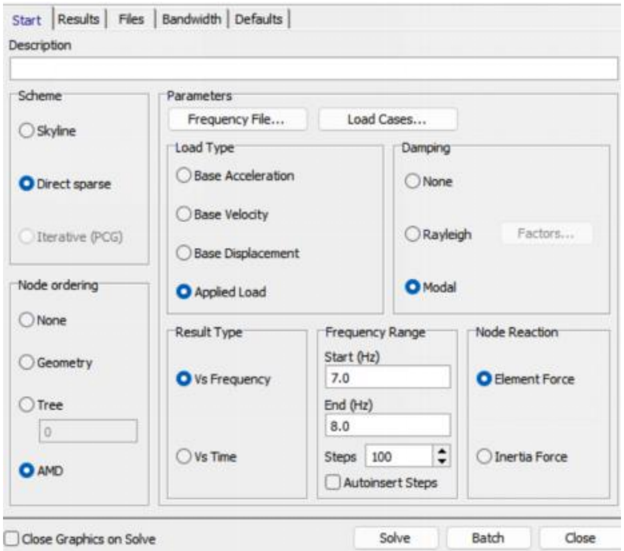

Figure 49. The solver for the harmonic response

Response Factor

The response factor is obtained by first calculating the amplitude baseline response factor based on the ratio of the peak value of the sine curve to the RMS of $\sqrt{2}$. The amplitude baseline response factor needs to be calculated according to the following equation.

$$R_{\text{base}} = \begin{cases} \sqrt{2}\dfrac{1}{100\sqrt{f}}, & f < 4Hz \\ \sqrt{2}\dfrac{1}{200}, & 4Hz \le f \le 8Hz \\ \sqrt{2}\dfrac{1}{200}\dfrac{f}{8}, & 8Hz < f \end{cases} \qquad (3)$$

Therefore, the response factor equation is as follows：

$$R = \frac{a_{vertical}}{a_{R=1}} \tag{4}$$

$a_{vertical}$ is the RMS acceleration obtained from the test; and

$a_{R=1}=R_{base}$.

In addition, the graph requires the calculation of the total response factor using the following equation:

$$R_{total} = \sqrt{R_1^2 + R_2^2 + R_3^2 + R_4^2} \tag{5}$$

Peak acceleration

In addition to the peak acceleration calculated by the solver(e.g., Figure 50), the graph needs to include Linear Acceleration Sum and SRSS.

Figure 50. Accelerated simulator

The acceleration formula used is as follows:

$$\text{Linear Acceleration Sum} = \sum_{Harmonics} A_{h,Peak} \tag{6}$$

$$\text{Total RMS Acceleration} = \sqrt{\sum_{Harmonics} A_{h,RMS}^{\;2}} \tag{7}$$

$$A_{h,RMS} = \frac{A_{h,Peak}}{\sqrt{2}} \tag{8}$$

$A_{h,Peak}$ is the peak acceleration of individual harmonics.

Peak Displacement

The primary use of the Strand7 software is the "Graphs" in the "Results" section (e.g., Figure 51).

Figure 51. Displacement simulator

Parameters are set according to the frequencies generated by human walking, as shown in Table 8. The fourth harmonic response was simulated for each of the three cases.

Harmonic	Start(Hz)	End(Hz)
First	1	2.8
Second	2	5.6
Third	3	8.4
Fourth	4	11.2

Table 8. Four sets of parameter settings for harmonic response

Case1

See Appendix C for data details. The curves for the individual harmonic response parameters are shown in Figure 52, Figure 53, and Figure 54.

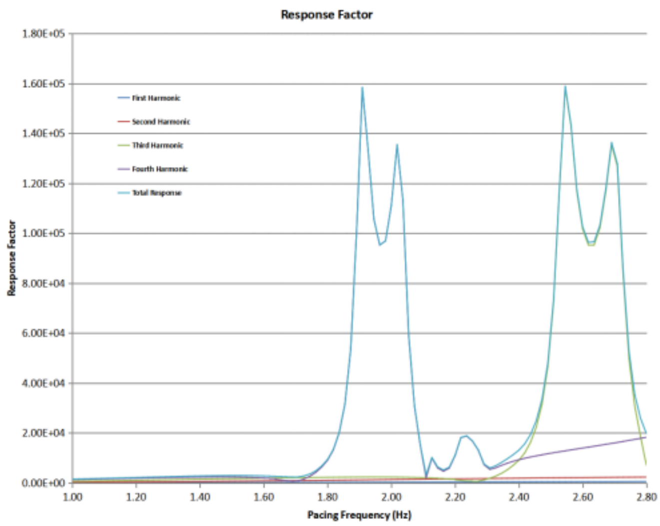

Figure 52. Response Factor(Case1)

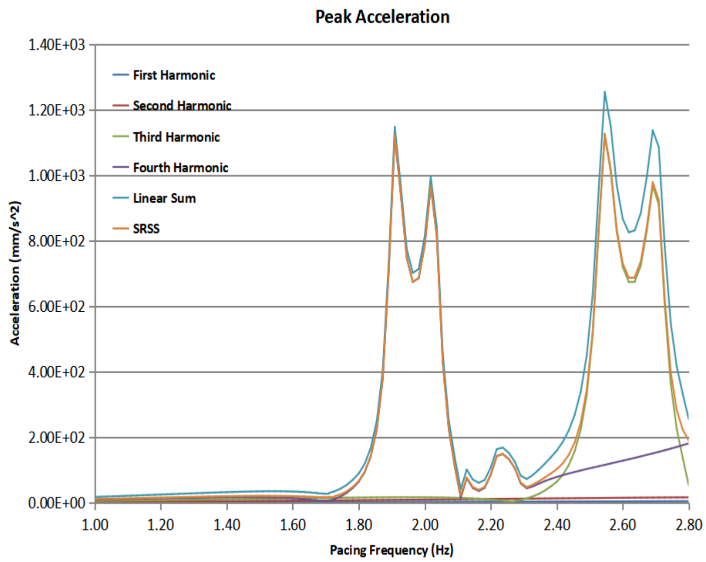

Figure 53. Peak Acceleration(Case1)

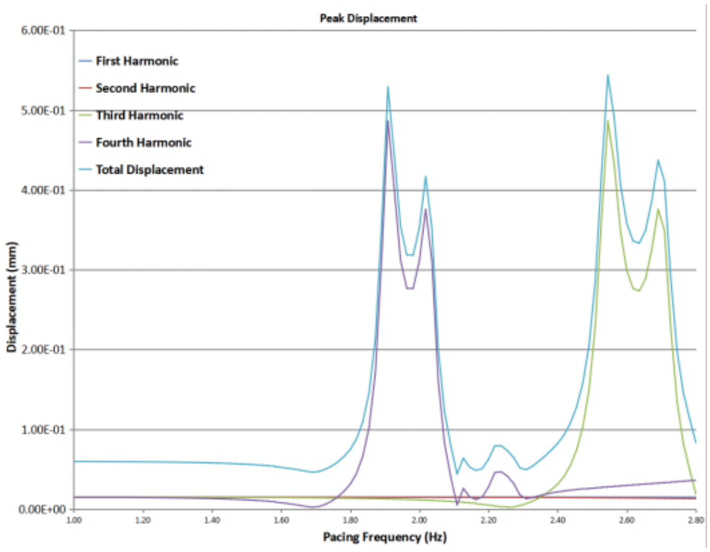

Figure 54. Peak Displacement(Case1)

Using the curves, it can be seen that the shapes of the curves for the response factor, peak acceleration, and peak displacement are similar and that the curve for the case1 has multiple peaks. For the execution of the fourth harmonic response, the peaks of the curve occur at the fourth harmonic and third harmonic, corresponding to a frequency of 7.64Hz, respectively. The maximum value of the response factor is $1.58*10^5$, and the peak acceleration and peak displacement at this frequency are also the largest, at $1.12*10^3 mm/s^2$ and 0.486mm. This indicates that a human walking frequency of 7.64Hz tends to cause a more significant response of the floor.

Case2

The data results are presented in Appendix C, and the curves are plotted in Figure55, Figure56, and Figure57.

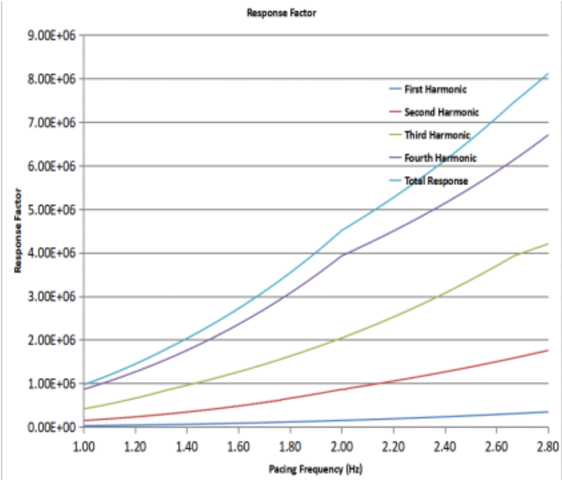

Figure 55. Response Factor(Case2)

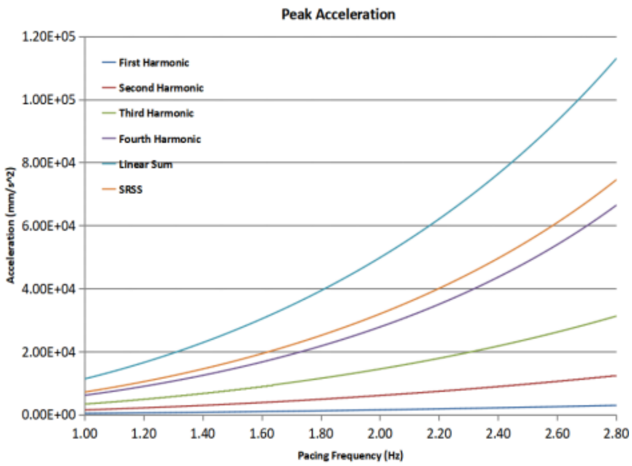

Figure 56. Peak Acceleration(Case2)

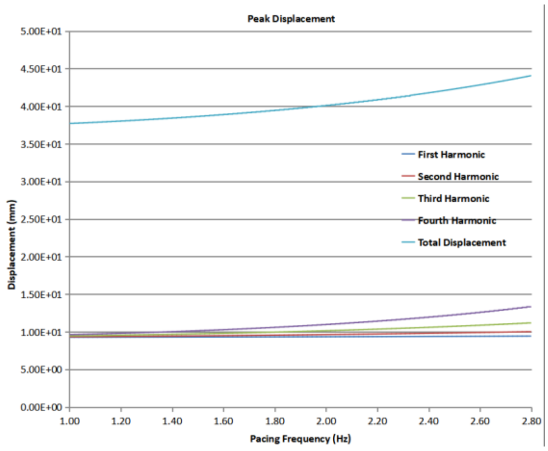

Figure 57. Peak Displacement(Case2)

The natural frequency bias of the case2 is relevant, resulting in no peak in the execution of the harmonic response between 1 and 11.2 Hz. However, the individual curves are incremental and increase with increasing frequency. Thus the curve corresponding to the Fourth harmonic has the most significant value. At 11.2 Hz, the individual parameters reach their maximum values. This frequency corresponds to a response factor of $6.7*10^6$, a peak acceleration of $6.64*10^4 mm/s^2$, a peak displacement, and 13.4mm. This indicates that the floor response of case2 increases with the increasing frequency of human walking.

Case3

The data results are presented in Appendix C, and the curves are plotted in Figure58, Figure59, and Figure60.

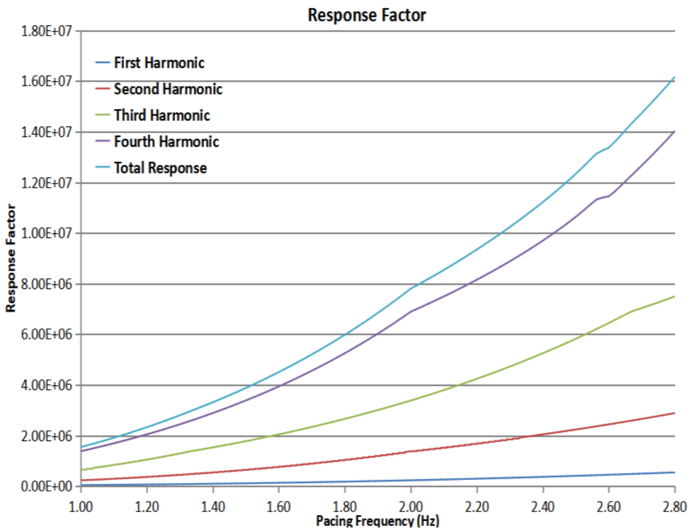

Figure 58. Response Factor(Case3)

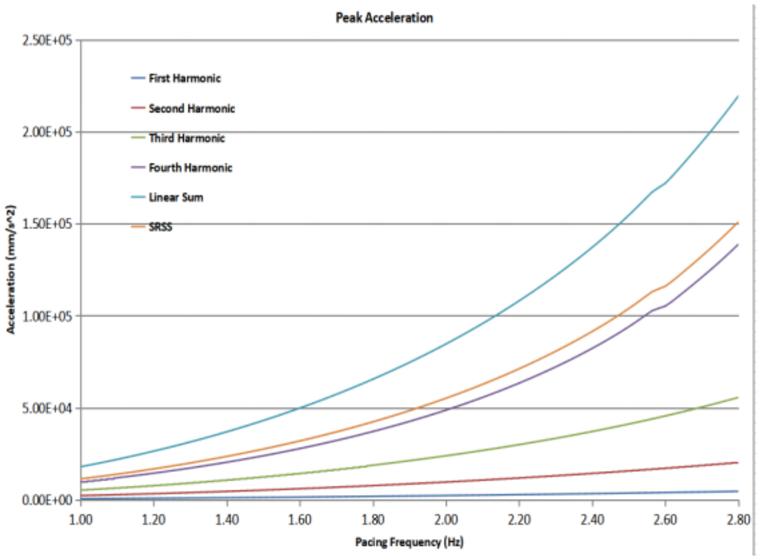

Figure 59. Peak Acceleration(Case3)

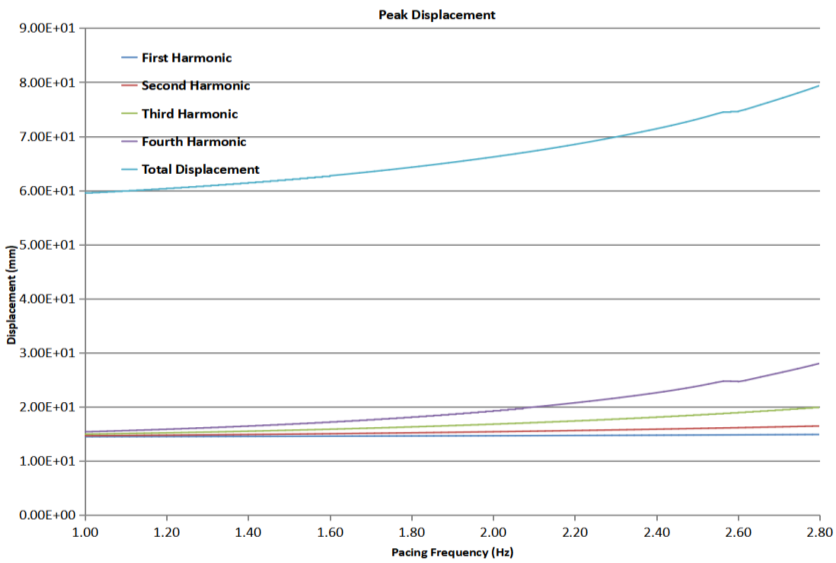

Figure 60. Peak Displacement(Case3)

Again due to the significant natural frequency of the case3, there is no peak in the execution of the harmonic response between 1 and 11.2 Hz. The individual curves are increasing. Therefore the curve corresponding to the Fourth harmonic has the most significant value. At 11.2 Hz, the individual parameters reach their maximum values. This frequency corresponds to a response factor of $1.4*10^7$, a peak acceleration of $1.39*10^5 mm/s^2$, and a peak displacement of 28mm.

4.3.2 Discussion

Similarly, the harmonic response is a dynamic parameter. Since case1 is modelled as a 'line element,' the parameters of the harmonic response of case1 are smaller. As the natural frequency (fundamental frequency) of both case2 and case3 is high, the frequency of human walking does not resonate with the floor, so their harmonic responses are similar. This is in line with Zhang and Xu's (2020) observation that "walking leads to a larger response when the fundamental frequency of the floor is close to a multiple of the human absorption frequency." In addition, it can be found that the higher the peak acceleration of the case3, the higher its peak displacement. It is also found that the exiles in the harmonic response of case2 and case3 are approximately twice as prominent as their static displacements. This suggests that the harmonic response is a more conservative result, a safer form. Moreover, the engineer refers more to the displacement parameter.

4.4 Elemental counts

4.4.1 Results

The data of different numbers of elements are shown in Table 9, and the curve of beam displacement with the number of elements is drawn (e.g., Figure 61). As can be seen from the curve, with the increase in the number of elements, the displacement trend gradually tends to be gentle, and finally, the numerical convergence to the correct result. Therefore, the more elements in the simulation, the more accurate the simulation results.

Number of elements	4	8	16	64
Displacement（mm）	9.246179	10.47088	11.05511	11.39527
Simulation time	6.219 Seconds (0:00:06)	16.469 Seconds (0:00:16)	41.812 Seconds (0:00:42)	265.781 Seconds (0:04:26)

Table 9. Data tables with different number of elements

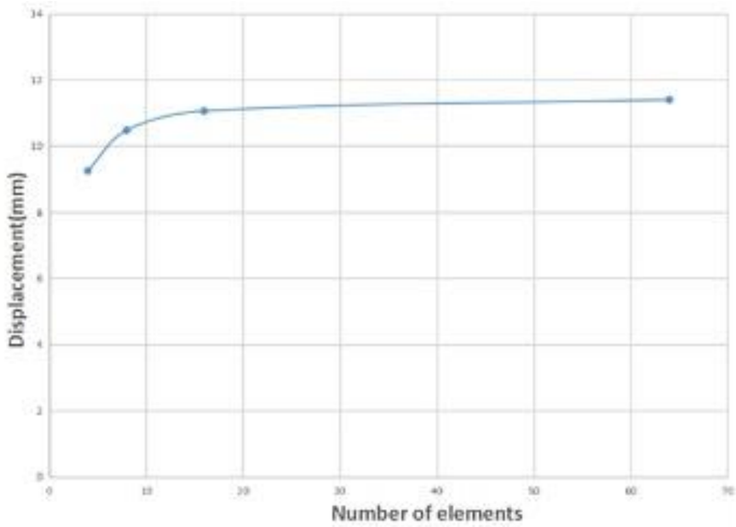

Figure 61. Displacement VS Number of elements

4.4.2 Discussion

The higher the number of elements found in the simulation, the higher the accuracy of the simulation results, but also the longer the simulation time; moreover, when the number of cells reaches a specific number, increasing the number of cells has less and less impact on the accuracy of the simulation results. Therefore, when selecting the number of elements, it is essential to consider both the accuracy and the simulation time.

5 CONCLUSIONS

In this project, the vibrations of CFS floors of 3 joist types were simulated and investigated using strand7 software. Based on the floor models developed, floor vibration parameters for static displacement, natural floor, and harmonic response were simulated and tested for the floor vibration analysis for the 3 cases. Some of the specifics of this study are summarized as follows：

- The type of joist affects floor vibrations, but the static displacements of the conventional joist type and the "C" type are not very different, and both comply with the L/480 standard. In addition, the more effective supports the engineered structure has, the less static displacement it will have.
- The magnitude of the natural frequency depends to a large extent on the flexural stiffness of the case structure. The bending stiffness of the "C" joist is significantly greater than that of the "dumbbell" type, so the "C" joist floor has a better bending capacity. The natural frequency range of the "C" joist and the "dumbbell" joist is far from the sensitive perceptual frequency region of 4-8Hz. This is very beneficial for reducing the occupants' perception of floor vibrations.
- The main factor influencing the results of the harmonic response is the relationship between the intrinsic frequency and the travel frequency. When there is a multiplicative relationship between the frequency at which the person walks and the fundamental frequency of the floor (the first peek of the natural frequency), resonance occurs, giving a peak in the harmonic response.

Finally, this project provides measurement data on floor vibrations of different joist types to help engineers determine the conditions and effects of floor vibrations in the three cases and ultimately design a more stable CFS floor.

6 REFERENCES

Allen, D.E., Onysko, D.M. and Murray, T.M. (1999). *Design Guide 1: Minimizing Floor Vibrations*, Applied Technology Council, USA.

CWC (1996). *Development of Designing Procedures for VibrationControlled Spans Using Engineered Wood Members*, Final report prepared for Canadian Construction Material Center and the Industry Partnership Consortium, Canadian Wood Council Ottawa.

Davis, B. W., Parnell, R. & Xu, L. (2008, August14-15). *Vibration performance of lightweight floor systems supported by cold-formed steel joists*[Conference proceedings]. 19th International Specialty Conference on Cold-Formed Steel Structures, Missouri, USA. https://scholarsmine.mst.edu/isccss/19iccfss/19iccfss-session6/1/

Dhanavade, P. V., Gawade, S. N., Mundhe, S. P., Lohar, R. R., Gaikwad, S. A., Petkar, A. T., & Kadam, R. R. (2021). Review Paper on Study and Analysis of Cold Formed Steel. *International Research Journal of Engineering and Technology (IRJET), 8*(5), 994-996.

Grether, W. F. (1971). Vibration and Human Performance. *Human Factors, 13*(3), 203－216. https://doi.org/10.1177/001872087101300301

Hancock, G.J.(2003). Cold-formed steel structures. *Journal of Constructional Steel Research, 59* (2003), 473－487.

Hagberg, K., Persson, T., & Hook, M. (2009, August). *Design of light weight constructions-risks and opportunities*[Conference Proceedings]. INTER-NOISE and NOISE-CONTROL Congress , Ottawa,Canada.

ISO.(1989). *Evaluation of human exposure to whole-body vibration–Part 2: Human Exposure to continuous and shock-induced vibrations in buildings (1 to 80 Hz)*(ISO 2631–2).

ISO. (1997). *Mechanical Vibration and Shock - Evaluation of Human Exposure to Whole-Body Vibration*(ISO 2631-1).

Johnson, J. (1994). Vibration acceptability of floor under impact vibration. *Department of Civil Engineering, Virginia Polytechnic Institute and State University, Blacksburg, Virginia, USA.*

Kraus, C. A., and Murray, T. M. (1997). *Floor vibration design criterion for cold-formed C-Shaped supported residential floor systems*[Doctoral dissertation, Virginia Tech]. Virginia Tech.http://hdl.handle.net/10919/36612

Lenzen, K.H. (1966). Vibration of steel joist-concrete slab floors. *Engineering Journal, American Institute of Steel Construction(AISC),* 3(1966), 133–136.

Laine, M., & Tuomala, M. (1999). Testing and design of gravity-loaded steel purlins restrained by sheeting. *Journal of Constructional Steel Research, 49*(2), 129-138. https://doi.org/10.1016/S0143-974X(98)00212-0

Lee, J., Kim, S., & Seon Park, H. (2006). Optimum design of cold-formed steel columns by using micro genetic algorithms. *Thin-Walled Structures, 44*(9), 952-960. https://doi.org/10.1016/j.tws.2006.08.021

Lakkavalli, B. S., & Liu, Y. (2006). Experimental study of composite cold-formed steel C-section floor joists. *Journal of Constructional Steel Research, 62*(10), 995-1006. https://doi.org/10.1016/j.jcsr.2006.02.003

Li, Q., Fan, J., Nie, J., Li, Q., & Chen, Y. (2010). Crowd-induced random vibration of footbridge and vibration control using multiple tuned mass dampers. *Journal of Sound and Vibration*, *329*(19), 4068-4092. https://doi.org/10.1016/j.jsv.2010.04.013

Reiher, H., & Meister, F. J. (1931). *The Effect of Vibration on People, Vol. 2, No. II, P381. Translation: Report No*. FTS-616-RE, Headquarters Air Material Command, Wright Field, Ohio.

Shahabpoor, E., Pavic, A., & Racic, V. (2017). Structural vibration serviceability: New design framework featuring human-structure interaction. *Engineering Structures*, *136*, 295-311. https://doi.org/10.1016/j.engstruct.2017.01.030

Ohmart, R. D. (1968). *an approximate method for the response of stiffened plates to aperiodic excitation*. University of Kansas.

Ohlsson, S. V. (1986). *Stiffness criteria and dynamic serviceability of light-weight steel floors*[Proceedings of IABSE]. In Colloquium: Thin-Walled Metal Structures in Buildings, Stockholm, Sweden.

Ohlsson, S. (1988). *Springiness and human-induced floor vibrations: a design guide*[Document D12]. Swedish Council for Building Research, Stockholm, Sweden.

Onysko DM, Hu LJ, Jones ED, et al. (2000, 31 July–3 August). *Serviceability design of residential wood framed floors in Canada*[Conference Proceedings]. In the world conference on timber engineering, Whistler, BC, Canada.

Parnell, R., Davis, B. W., & Xu, L. (2010). Vibration performance of lightweight cold-formed steel floors. *Journal of Structural Engineering (New York, N.Y.), 136*(6), 645-653. https://doi.org/10.1061/(ASCE)ST.1943-541X.0000168

Pedersen, L. (2011). *Interaction between structures and their occupants*[Conference Proceedings]. In Modal Analysis Topics, Springer, New York.

Qi, Y. S., Zhao, F. H. & He, Y. (2015). Teaching analysis of steel structure engineering catastrophic accident case. *Journal of Changzhou Institute of Technology*, 28(4), 88-92.

Rencis, J. J., Jolley, W. O., & Grandin, H. T. (2007). Teaching fundamentals of finite-element theory and applications using sophomore-level strength-of-materials theory. *International Journal of Mechanical Engineering Education, 35*(2), 114-137. https://doi.org/10.7227/IJMEE.35.2.3

Strand7. (1996). *Developers of Strand7*. Retrieved May 10, 2022 from https://www.strand7.com/html/Strand7PtyLtd.htm

Strand7. (n.d.). *ST7-1.40.60.1 Footfall Analysis of Low Frequency Vibration Sensitive*

Structures. Strand7 Webnotes. Retrieved May 18, 2022 from https://www.strand7.com/webnotes/request/?w=ST7-1.40.60.1&origin=direct

Shaikh, F. U. A. (2012). Role of commercial software in teaching finite element analysis at undergraduate level: A case study. *Engineering Education (Loughborough), 7*(2), 2-6. https://doi.org/10.11120/ened.2012.07020002

Tahir, M. M., Siang, T. C., & Ngian, S. P. (2006,September). *Typical tests on cold-formed steel structures*[Conference Proceedings]. Proceedings of the Asia-Pacific Structural Engineering , Kuala Lumper, Malaysia.

Wyatt, T. A. (1989). Design guide on the vibration of floors. SCI Standard P076. *Steel Construction Institute, Ascot, Berkshire, UK*.

Williams, M. S. & Blakeborough, A., (2003). Measurement of floor vibrations using a heel drop test. *Proceedings of the Institution of Civil Engineers-Structures and Buildings*, *156*(4), 367-371. https://doi.org/10.1680/stbu.2003.156.4.367

Xu, L., & Tangorra, F. M. (2007). Experimental investigation of lightweight residential floors supported by cold-formed steel C-shape joists. *Journal of Constructional Steel Research*, *63*(3), 422-435. https://doi.org/10.1016/j.jcsr.2006.05.010

Xu, L. (2011). Floor vibration in lightweight cold-formed steel framing. *Advances in Structural Engineering*, *14*(4), 659-672. https://doi.org/10.1260/1369-4332.14.4.659

Young, P. (2001, October 4). *Improved floor vibration prediction methodologies* [Conference Proceedings]. In: ARUP vibration seminar on engineering for structural vibration: current developments in research and practice, London, England.

Zhang, S., Xu, L., & Qin, J. (2017). Vibration of lightweight steel floor systems with occupants: Modelling, formulation and dynamic properties. *Engineering Structures*, *147*, 652-665. https://doi.org/10.1016/j.engstruct.2017.06.008

Zhang, S., & Xu, L. (2020). Human-induced vibration of cold-formed steel floor systems: Parametric studies. *Advances in Structural Engineering*, *23*(10), 2030-2043. https://doi.org/10.1177/1369433220904013

7 APPENDICES

7.1 APPENDIX A—Static displacement simulation process

Case1

```
TOTALS
 Nodes              : 2378
 Beams              :  770
 Plates             : 1990
 Bricks             :    0
 Links              :   64

 SOLVER UNITS
 Length             : mm
 Mass               : t
 Force              : N
 Stress             : MPa

 FREEDOM CASE           : "Freedom Case 1"

 LOAD CASES             : "Load Case 1"

 STORAGE SCHEME          : Sparse
 SORTING METHOD          : AMD
 SOLUTION TYPE           : Direct

 NUMBER OF EQUATIONS     : 13751
 MATRIX FILL-IN          : 77.4%
 [K] MATRIX SIZE         : 12.0 MB
 OPTIMUM RAM NEEDED      : 2.6 MB
 FREE SCRATCH SPACE      : 78.4 GB

 SUMMATION OF APPLIED LOADS (Name: "Load Case 1")
          FX          FY          FZ          MX          MY          MZ
 Beams   -1.45269E-15 -4.09291E+03 4.12821E-15 2.31811E+00 -9.48098E-14 -6.53381E+02
 Plates  -3.11130E+02 -9.28232E+04 -6.62586E-01 -1.28445E-01 5.38605E-02 -9.72018E+01
 Total   -3.11130E+02 -9.69161E+04 -6.62586E-01 2.18967E+00 5.38605E-02 -7.50583E+02
 Vector  -3.09562E+02 -9.53456E+04 -6.62586E-01 8.96138E+01 5.38605E-02 5.69891E+05

 SUMMATION OF MOMENTS OF APPLIED LOADS ABOUT THE ORIGIN [Load Vector]
         MXo         MYo         MZo
      1.06004E+06 -7.05158E+05 -2.15295E+08

 Reducing 13751 Equations (Using 12.1 MB RAM)...

 MAXIMUM PIVOT           : 5.705346E+10 (Node 618 RZ)
 MINIMUM PIVOT           : 2.064255E+01 (Node 588 DX)

 Results for 1 Load Case...

 MAXIMUM DISPLACEMENT MAGNITUDES
  Case     DX          DY          DZ          RX          RY          RZ          Name
    1    6.67699E+00 5.14764E+00 1.66824E+00 4.47157E-02 3.40980E-02 1.91204E-01 "Load Case 1"

 TOTAL CPU TIME: 0.625 Seconds

*Solution completed on 07/06/2022 at 16:39:36
*Solution time: 1 Second

*SUMMARY OF MESSAGES
*Number of Notes    : 0
*Number of Warnings :0
*Number of Errors   : 0
```

Case2

```
 TOTALS
 Nodes                         : 11808
 Beams                         :     0
 Plates                        : 10850
 Bricks                        :     0
 Links                         :   152

 SOLVER UNITS
 Length                        : mm
 Mass                          : t
 Force                         : N
 Stress                        : MPa

 FREEDOM CASE                  : "Freedom Case 1"

 LOAD CASES                    : "Load Case 1"

 STORAGE SCHEME                : Sparse
 SORTING METHOD                : AMD
 SOLUTION TYPE                 : Direct

 NUMBER OF EQUATIONS           : 69982
 MATRIX FILL-IN                : 72.5%
 [K] MATRIX SIZE               : 50.7 MB
 OPTIMUM RAM NEEDED            : 4.0 MB
 FREE SCRATCH SPACE            : 80.2 GB

*NOTE[  4]:Link forces are added to node reaction calculations.

 SUMMATION OF APPLIED LOADS (Name: "Load Case 1")
             FX           FY           FZ           MX           MY           MZ
 Plates  -1.14015E-31 -9.87526E+04  0.00000E+00  0.00000E+00  0.00000E+00  0.00000E+00
 Total   -1.14015E-31 -9.87526E+04  0.00000E+00  0.00000E+00  0.00000E+00  0.00000E+00
 Vector  -1.01689E-31 -9.41333E+04  0.00000E+00 -1.23102E-12  2.95884E-29 -1.30193E+05

 SUMMATION OF MOMENTS OF APPLIED LOADS ABOUT THE ORIGIN [Load Vector]
             MXo          MYo          MZo
         2.07093E+05  7.88861E-31 -2.11838E+08

 Reducing 69982 Equations (Using 50.7 MB RAM)...

 MAXIMUM PIVOT                 : 4.403550E+10 (Node 691 RZ)
 MINIMUM PIVOT                 : 3.220259E+01 (Node 9628 DX)

 Results for 1 Load Case...

 MAXIMUM DISPLACEMENT MAGNITUDES
   Case        DX           DY           DZ           RX           RY           RZ          Name
     1     1.06683E+00  8.39519E+00  1.22086E+00  5.99404E-02  3.39081E-02  1.55018E-02  "Load Case 1"

 DIRECT SUMMATION OF NODE REACTION FORCES
   Case        FX           FY           FZ           MX           MY           MZ          Name
     1     6.77305E-07  9.87526E+04  1.26219E-08 -7.54881E-07  1.96572E-08 -1.28467E-02  "Load Case 1"

 TOTAL CPU TIME                : 1.453 Seconds ( 0:00:01)

*Solution completed on 08/06/2022 at 14:28:16
*Solution time: 2 Seconds

*SUMMARY OF MESSAGES
*Number of Notes    : 1
*Number of Warnings : 0
*Number of Errors   : 0
```

Case3

```
TOTALS
Nodes              : 17616
Beams              :    0
Plates             : 16130
Bricks             :    0
Links              :   64

SOLVER UNITS
Length             : mm
Mass               : t
Force              : N
Stress             : MPa

FREEDOM CASE             : "Freedom Case 1"

LOAD CASES               : "Load Case 1"

STORAGE SCHEME           : Sparse
SORTING METHOD           : AMD
SOLUTION TYPE            : Direct

NUMBER OF EQUATIONS      : 103758
MATRIX FILL-IN           : 71.7%
[K] MATRIX SIZE          : 72.7 MB
OPTIMUM RAM NEEDED       : 5.1 MB
FREE SCRATCH SPACE       : 78.4 GB

*NOTE[  4]:Link forces are added to node reaction calculations.

SUMMATION OF APPLIED LOADS (Name: "Load Case 1")
            FX           FY           FZ           MX           MY           MZ
Plates  -9.55261E-32 -1.09034E+05  0.00000E+00  0.00000E+00  0.00000E+00  0.00000E+00
Total   -9.55261E-32 -1.09034E+05  0.00000E+00  0.00000E+00  0.00000E+00  0.00000E+00
Vector   2.43084E-18 -1.03871E+05  0.00000E+00 -2.70325E+01  4.93038E-32 -1.21102E+04

SUMMATION OF MOMENTS OF APPLIED LOADS ABOUT THE ORIGIN [Load Vector]
        MXo          MYo          MZo
    2.28516E+05  5.34785E-18 -2.36184E+08

Reducing 103758 Equations (Using 72.8 MB RAM)...

MAXIMUM PIVOT            : 9.984418E+09 (Node 5848 RZ)
MINIMUM PIVOT            : 1.407798E+02 (Node 4082 DX)

Results for 1 Load Case...

MAXIMUM DISPLACEMENT MAGNITUDES
 Case      DX           DY           DZ           RX           RY           RZ        Name
   1   8.39598E+00  1.36646E+01  2.19028E+00  1.18840E-01  7.47333E-02  1.29419E-01  "Load Case 1"

DIRECT SUMMATION OF NODE REACTION FORCES
 Case      FX           FY           FZ           MX           MY           MZ        Name
   1  -6.30413E-06  1.09034E+05  2.09090E-07 -3.23966E-07 -2.84522E-07  2.76153E-03  "Load Case 1"

TOTAL CPU TIME           : 2.016 Seconds ( 0:00:02)

*Solution completed on 07/06/2022 at 16:22:23
*Solution time: 2 Seconds

*SUMMARY OF MESSAGES
*Number of Notes    : 1
*Number of Warnings : 0
*Number of Errors   : 0
```

7.2 APPENDIX B—Natural frequency simulation process

Case1

```
FINAL FREQUENCY RESULTS
Mode        Eigenvalue          Frequency (rad/s)     Frequency (Hz)
  1       2.03429823E+03        4.51031953E+01        7.17839649E+00
  2       2.25304234E+03        4.74662232E+01        7.55448405E+00
  3       2.29854668E+03        4.79431610E+01        7.63039105E+00
  4       2.58931525E+03        5.08853147E+01        8.09864936E+00
  5       2.60018917E+03        5.09920500E+01        8.11563682E+00
  6       2.77946139E+03        5.27206164E+01        8.39074670E+00
  7       2.80204928E+03        5.29343866E+01        8.42476928E+00
  8       2.84552225E+03        5.33434368E+01        8.48987164E+00
  9       3.07181615E+03        5.54239673E+01        8.82099836E+00
 10       3.07837364E+03        5.54830933E+01        8.83040855E+00
 11       3.14538217E+03        5.60837068E+01        8.92599917E+00
 12       3.18097049E+03        5.64000930E+01        8.97615360E+00
 13       3.19102788E+03        5.64891838E+01        8.99053283E+00
 14       3.22170489E+03        5.67600642E+01        9.03364479E+00
 15       3.22217058E+03        5.67641664E+01        9.03429767E+00
 16       3.23011063E+03        5.68340622E+01        9.04542194E+00
 17       3.23175831E+03        5.68485559E+01        9.04772868E+00
 18       3.23472518E+03        5.68746444E+01        9.05188080E+00
 19       3.24409088E+03        5.69569213E+01        9.06497556E+00
 20       3.28007326E+03        5.72719238E+01        9.11510978E+00
 21       3.31083908E+03        5.75398912E+01        9.15775812E+00
 22       3.32098184E+03        5.76279606E+01        9.17177479E+00
 23       6.39492192E+03        7.99682557E+01        1.27273432E+01
 24       8.81967805E+03        9.39131410E+01        1.49467406E+01
 25       8.86656751E+03        9.41624528E+01        1.49864198E+01
 26       9.04670756E+03        9.51141817E+01        1.51378922E+01
 27       9.08512883E+03        9.53159422E+01        1.51700034E+01
 28       9.11876429E+03        9.54922211E+01        1.51980590E+01
 29       9.13114980E+03        9.55570500E+01        1.52083769E+01
 30       9.19326241E+03        9.58815019E+01        1.52600150E+01

COUNTING MODES IN RANGE     :   7.17031487E+00 to  1.52680966E+01

Reducing 13751 Equations (Using 12.1 MB RAM)...

Reducing 13751 Equations (Using 12.1 MB RAM)...

STURM CHECK RESULTS
There is no natural frequency below 7.170E+00 Hz.
There are 30 frequencies below 1.527E+01 Hz.
All eigenvalues are found.

TOTAL CPU TIME                  : 8.703 Seconds ( 0:00:09)

*Solution completed on 08/06/2022 at 14:31:51
*Solution time: 9 Seconds

*SUMMARY OF MESSAGES
*Number of Notes    : 0
*Number of Warnings : 0
*Number of Errors   : 0
```

Case2

```
THE FIRST 30 EIGENVALUES HAVE CONVERGED

FINAL FREQUENCY RESULTS
Mode        Eigenvalue          Frequency (rad/s)     Frequency (Hz)
  1       1.59738898E+04        1.26387855E+02        2.01152518E+01
  2       1.60623371E+04        1.26737276E+02        2.01708639E+01
  3       2.84186776E+04        1.68578402E+02        2.68300860E+01
  4       2.85607082E+04        1.68999137E+02        2.68970480E+01
  5       2.86100343E+04        1.69145010E+02        2.69202644E+01
  6       2.86548016E+04        1.69277292E+02        2.69413178E+01
  7       2.87466621E+04        1.69548406E+02        2.69844670E+01
  8       2.87652883E+04        1.69603326E+02        2.69932078E+01
  9       2.88607636E+04        1.69884560E+02        2.70379674E+01
 10       2.89122554E+04        1.70036041E+02        2.70620765E+01
 11       2.89839166E+04        1.70246635E+02        2.70955935E+01
 12       2.90064680E+04        1.70312853E+02        2.71061325E+01
 13       2.91820571E+04        1.70827565E+02        2.71880514E+01
 14       2.91975731E+04        1.70872974E+02        2.71952784E+01
 15       2.93595505E+04        1.71346288E+02        2.72706087E+01
 16       2.93778461E+04        1.71399668E+02        2.72791044E+01
 17       2.96191220E+04        1.72102068E+02        2.73908949E+01
 18       2.96374332E+04        1.72155259E+02        2.73993605E+01
 19       2.99024456E+04        1.72923236E+02        2.75215878E+01
 20       2.99354784E+04        1.73018723E+02        2.75367850E+01
 21       3.02027106E+04        1.73789271E+02        2.76594215E+01
 22       3.02437672E+04        1.73907352E+02        2.76782148E+01
 23       3.04382789E+04        1.74465695E+02        2.77670778E+01
 24       3.04850440E+04        1.74599668E+02        2.77884002E+01
 25       3.23357962E+04        1.79821568E+02        2.86194914E+01
 26       3.91906825E+04        1.97966367E+02        3.15073259E+01
 27       4.41429467E+04        2.10102229E+02        3.34388083E+01
 28       5.17243120E+04        2.27429796E+02        3.61965762E+01
 29       5.17913772E+04        2.27577190E+02        3.62200347E+01
 30       5.22673081E+04        2.28620446E+02        3.63860740E+01

COUNTING MODES IN RANGE     :   2.00989810E+01 to  3.64023448E+01

Reducing 69982 Equations (Using 50.7 MB RAM)...

Reducing 69982 Equations (Using 50.7 MB RAM)...

STURM CHECK RESULTS
There is no natural frequency below 2.010E+01 Hz.
There are 30 frequencies below 3.640E+01 Hz.
All eigenvalues are found.

TOTAL CPU TIME                  : 30.859 Seconds ( 0:00:31)

*Solution completed on 08/06/2022 at 14:30:06
*Solution time: 31 Seconds

*SUMMARY OF MESSAGES
*Number of Notes    : 0
*Number of Warnings: 0
*Number of Errors   : 0
```

Case3

```
THE FIRST 30 EIGENVALUES HAVE CONVERGED

 FINAL FREQUENCY RESULTS
 Mode       Eigenvalue        Frequency (rad/s)     Frequency (Hz)
    1     4.21373888E+03      6.49133182E+01      1.03312755E+01
    2     1.05425659E+04      1.02676998E+02      1.63415517E+01
    3     1.76747592E+04      1.32946452E+02      2.11590850E+01
    4     1.91401547E+04      1.38347948E+02      2.20187598E+01
    5     2.18313516E+04      1.47754362E+02      2.35158371E+01
    6     2.22510329E+04      1.49167801E+02      2.37407929E+01
    7     2.48726848E+04      1.57710763E+02      2.51004475E+01
    8     2.49290497E+04      1.57889359E+02      2.51288720E+01
    9     2.49321357E+04      1.57899131E+02      2.51304273E+01
   10     2.49505429E+04      1.57957408E+02      2.51397023E+01
   11     2.49653440E+04      1.58004253E+02      2.51471579E+01
   12     2.49918972E+04      1.58088258E+02      2.51605277E+01
   13     2.50091285E+04      1.58142747E+02      2.51691999E+01
   14     2.50187192E+04      1.58173067E+02      2.51740255E+01
   15     2.50526134E+04      1.58280174E+02      2.51910720E+01
   16     2.50601550E+04      1.58303995E+02      2.51948634E+01
   17     2.50785473E+04      1.58362076E+02      2.52041073E+01
   18     2.50854578E+04      1.58383894E+02      2.52075796E+01
   19     2.50944374E+04      1.58412239E+02      2.52120908E+01
   20     2.50976971E+04      1.58422527E+02      2.52137283E+01
   21     2.51082539E+04      1.58455842E+02      2.52190305E+01
   22     2.51266067E+04      1.58513743E+02      2.52282457E+01
   23     2.51338311E+04      1.58536529E+02      2.52318723E+01
   24     2.51367383E+04      1.58545698E+02      2.52333315E+01
   25     2.51386811E+04      1.58551825E+02      2.52343066E+01
   26     2.53887717E+04      1.59338544E+02      2.53595169E+01
   27     2.80082117E+04      1.67356541E+02      2.66356207E+01
   28     2.97534878E+04      1.72491993E+02      2.74529534E+01
   29     3.13746567E+04      1.77128927E+02      2.81909443E+01
   30     3.43346674E+04      1.85296161E+02      2.94908000E+01

 COUNTING MODES IN RANGE     :   1.03121159E+01 to  2.95099595E+01

 Reducing 103758 Equations (Using 72.8 MB RAM)...

 Reducing 103758 Equations (Using 72.8 MB RAM)...

 STURM CHECK RESULTS
 There is no natural frequency below 1.031E+01 Hz.
 There are 30 frequencies below 2.951E+01 Hz.
 All eigenvalues are found.

 TOTAL CPU TIME              : 23.766 Seconds ( 0:00:24)

*Solution completed on 08/06/2022 at 22:39:19
*Solution time: 24 Seconds

*SUMMARY OF MESSAGES
*Number of Notes    : 0
*Number of Warnings : 0
*Number of Errors   : 0
```

7.3 APPENDIX C—Harmonic response simulation process

Case1

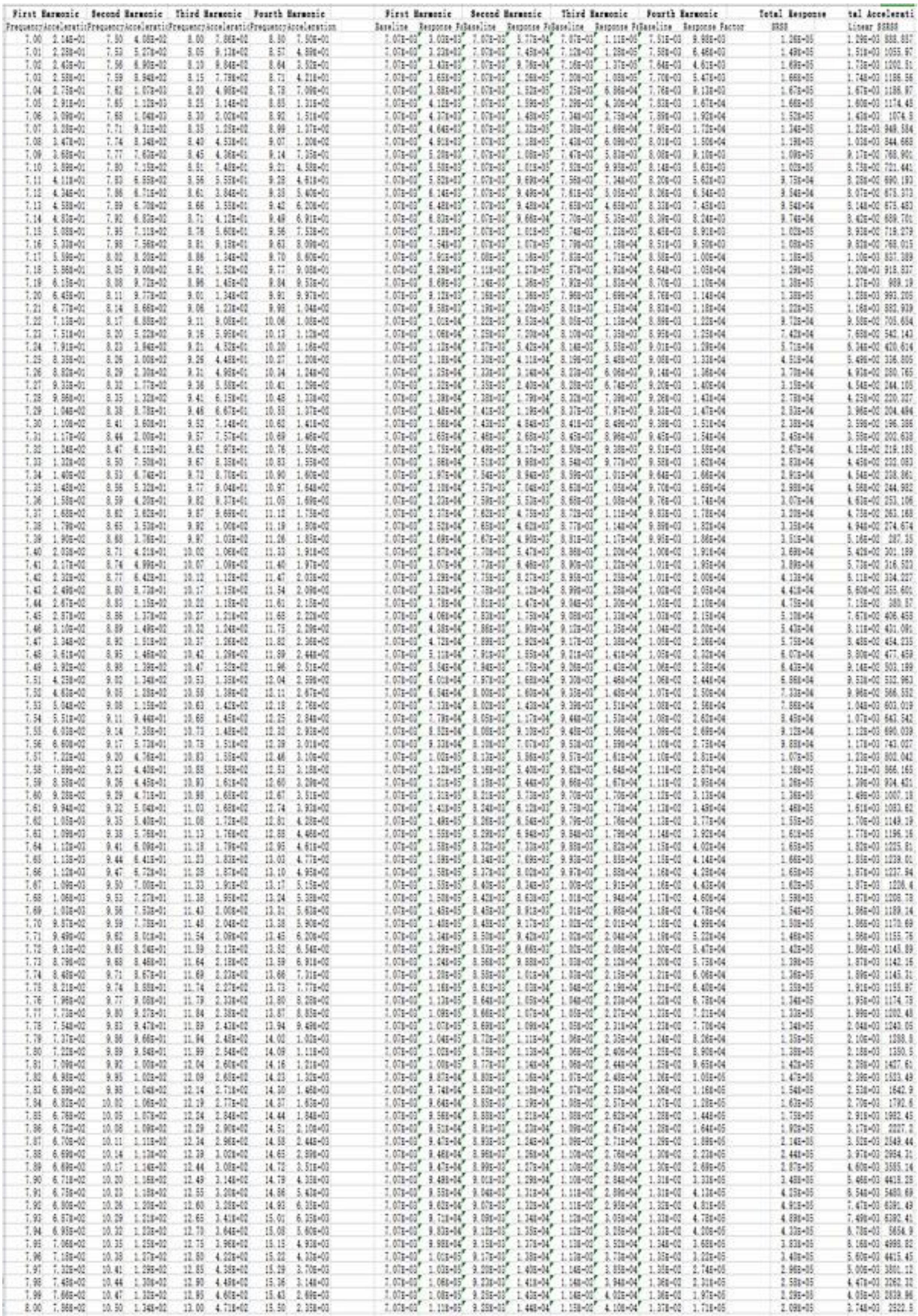

First Harmonic		Second Harmonic		Third Harmonic		Fourth Harmonic		First Harmonic		Second Harmonic		Third Harmonic		Fourth Harmonic		Total Response	tal Accelerati
Frequency	Acceleratio	Frequency	Acceleratio	Frequency	Acceleratio	Frequency	Acceleration	Baseline	Response F	Baseline	Response F	Baseline	Response F	Baseline	Response Factor	SRSS	Linear SSRSS

First Harmonic		Second Harmonic		Third Harmonic		Fourth Harmonic		Sum		TO PASTE							TO PASTE AGAIN		DROP TO PASTE
[illegible]	[illegible]	[illegible]	[illegible]	[illegible]	[illegible]	[illegible]	[illegible]	[illegible]	[illegible]	[illegible]	[illegible]	[illegible]	[illegible]	[illegible]	[illegible]	[illegible]	[illegible]	[illegible]	[illegible]

Case2

First Harmonic		Second Harmonic		Third Harmonic		Fourth Harmonic	
Frequency	Acceleration	Frequency	Acceleration	Frequency	Acceleration	Frequency	Acceleration
1.00	3.66E+02	2.00	1.43E+03	3.00	3.36E+03	4.00	6.09E+03
1.02	3.80E+02	2.04	1.53E+03	3.05	3.49E+03	4.07	6.32E+03
1.04	3.93E+02	2.07	1.59E+03	3.11	3.62E+03	4.15	6.56E+03
1.05	4.07E+02	2.11	1.64E+03	3.16	3.75E+03	4.22	6.80E+03
1.07	4.22E+02	2.15	1.70E+03	3.22	3.88E+03	4.29	7.05E+03
1.09	4.36E+02	2.18	1.76E+03	3.27	4.02E+03	4.36	7.30E+03
1.11	4.51E+02	2.22	1.82E+03	3.33	4.16E+03	4.44	7.56E+03
1.13	4.66E+02	2.25	1.88E+03	3.38	4.30E+03	4.51	7.82E+03
1.15	4.81E+02	2.29	1.94E+03	3.44	4.44E+03	4.58	8.09E+03
1.16	4.96E+02	2.33	2.01E+03	3.49	4.59E+03	4.65	8.36E+03
1.18	5.12E+02	2.36	2.07E+03	3.55	4.74E+03	4.73	8.64E+03
1.20	5.28E+02	2.40	2.13E+03	3.60	4.89E+03	4.80	8.92E+03
1.22	5.44E+02	2.44	2.20E+03	3.65	5.05E+03	4.87	9.21E+03
1.24	5.61E+02	2.47	2.27E+03	3.71	5.20E+03	4.95	9.51E+03
1.25	5.77E+02	2.51	2.34E+03	3.76	5.36E+03	5.02	9.81E+03
1.27	5.94E+02	2.55	2.41E+03	3.82	5.52E+03	5.09	1.01E+04
1.29	6.11E+02	2.58	2.48E+03	3.87	5.69E+03	5.16	1.04E+04
1.31	6.29E+02	2.62	2.55E+03	3.93	5.86E+03	5.24	1.07E+04
1.33	6.46E+02	2.65	2.62E+03	3.98	6.03E+03	5.31	1.11E+04
1.35	6.64E+02	2.69	2.69E+03	4.04	6.20E+03	5.38	1.14E+04
1.36	6.82E+02	2.73	2.77E+03	4.09	6.38E+03	5.45	1.17E+04
1.38	7.01E+02	2.76	2.84E+03	4.15	6.56E+03	5.53	1.21E+04
1.40	7.20E+02	2.80	2.92E+03	4.20	6.74E+03	5.60	1.24E+04
1.42	7.38E+02	2.84	3.00E+03	4.25	6.92E+03	5.67	1.28E+04
1.44	7.58E+02	2.87	3.08E+03	4.31	7.11E+03	5.75	1.31E+04
1.45	7.77E+02	2.91	3.16E+03	4.36	7.30E+03	5.82	1.35E+04
1.47	7.97E+02	2.95	3.24E+03	4.42	7.49E+03	5.89	1.39E+04
1.49	8.17E+02	2.98	3.32E+03	4.47	7.69E+03	5.96	1.42E+04
1.51	8.37E+02	3.02	3.40E+03	4.53	7.89E+03	6.04	1.46E+04
1.53	8.57E+02	3.05	3.49E+03	4.58	8.09E+03	6.11	1.50E+04
1.55	8.78E+02	3.09	3.57E+03	4.64	8.29E+03	6.18	1.54E+04
1.56	8.99E+02	3.13	3.66E+03	4.69	8.50E+03	6.25	1.58E+04
1.58	9.20E+02	3.16	3.75E+03	4.75	8.71E+03	6.33	1.62E+04
1.60	9.41E+02	3.20	3.84E+03	4.80	8.92E+03	6.40	1.66E+04
1.62	9.63E+02	3.24	3.93E+03	4.85	9.14E+03	6.47	1.71E+04
1.64	9.85E+02	3.27	4.02E+03	4.91	9.36E+03	6.55	1.75E+04
1.65	1.01E+03	3.31	4.11E+03	4.96	9.58E+03	6.62	1.79E+04
1.67	1.03E+03	3.35	4.20E+03	5.02	9.81E+03	6.69	1.84E+04
1.69	1.05E+03	3.38	4.30E+03	5.07	1.00E+04	6.76	1.88E+04
1.71	1.07E+03	3.42	4.40E+03	5.13	1.03E+04	6.84	1.93E+04
1.73	1.10E+03	3.45	4.49E+03	5.18	1.05E+04	6.91	1.98E+04
1.75	1.12E+03	3.49	4.59E+03	5.24	1.07E+04	6.98	2.02E+04
1.76	1.15E+03	3.53	4.69E+03	5.29	1.10E+04	7.05	2.07E+04
1.78	1.17E+03	3.56	4.79E+03	5.35	1.12E+04	7.13	2.12E+04
1.80	1.19E+03	3.60	4.89E+03	5.40	1.15E+04	7.20	2.17E+04
1.82	1.22E+03	3.64	4.99E+03	5.45	1.17E+04	7.27	2.22E+04
1.84	1.24E+03	3.67	5.10E+03	5.51	1.20E+04	7.35	2.27E+04
1.85	1.27E+03	3.71	5.20E+03	5.56	1.22E+04	7.42	2.33E+04
1.87	1.29E+03	3.75	5.31E+03	5.62	1.25E+04	7.49	2.38E+04
1.89	1.32E+03	3.78	5.42E+03	5.67	1.28E+04	7.56	2.43E+04
1.91	1.34E+03	3.82	5.52E+03	5.73	1.30E+04	7.64	2.49E+04
1.93	1.37E+03	3.85	5.63E+03	5.78	1.33E+04	7.71	2.54E+04
1.95	1.40E+03	3.89	5.75E+03	5.84	1.36E+04	7.78	2.60E+04
1.96	1.42E+03	3.93	5.86E+03	5.89	1.39E+04	7.85	2.66E+04
1.98	1.45E+03	3.96	5.97E+03	5.95	1.41E+04	7.93	2.72E+04
2.00	1.48E+03	4.00	6.09E+03	6.00	1.44E+04	8.00	2.78E+04
2.02	1.50E+03	4.04	6.20E+03	6.05	1.47E+04	8.07	2.84E+04
2.04	1.53E+03	4.07	6.32E+03	6.11	1.50E+04	8.15	2.90E+04
2.05	1.56E+03	4.11	6.44E+03	6.16	1.53E+04	8.22	2.96E+04
2.07	1.59E+03	4.15	6.56E+03	6.22	1.56E+04	8.29	3.02E+04
2.09	1.61E+03	4.18	6.68E+03	6.27	1.59E+04	8.36	3.09E+04
2.11	1.64E+03	4.22	6.80E+03	6.33	1.62E+04	8.44	3.15E+04
2.13	1.67E+03	4.25	6.92E+03	6.38	1.65E+04	8.51	3.22E+04
2.15	1.70E+03	4.29	7.05E+03	6.44	1.69E+04	8.58	3.29E+04
2.16	1.73E+03	4.33	7.17E+03	6.49	1.72E+04	8.65	3.36E+04
2.18	1.76E+03	4.36	7.30E+03	6.55	1.75E+04	8.73	3.43E+04
2.20	1.79E+03	4.40	7.43E+03	6.60	1.78E+04	8.80	3.50E+04
2.22	1.82E+03	4.44	7.56E+03	6.65	1.82E+04	8.87	3.57E+04
2.24	1.85E+03	4.47	7.69E+03	6.71	1.85E+04	8.95	3.64E+04
2.25	1.88E+03	4.51	7.82E+03	6.76	1.88E+04	9.02	3.72E+04
2.27	1.91E+03	4.55	7.95E+03	6.82	1.92E+04	9.09	3.79E+04
2.29	1.94E+03	4.58	8.09E+03	6.87	1.95E+04	9.16	3.87E+04
2.31	1.97E+03	4.62	8.22E+03	6.93	1.99E+04	9.24	3.95E+04
2.33	2.01E+03	4.65	8.36E+03	6.98	2.02E+04	9.31	4.03E+04
2.35	2.04E+03	4.69	8.50E+03	7.04	2.06E+04	9.38	4.11E+04
2.36	2.07E+03	4.73	8.64E+03	7.09	2.10E+04	9.45	4.19E+04
2.38	2.10E+03	4.76	8.78E+03	7.15	2.13E+04	9.53	4.27E+04
2.40	2.13E+03	4.80	8.92E+03	7.20	2.17E+04	9.60	4.36E+04
2.42	2.17E+03	4.84	9.07E+03	7.25	2.21E+04	9.67	4.44E+04
2.44	2.20E+03	4.87	9.21E+03	7.31	2.25E+04	9.75	4.53E+04
2.45	2.23E+03	4.91	9.36E+03	7.36	2.29E+04	9.82	4.62E+04
2.47	2.27E+03	4.95	9.51E+03	7.42	2.33E+04	9.89	4.71E+04
2.49	2.30E+03	4.98	9.66E+03	7.47	2.37E+04	9.96	4.80E+04
2.51	2.34E+03	5.02	9.81E+03	7.53	2.41E+04	10.04	4.90E+04
2.53	2.37E+03	5.05	9.96E+03	7.58	2.45E+04	10.11	4.99E+04
2.55	2.41E+03	5.09	1.01E+04	7.64	2.49E+04	10.18	5.09E+04
2.56	2.44E+03	5.13	1.03E+04	7.69	2.53E+04	10.25	5.19E+04
2.58	2.48E+03	5.16	1.04E+04	7.75	2.57E+04	10.33	5.29E+04
2.60	2.51E+03	5.20	1.06E+04	7.80	2.62E+04	10.40	5.39E+04
2.62	2.55E+03	5.24	1.07E+04	7.85	2.66E+04	10.47	5.49E+04
2.64	2.58E+03	5.27	1.09E+04	7.91	2.70E+04	10.55	5.60E+04
2.65	2.62E+03	5.31	1.11E+04	7.96	2.75E+04	10.62	5.71E+04
2.67	2.66E+03	5.35	1.12E+04	8.02	2.79E+04	10.69	5.82E+04
2.69	2.69E+03	5.38	1.14E+04	8.07	2.84E+04	10.76	5.93E+04
2.71	2.73E+03	5.42	1.16E+04	8.13	2.88E+04	10.84	6.04E+04
2.73	2.77E+03	5.45	1.17E+04	8.18	2.93E+04	10.91	6.16E+04
2.75	2.81E+03	5.49	1.19E+04	8.24	2.98E+04	10.98	6.27E+04
2.76	2.84E+03	5.53	1.21E+04	8.29	3.02E+04	11.05	6.39E+04
2.78	2.88E+03	5.56	1.22E+04	8.35	3.07E+04	11.13	6.51E+04
2.80	2.92E+03	5.60	1.24E+04	8.40	3.12E+04	11.20	6.64E+04

First Harmonic		Second Harmonic		Third Harmonic		Fourth Harmonic		Total Response	Total Acceleration	
Baseline	Response Factor	Baseline	Response Factor	Baseline	Response Factor	Baseline	Response Factor	SRSS	Linear SRSS	
1.41E-02	2.59E-07	1.00E-02	1.48E-07	8.16E-03	4.12E-07	7.07E-03	8.61E-07	9.66E-07	1.13E-04	7117.10213
1.40E-02	2.71E-07	9.91E-03	1.54E-07	8.09E-03	4.31E-07	7.07E-03	8.94E-07	1.00E-06	1.17E-04	7387.89756
1.39E-02	2.83E-07	9.82E-03	1.61E-07	8.02E-03	4.51E-07	7.07E-03	9.27E-07	1.04E-06	1.22E-04	7664.30254
1.38E-02	2.96E-07	9.74E-03	1.69E-07	7.95E-03	4.72E-07	7.07E-03	9.61E-07	1.08E-06	1.26E-04	7946.36085
1.37E-02	3.09E-07	9.66E-03	1.76E-07	7.88E-03	4.93E-07	7.07E-03	9.97E-07	1.13E-06	1.31E-04	8234.11524
1.35E-02	3.22E-07	9.57E-03	1.84E-07	7.82E-03	5.14E-07	7.07E-03	1.03E-06	1.17E-06	1.35E-04	8527.60944
1.34E-02	3.36E-07	9.50E-03	1.92E-07	7.75E-03	5.36E-07	7.07E-03	1.07E-06	1.21E-06	1.40E-04	8826.89004
1.33E-02	3.50E-07	9.42E-03	2.00E-07	7.69E-03	5.59E-07	7.07E-03	1.11E-06	1.26E-06	1.45E-04	9132.00422
1.32E-02	3.64E-07	9.34E-03	2.08E-07	7.63E-03	5.82E-07	7.07E-03	1.14E-06	1.30E-06	1.50E-04	9442.99919
1.31E-02	3.79E-07	9.27E-03	2.16E-07	7.57E-03	6.06E-07	7.07E-03	1.18E-06	1.35E-06	1.55E-04	9759.92481
1.30E-02	3.94E-07	9.20E-03	2.25E-07	7.51E-03	6.31E-07	7.07E-03	1.22E-06	1.39E-06	1.60E-04	10082.8327
1.29E-02	4.09E-07	9.13E-03	2.34E-07	7.45E-03	6.56E-07	7.07E-03	1.26E-06	1.44E-06	1.65E-04	10411.7718
1.28E-02	4.25E-07	9.06E-03	2.43E-07	7.40E-03	6.82E-07	7.07E-03	1.30E-06	1.49E-06	1.70E-04	10746.7976
1.27E-02	4.41E-07	8.99E-03	2.52E-07	7.34E-03	7.08E-07	7.07E-03	1.34E-06	1.54E-06	1.75E-04	11087.963
1.26E-02	4.57E-07	8.93E-03	2.62E-07	7.29E-03	7.36E-07	7.07E-03	1.39E-06	1.59E-06	1.81E-04	11435.3229
1.25E-02	4.74E-07	8.86E-03	2.71E-07	7.24E-03	7.63E-07	7.07E-03	1.43E-06	1.64E-06	1.86E-04	11788.9398
1.24E-02	4.91E-07	8.80E-03	2.81E-07	7.19E-03	7.92E-07	7.07E-03	1.47E-06	1.70E-06	1.92E-04	12148.8567
1.24E-02	5.09E-07	8.74E-03	2.91E-07	7.14E-03	8.21E-07	7.07E-03	1.52E-06	1.75E-06	1.98E-04	12515.1479
1.23E-02	5.27E-07	8.68E-03	3.02E-07	7.09E-03	8.51E-07	7.07E-03	1.57E-06	1.81E-06	2.04E-04	12887.8728
1.22E-02	5.45E-07	8.62E-03	3.12E-07	7.07E-03	8.77E-07	7.07E-03	1.61E-06	1.86E-06	2.10E-04	13267.0917
1.21E-02	5.64E-07	8.56E-03	3.23E-07	7.07E-03	9.02E-07	7.07E-03	1.66E-06	1.92E-06	2.16E-04	13652.866
1.20E-02	5.83E-07	8.51E-03	3.34E-07	7.07E-03	9.27E-07	7.07E-03	1.71E-06	1.97E-06	2.22E-04	14045.2556
1.20E-02	6.02E-07	8.45E-03	3.46E-07	7.07E-03	9.53E-07	7.07E-03	1.76E-06	2.03E-06	2.28E-04	14444.3479
1.19E-02	6.22E-07	8.40E-03	3.57E-07	7.07E-03	9.79E-07	7.07E-03	1.81E-06	2.09E-06	2.34E-04	14850.1967
1.18E-02	6.42E-07	8.34E-03	3.69E-07	7.07E-03	1.01E-06	7.07E-03	1.86E-06	2.14E-06	2.41E-04	15262.8591
1.17E-02	6.63E-07	8.29E-03	3.81E-07	7.07E-03	1.03E-06	7.07E-03	1.91E-06	2.20E-06	2.47E-04	15682.4269
1.17E-02	6.84E-07	8.24E-03	3.93E-07	7.07E-03	1.06E-06	7.07E-03	1.96E-06	2.26E-06	2.54E-04	16108.9771
1.16E-02	7.05E-07	8.19E-03	4.06E-07	7.07E-03	1.09E-06	7.07E-03	2.01E-06	2.33E-06	2.61E-04	16542.5641
1.15E-02	7.27E-07	8.14E-03	4.18E-07	7.07E-03	1.12E-06	7.07E-03	2.07E-06	2.39E-06	2.68E-04	16983.2836
1.14E-02	7.49E-07	8.09E-03	4.31E-07	7.07E-03	1.14E-06	7.07E-03	2.12E-06	2.45E-06	2.75E-04	17431.1988
1.14E-02	7.72E-07	8.04E-03	4.44E-07	7.07E-03	1.17E-06	7.07E-03	2.18E-06	2.52E-06	2.82E-04	17886.4063
1.13E-02	7.95E-07	8.00E-03	4.58E-07	7.07E-03	1.20E-06	7.07E-03	2.24E-06	2.58E-06	2.89E-04	18348.9784
1.12E-02	8.18E-07	7.95E-03	4.72E-07	7.07E-03	1.23E-06	7.07E-03	2.30E-06	2.65E-06	2.96E-04	18819.0033
1.12E-02	8.42E-07	7.91E-03	4.85E-07	7.07E-03	1.26E-06	7.07E-03	2.35E-06	2.72E-06	3.03E-04	19296.5619
1.11E-02	8.66E-07	7.86E-03	5.00E-07	7.07E-03	1.29E-06	7.07E-03	2.41E-06	2.79E-06	3.11E-04	19781.7522
1.11E-02	8.91E-07	7.82E-03	5.14E-07	7.07E-03	1.32E-06	7.07E-03	2.48E-06	2.86E-06	3.19E-04	20274.6559
1.10E-02	9.16E-07	7.77E-03	5.29E-07	7.07E-03	1.36E-06	7.07E-03	2.54E-06	2.93E-06	3.26E-04	20775.3709
1.09E-02	9.41E-07	7.73E-03	5.44E-07	7.07E-03	1.39E-06	7.07E-03	2.60E-06	3.00E-06	3.34E-04	21283.9875
1.09E-02	9.67E-07	7.69E-03	5.59E-07	7.07E-03	1.42E-06	7.07E-03	2.66E-06	3.07E-06	3.42E-04	21800.6038
1.08E-02	9.94E-07	7.65E-03	5.75E-07	7.07E-03	1.45E-06	7.07E-03	2.72E-06	3.15E-06	3.50E-04	22325.3222
1.08E-02	1.02E-06	7.61E-03	5.90E-07	7.07E-03	1.49E-06	7.07E-03	2.80E-06	3.22E-06	3.59E-04	22858.2428
1.07E-02	1.05E-06	7.57E-03	6.06E-07	7.07E-03	1.52E-06	7.07E-03	2.86E-06	3.30E-06	3.67E-04	23399.4756
1.06E-02	1.08E-06	7.53E-03	6.22E-07	7.07E-03	1.55E-06	7.07E-03	2.93E-06	3.38E-06	3.75E-04	23949.1151
1.06E-02	1.10E-06	7.49E-03	6.39E-07	7.07E-03	1.59E-06	7.07E-03	3.00E-06	3.46E-06	3.84E-04	24507.2755
1.05E-02	1.13E-06	7.45E-03	6.56E-07	7.07E-03	1.62E-06	7.07E-03	3.07E-06	3.54E-06	3.93E-04	25074.0769
1.05E-02	1.16E-06	7.42E-03	6.73E-07	7.07E-03	1.66E-06	7.07E-03	3.14E-06	3.62E-06	4.02E-04	25649.6216
1.04E-02	1.19E-06	7.38E-03	6.91E-07	7.07E-03	1.69E-06	7.07E-03	3.22E-06	3.70E-06	4.11E-04	26234.0379
1.04E-02	1.22E-06	7.34E-03	7.08E-07	7.07E-03	1.73E-06	7.07E-03	3.29E-06	3.79E-06	4.20E-04	26827.4331
1.03E-02	1.25E-06	7.31E-03	7.26E-07	7.07E-03	1.77E-06	7.07E-03	3.37E-06	3.87E-06	4.29E-04	27429.94
1.03E-02	1.28E-06	7.27E-03	7.45E-07	7.07E-03	1.81E-06	7.07E-03	3.44E-06	3.96E-06	4.38E-04	28041.6876
1.02E-02	1.31E-06	7.24E-03	7.63E-07	7.07E-03	1.84E-06	7.07E-03	3.52E-06	4.05E-06	4.48E-04	28662.7958
1.02E-02	1.34E-06	7.20E-03	7.82E-07	7.07E-03	1.88E-06	7.07E-03	3.60E-06	4.14E-06	4.58E-04	29293.4028
1.01E-02	1.38E-06	7.17E-03	8.01E-07	7.07E-03	1.92E-06	7.07E-03	3.68E-06	4.23E-06	4.67E-04	29933.6375
1.01E-02	1.41E-06	7.14E-03	8.21E-07	7.07E-03	1.96E-06	7.07E-03	3.76E-06	4.32E-06	4.77E-04	30583.651
1.00E-02	1.44E-06	7.10E-03	8.41E-07	7.07E-03	2.00E-06	7.07E-03	3.84E-06	4.42E-06	4.87E-04	31243.5727
1.00E-02	1.48E-06	7.07E-03	8.61E-07	7.07E-03	2.04E-06	7.07E-03	3.93E-06	4.51E-06	4.98E-04	31913.5628
9.95E-03	1.51E-06	7.07E-03	8.77E-07	7.07E-03	2.08E-06	7.14E-03	3.98E-06	4.58E-06	5.08E-04	32593.7592
9.91E-03	1.54E-06	7.07E-03	8.94E-07	7.07E-03	2.12E-06	7.20E-03	4.03E-06	4.64E-06	5.19E-04	33284.314
9.87E-03	1.58E-06	7.07E-03	9.10E-07	7.07E-03	2.17E-06	7.26E-03	4.08E-06	4.71E-06	5.29E-04	33985.3921
9.82E-03	1.61E-06	7.07E-03	9.27E-07	7.07E-03	2.21E-06	7.33E-03	4.13E-06	4.77E-06	5.40E-04	34697.1491
9.78E-03	1.65E-06	7.07E-03	9.44E-07	7.07E-03	2.25E-06	7.39E-03	4.18E-06	4.84E-06	5.51E-04	35419.7595
9.74E-03	1.69E-06	7.07E-03	9.61E-07	7.07E-03	2.30E-06	7.46E-03	4.23E-06	4.91E-06	5.62E-04	36153.3839
9.70E-03	1.72E-06	7.07E-03	9.79E-07	7.07E-03	2.34E-06	7.52E-03	4.28E-06	4.98E-06	5.73E-04	36898.1968
9.66E-03	1.76E-06	7.07E-03	9.97E-07	7.07E-03	2.38E-06	7.59E-03	4.33E-06	5.05E-06	5.85E-04	37654.3808
9.61E-03	1.80E-06	7.07E-03	1.01E-06	7.07E-03	2.43E-06	7.65E-03	4.39E-06	5.12E-06	5.96E-04	38422.1196
9.57E-03	1.84E-06	7.07E-03	1.03E-06	7.07E-03	2.48E-06	7.71E-03	4.44E-06	5.19E-06	6.08E-04	39201.5964
9.53E-03	1.88E-06	7.07E-03	1.05E-06	7.07E-03	2.52E-06	7.78E-03	4.50E-06	5.26E-06	6.20E-04	39993.0124
9.50E-03	1.92E-06	7.07E-03	1.07E-06	7.07E-03	2.57E-06	7.84E-03	4.55E-06	5.34E-06	6.32E-04	40796.5516
9.46E-03	1.96E-06	7.07E-03	1.09E-06	7.07E-03	2.62E-06	7.91E-03	4.61E-06	5.41E-06	6.45E-04	41612.4206
9.42E-03	2.00E-06	7.07E-03	1.11E-06	7.07E-03	2.66E-06	7.97E-03	4.66E-06	5.49E-06	6.57E-04	42440.854
9.38E-03	2.04E-06	7.07E-03	1.12E-06	7.07E-03	2.71E-06	8.04E-03	4.72E-06	5.56E-06	6.70E-04	43282.034
9.34E-03	2.08E-06	7.07E-03	1.14E-06	7.07E-03	2.76E-06	8.10E-03	4.78E-06	5.64E-06	6.83E-04	44136.1929
9.31E-03	2.12E-06	7.07E-03	1.16E-06	7.07E-03	2.81E-06	8.16E-03	4.84E-06	5.72E-06	6.96E-04	45003.5462
9.27E-03	2.16E-06	7.07E-03	1.18E-06	7.07E-03	2.86E-06	8.23E-03	4.89E-06	5.80E-06	7.09E-04	45884.3449
9.23E-03	2.21E-06	7.07E-03	1.20E-06	7.07E-03	2.91E-06	8.29E-03	4.95E-06	5.88E-06	7.22E-04	46778.8141
9.20E-03	2.25E-06	7.07E-03	1.22E-06	7.07E-03	2.97E-06	8.36E-03	5.01E-06	5.96E-06	7.36E-04	47687.2138
9.16E-03	2.29E-06	7.07E-03	1.24E-06	7.07E-03	3.02E-06	8.42E-03	5.07E-06	6.04E-06	7.50E-04	48609.7781
9.13E-03	2.34E-06	7.07E-03	1.26E-06	7.07E-03	3.07E-06	8.49E-03	5.14E-06	6.12E-06	7.64E-04	49546.7638
9.09E-03	2.38E-06	7.07E-03	1.28E-06	7.07E-03	3.12E-06	8.55E-03	5.20E-06	6.20E-06	7.78E-04	50498.4582
9.06E-03	2.43E-06	7.07E-03	1.30E-06	7.07E-03	3.18E-06	8.61E-03	5.26E-06	6.29E-06	7.92E-04	51465.1273
9.03E-03	2.48E-06	7.07E-03	1.32E-06	7.07E-03	3.23E-06	8.68E-03	5.32E-06	6.37E-06	8.07E-04	52447.0416
8.99E-03	2.52E-06	7.07E-03	1.34E-06	7.07E-03	3.29E-06	8.74E-03	5.39E-06	6.46E-06	8.22E-04	53444.4896
8.96E-03	2.57E-06	7.07E-03	1.37E-06	7.07E-03	3.35E-06	8.81E-03	5.45E-06	6.55E-06	8.37E-04	54457.8001
8.93E-03	2.62E-06	7.07E-03	1.39E-06	7.07E-03	3.40E-06	8.87E-03	5.52E-06	6.64E-06	8.52E-04	55487.2489
8.90E-03	2.67E-06	7.07E-03	1.41E-06	7.07E-03	3.46E-06	8.94E-03	5.59E-06	6.73E-06	8.67E-04	56533.1653
8.86E-03	2.71E-06	7.07E-03	1.43E-06	7.07E-03	3.52E-06	9.00E-03	5.65E-06	6.82E-06	8.83E-04	57595.8712
8.83E-03	2.76E-06	7.07E-03	1.45E-06	7.07E-03	3.58E-06	9.06E-03	5.72E-06	6.91E-06	8.99E-04	58675.698
8.80E-03	2.81E-06	7.07E-03	1.47E-06	7.07E-03	3.64E-06	9.13E-03	5.79E-06	7.00E-06	9.15E-04	59772.9934
8.77E-03	2.86E-06	7.07E-03	1.50E-06	7.07E-03	3.70E-06	9.19E-03	5.86E-06	7.10E-06	9.31E-04	60888.1135
8.74E-03	2.91E-06	7.07E-03	1.52E-06	7.07E-03	3.76E-06	9.26E-03	5.93E-06	7.19E-06	9.48E-04	62021.4151
8.71E-03	2.97E-06	7.07E-03	1.54E-06	7.07E-03	3.82E-06	9.32E-03	6.01E-06	7.29E-06	9.65E-04	63173.2984
8.68E-03	3.02E-06	7.07E-03	1.57E-06	7.07E-03	3.88E-06	9.39E-03	6.08E-06	7.39E-06	9.82E-04	64344.1346
8.65E-03	3.07E-06	7.07E-03	1.59E-06	7.09E-03	3.94E-06	9.45E-03	6.15E-06	7.48E-06	1.00E-03	65534.319
8.62E-03	3.12E-06	7.07E-03	1.61E-06	7.14E-03	3.98E-06	9.51E-03	6.23E-06	7.57E-06	1.02E-03	66744.287
8.59E-03	3.18E-06	7.07E-03	1.64E-06	7.18E-03	4.01E-06	9.58E-03	6.31E-06	7.66E-06	1.04E-03	67974.4472
8.56E-03	3.23E-06	7.07E-03	1.66E-06	7.23E-03	4.05E-06	9.64E-03	6.38E-06	7.75E-06	1.05E-03	69225.2421
8.54E-03	3.29E-06	7.07E-03	1.68E-06	7.28E-03	4.09E-06	9.71E-03	6.46E-06	7.84E-06	1.07E-03	70497.1301
8.51E-03	3.34E-06	7.07E-03	1.71E-06	7.33E-03	4.13E-06	9.77E-03	6.54E-06	7.93E-06	1.09E-03	71790.5741
8.48E-03	3.40E-06	7.07E-03	1.73E-06	7.38E-03	4.17E-06	9.84E-03	6.62E-06	8.02E-06	1.11E-03	73106.0651
8.45E-03	3.46E-06	7.07E-03	1.76E-06	7.42E-03	4.20E-06	9.90E-03	6.70E-06	8.11E-06	1.13E-03	74444.0901

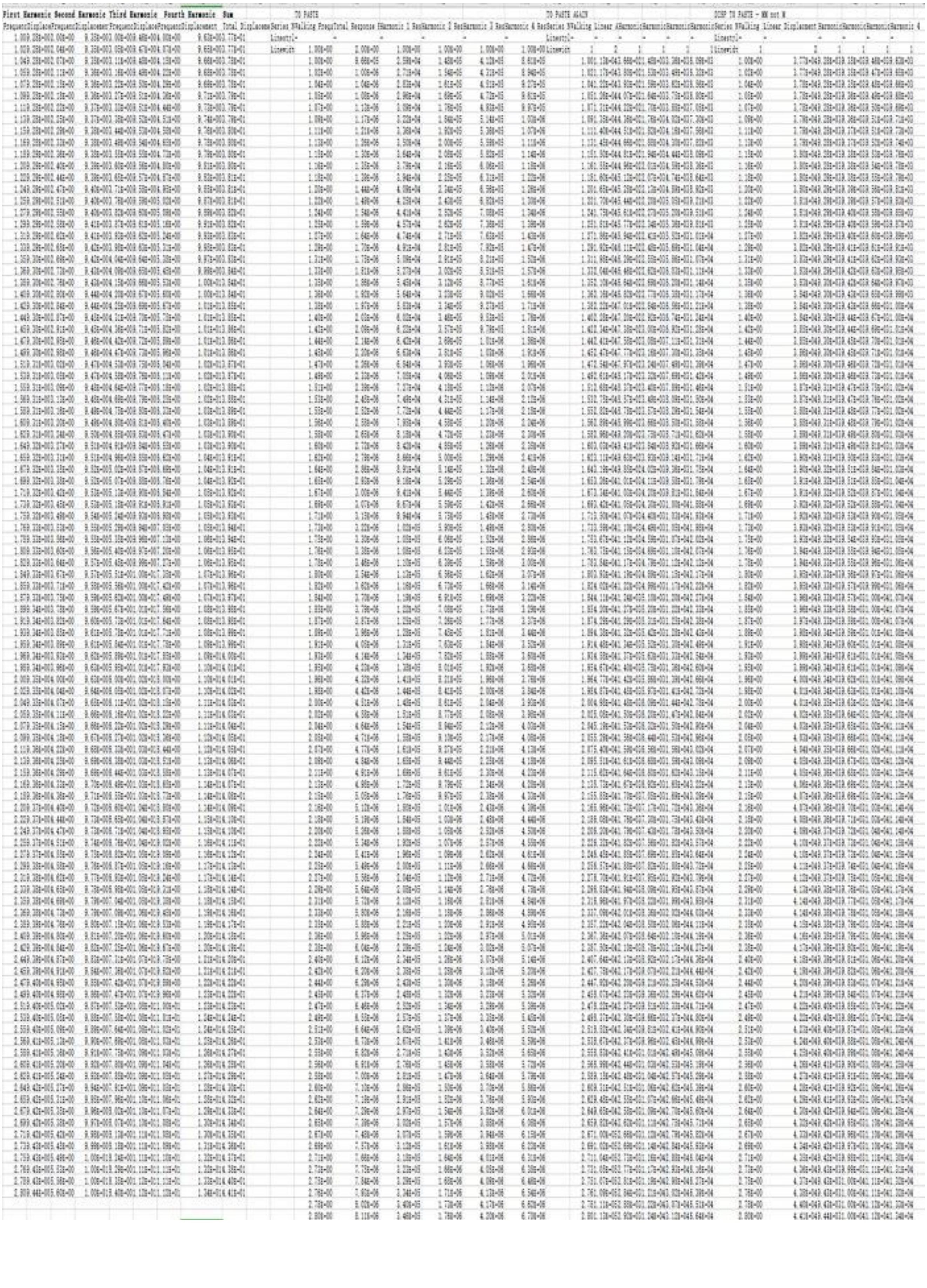
First Harmonic Second Harmonic Third Harmonic Fourth Harmonic Sum
TO PASTE
TO PASTE AGAIN

Case3

First Harmonic		Second Harmonic		Third Harmonic		Fourth Harmonic		First Harmonic		Second Harmonic		Third Harmonic		Fourth Harmonic		Total Response	tal Accelerati	
Frequency	Acceleration	Frequency	Acceleration	Frequency	Acceleration	Frequency	Acceleration	Baseline	Response Factor	Baseline	Response Factor	Baseline	Response Factor	Baseline	Response Factor	SRSS	Linear	SRSS
1.00	5.72E+02	2.00	2.32E+03	3.00	5.32E+03	4.00	9.73E+03	1.41E-02	4.05E-04	1.00E-02	2.32E-05	8.16E-03	6.51E-05	7.07E-03	1.38E-06	1.54E-06	1.79E-04	11343.9
1.02	5.93E+02	2.04	2.40E+03	3.05	5.52E+03	4.07	1.01E+04	1.40E-02	4.23E-04	9.91E-03	2.42E-05	8.09E-03	6.82E-05	7.07E-03	1.43E-06	1.60E-06	1.86E-04	11785.4
1.04	6.15E+02	2.07	2.49E+03	3.11	5.73E+03	4.15	1.05E+04	1.39E-02	4.42E-04	9.82E-03	2.54E-05	8.02E-03	7.14E-05	7.07E-03	1.49E-06	1.67E-06	1.93E-04	12236.8
1.05	6.36E+02	2.11	2.58E+03	3.16	5.94E+03	4.22	1.09E+04	1.38E-02	4.62E-04	9.74E-03	2.65E-05	7.95E-03	7.47E-05	7.07E-03	1.54E-06	1.73E-06	2.01E-04	12698.2
1.07	6.59E+02	2.15	2.67E+03	3.22	6.15E+03	4.29	1.13E+04	1.37E-02	4.82E-04	9.66E-03	2.77E-05	7.88E-03	7.81E-05	7.07E-03	1.60E-06	1.80E-06	2.08E-04	13169.8
1.09	6.81E+02	2.18	2.76E+03	3.27	6.37E+03	4.36	1.17E+04	1.35E-02	5.03E-04	9.57E-03	2.89E-05	7.82E-03	8.15E-05	7.07E-03	1.66E-06	1.87E-06	2.16E-04	13651.7
1.11	7.04E+02	2.22	2.86E+03	3.33	6.60E+03	4.44	1.22E+04	1.34E-02	5.25E-04	9.50E-03	3.01E-05	7.75E-03	8.51E-05	7.07E-03	1.72E-06	1.94E-06	2.23E-04	14144
1.13	7.28E+02	2.25	2.96E+03	3.38	6.83E+03	4.51	1.26E+04	1.33E-02	5.46E-04	9.42E-03	3.14E-05	7.69E-03	8.88E-05	7.07E-03	1.78E-06	2.02E-06	2.31E-04	14646.9
1.15	7.52E+02	2.29	3.05E+03	3.44	7.06E+03	4.58	1.30E+04	1.32E-02	5.69E-04	9.34E-03	3.27E-05	7.63E-03	9.25E-05	7.07E-03	1.84E-06	2.09E-06	2.39E-04	15160.4
1.16	7.76E+02	2.33	3.15E+03	3.49	7.30E+03	4.65	1.35E+04	1.31E-02	5.92E-04	9.27E-03	3.40E-05	7.57E-03	9.64E-05	7.07E-03	1.91E-06	2.17E-06	2.47E-04	15684.8
1.18	8.00E+02	2.36	3.26E+03	3.55	7.54E+03	4.73	1.40E+04	1.30E-02	6.15E-04	9.20E-03	3.54E-05	7.51E-03	1.00E-06	7.07E-03	1.98E-06	2.24E-06	2.56E-04	16220.2
1.20	8.25E+02	2.40	3.36E+03	3.60	7.78E+03	4.80	1.44E+04	1.29E-02	6.39E-04	9.13E-03	3.68E-05	7.45E-03	1.04E-06	7.07E-03	2.04E-06	2.32E-06	2.64E-04	16766.6
1.22	8.51E+02	2.44	3.46E+03	3.65	8.03E+03	4.87	1.49E+04	1.28E-02	6.64E-04	9.06E-03	3.82E-05	7.40E-03	1.09E-06	7.07E-03	2.11E-06	2.41E-06	2.73E-04	17324.4
1.24	8.76E+02	2.47	3.57E+03	3.71	8.29E+03	4.95	1.54E+04	1.27E-02	6.89E-04	8.99E-03	3.97E-05	7.34E-03	1.13E-06	7.07E-03	2.18E-06	2.49E-06	2.82E-04	17893.6
1.25	9.02E+02	2.51	3.68E+03	3.76	8.55E+03	5.02	1.59E+04	1.26E-02	7.15E-04	8.93E-03	4.12E-05	7.29E-03	1.17E-06	7.07E-03	2.25E-06	2.57E-06	2.91E-04	18474.4
1.27	9.29E+02	2.55	3.79E+03	3.82	8.81E+03	5.09	1.65E+04	1.25E-02	7.41E-04	8.86E-03	4.27E-05	7.24E-03	1.22E-06	7.07E-03	2.33E-06	2.66E-06	3.00E-04	19067
1.29	9.56E+02	2.58	3.90E+03	3.87	9.08E+03	5.16	1.70E+04	1.24E-02	7.68E-04	8.80E-03	4.43E-05	7.19E-03	1.26E-06	7.07E-03	2.40E-06	2.75E-06	3.09E-04	19671.5
1.31	9.83E+02	2.62	4.01E+03	3.93	9.36E+03	5.24	1.75E+04	1.24E-02	7.95E-04	8.74E-03	4.59E-05	7.14E-03	1.31E-06	7.07E-03	2.48E-06	2.84E-06	3.19E-04	20288.2
1.33	1.01E+03	2.65	4.13E+03	3.98	9.64E+03	5.31	1.81E+04	1.23E-02	8.23E-04	8.68E-03	4.76E-05	7.09E-03	1.36E-06	7.07E-03	2.56E-06	2.93E-06	3.29E-04	20917.2
1.35	1.04E+03	2.69	4.25E+03	4.04	9.92E+03	5.38	1.86E+04	1.22E-02	8.52E-04	8.62E-03	4.93E-05	7.07E-03	1.40E-06	7.07E-03	2.64E-06	3.03E-06	3.39E-04	21558.6
1.36	1.07E+03	2.73	4.37E+03	4.09	1.02E+04	5.45	1.92E+04	1.21E-02	8.81E-04	8.56E-03	5.10E-05	7.07E-03	1.44E-06	7.07E-03	2.72E-06	3.12E-06	3.49E-04	22212.8
1.38	1.10E+03	2.76	4.49E+03	4.15	1.05E+04	5.53	1.98E+04	1.20E-02	9.11E-04	8.51E-03	5.28E-05	7.07E-03	1.49E-06	7.07E-03	2.80E-06	3.21E-06	3.59E-04	22879.9
1.40	1.13E+03	2.80	4.61E+03	4.20	1.08E+04	5.60	2.04E+04	1.20E-02	9.42E-04	8.45E-03	5.45E-05	7.07E-03	1.53E-06	7.07E-03	2.88E-06	3.31E-06	3.69E-04	23560.1
1.42	1.16E+03	2.84	4.73E+03	4.25	1.11E+04	5.67	2.10E+04	1.19E-02	9.73E-04	8.40E-03	5.64E-05	7.07E-03	1.57E-06	7.07E-03	2.97E-06	3.41E-06	3.80E-04	24253.6
1.44	1.19E+03	2.87	4.86E+03	4.31	1.14E+04	5.75	2.16E+04	1.18E-02	1.00E-05	8.34E-03	5.83E-05	7.07E-03	1.61E-06	7.07E-03	3.06E-06	3.51E-06	3.91E-04	24960.6
1.45	1.22E+03	2.91	4.99E+03	4.36	1.17E+04	5.82	2.23E+04	1.17E-02	1.04E-05	8.29E-03	6.02E-05	7.07E-03	1.66E-06	7.07E-03	3.15E-06	3.61E-06	4.02E-04	25681.5
1.47	1.25E+03	2.95	5.12E+03	4.42	1.21E+04	5.89	2.29E+04	1.17E-02	1.07E-05	8.24E-03	6.21E-05	7.07E-03	1.70E-06	7.07E-03	3.24E-06	3.71E-06	4.13E-04	26416.3
1.49	1.28E+03	2.98	5.25E+03	4.47	1.24E+04	5.96	2.36E+04	1.16E-02	1.10E-05	8.19E-03	6.41E-05	7.07E-03	1.75E-06	7.07E-03	3.33E-06	3.82E-06	4.25E-04	27165.4
1.51	1.31E+03	3.02	5.38E+03	4.53	1.27E+04	6.04	2.42E+04	1.15E-02	1.14E-05	8.14E-03	6.61E-05	7.07E-03	1.80E-06	7.07E-03	3.43E-06	3.93E-06	4.36E-04	27928.9
1.53	1.34E+03	3.05	5.52E+03	4.58	1.30E+04	6.11	2.49E+04	1.14E-02	1.17E-05	8.09E-03	6.82E-05	7.07E-03	1.84E-06	7.07E-03	3.53E-06	4.04E-06	4.48E-04	28707.2
1.55	1.37E+03	3.09	5.66E+03	4.64	1.34E+04	6.18	2.56E+04	1.14E-02	1.21E-05	8.04E-03	7.03E-05	7.07E-03	1.89E-06	7.07E-03	3.63E-06	4.15E-06	4.61E-04	29500.6
1.56	1.41E+03	3.13	5.80E+03	4.69	1.37E+04	6.25	2.64E+04	1.13E-02	1.24E-05	8.00E-03	7.25E-05	7.07E-03	1.94E-06	7.07E-03	3.73E-06	4.27E-06	4.73E-04	30309.2
1.58	1.44E+03	3.16	5.94E+03	4.75	1.41E+04	6.33	2.71E+04	1.12E-02	1.28E-05	7.95E-03	7.47E-05	7.07E-03	1.99E-06	7.07E-03	3.83E-06	4.38E-06	4.85E-04	31133.3
1.60	1.47E+03	3.20	6.08E+03	4.80	1.44E+04	6.40	2.78E+04	1.12E-02	1.32E-05	7.91E-03	7.69E-05	7.07E-03	2.04E-06	7.07E-03	3.94E-06	4.50E-06	4.98E-04	31973.4
1.62	1.51E+03	3.24	6.23E+03	4.85	1.48E+04	6.47	2.86E+04	1.11E-02	1.36E-05	7.86E-03	7.92E-05	7.07E-03	2.09E-06	7.07E-03	4.04E-06	4.62E-06	5.11E-04	32829.5
1.64	1.54E+03	3.27	6.37E+03	4.91	1.52E+04	6.55	2.94E+04	1.11E-02	1.39E-05	7.82E-03	8.15E-05	7.07E-03	2.15E-06	7.07E-03	4.15E-06	4.75E-06	5.25E-04	33702.2
1.65	1.58E+03	3.31	6.52E+03	4.96	1.56E+04	6.62	3.02E+04	1.10E-02	1.43E-05	7.77E-03	8.39E-05	7.07E-03	2.20E-06	7.07E-03	4.27E-06	4.87E-06	5.38E-04	34591.6
1.67	1.61E+03	3.35	6.67E+03	5.02	1.59E+04	6.69	3.10E+04	1.09E-02	1.47E-05	7.73E-03	8.63E-05	7.07E-03	2.25E-06	7.07E-03	4.38E-06	5.00E-06	5.52E-04	35498.1
1.69	1.65E+03	3.38	6.83E+03	5.07	1.63E+04	6.76	3.18E+04	1.09E-02	1.52E-05	7.69E-03	8.88E-05	7.07E-03	2.31E-06	7.07E-03	4.50E-06	5.13E-06	5.66E-04	36422
1.71	1.68E+03	3.42	6.98E+03	5.13	1.67E+04	6.84	3.26E+04	1.08E-02	1.56E-05	7.65E-03	9.13E-05	7.07E-03	2.36E-06	7.07E-03	4.62E-06	5.27E-06	5.80E-04	37363.7
1.73	1.72E+03	3.45	7.14E+03	5.18	1.71E+04	6.91	3.35E+04	1.08E-02	1.60E-05	7.61E-03	9.38E-05	7.07E-03	2.42E-06	7.07E-03	4.74E-06	5.40E-06	5.95E-04	38323.6
1.75	1.76E+03	3.49	7.30E+03	5.24	1.75E+04	6.98	3.44E+04	1.07E-02	1.64E-05	7.57E-03	9.64E-05	7.07E-03	2.48E-06	7.07E-03	4.86E-06	5.54E-06	6.09E-04	39302
1.76	1.79E+03	3.53	7.46E+03	5.29	1.79E+04	7.05	3.53E+04	1.06E-02	1.69E-05	7.53E-03	9.90E-05	7.07E-03	2.54E-06	7.07E-03	4.99E-06	5.68E-06	6.24E-04	40299.3
1.78	1.83E+03	3.56	7.62E+03	5.35	1.84E+04	7.13	3.62E+04	1.06E-02	1.73E-05	7.49E-03	1.02E-06	7.07E-03	2.60E-06	7.07E-03	5.12E-06	5.83E-06	6.40E-04	41316
1.80	1.87E+03	3.60	7.79E+03	5.40	1.88E+04	7.20	3.71E+04	1.05E-02	1.77E-05	7.45E-03	1.04E-06	7.07E-03	2.66E-06	7.07E-03	5.25E-06	5.98E-06	6.55E-04	42352.3
1.82	1.91E+03	3.64	7.95E+03	5.45	1.92E+04	7.27	3.81E+04	1.05E-02	1.82E-05	7.42E-03	1.07E-06	7.07E-03	2.72E-06	7.07E-03	5.38E-06	6.13E-06	6.71E-04	43408.8
1.84	1.95E+03	3.67	8.12E+03	5.51	1.96E+04	7.35	3.90E+04	1.04E-02	1.87E-05	7.38E-03	1.10E-06	7.07E-03	2.78E-06	7.07E-03	5.52E-06	6.28E-06	6.87E-04	44485.8
1.85	1.99E+03	3.71	8.29E+03	5.56	2.01E+04	7.42	4.00E+04	1.04E-02	1.91E-05	7.34E-03	1.13E-06	7.07E-03	2.84E-06	7.07E-03	5.66E-06	6.44E-06	7.04E-04	45583.9
1.87	2.03E+03	3.75	8.46E+03	5.62	2.05E+04	7.49	4.10E+04	1.03E-02	1.96E-05	7.31E-03	1.16E-06	7.07E-03	2.91E-06	7.07E-03	5.80E-06	6.59E-06	7.21E-04	46703.4
1.89	2.07E+03	3.78	8.64E+03	5.67	2.10E+04	7.56	4.21E+04	1.03E-02	2.01E-05	7.27E-03	1.19E-06	7.07E-03	2.97E-06	7.07E-03	5.95E-06	6.76E-06	7.38E-04	47845
1.91	2.11E+03	3.82	8.81E+03	5.73	2.15E+04	7.64	4.31E+04	1.02E-02	2.06E-05	7.24E-03	1.22E-06	7.07E-03	3.04E-06	7.07E-03	6.10E-06	6.92E-06	7.55E-04	49009.1
1.93	2.15E+03	3.85	8.99E+03	5.78	2.19E+04	7.71	4.42E+04	1.02E-02	2.11E-05	7.20E-03	1.25E-06	7.07E-03	3.10E-06	7.07E-03	6.25E-06	7.09E-06	7.73E-04	50196.1
1.95	2.19E+03	3.89	9.18E+03	5.84	2.24E+04	7.78	4.53E+04	1.01E-02	2.16E-05	7.17E-03	1.28E-06	7.07E-03	3.17E-06	7.07E-03	6.40E-06	7.26E-06	7.91E-04	51406.7
1.96	2.23E+03	3.93	9.36E+03	5.89	2.29E+04	7.85	4.64E+04	1.01E-02	2.21E-05	7.14E-03	1.31E-06	7.07E-03	3.24E-06	7.07E-03	6.56E-06	7.44E-06	8.09E-04	52641.5
1.98	2.27E+03	3.96	9.54E+03	5.95	2.34E+04	7.93	4.76E+04	1.00E-02	2.26E-05	7.10E-03	1.34E-06	7.07E-03	3.31E-06	7.07E-03	6.73E-06	7.62E-06	8.28E-04	53900.9
2.00	2.32E+03	4.00	9.73E+03	6.00	2.39E+04	8.00	4.87E+04	1.00E-02	2.32E-05	7.07E-03	1.38E-06	7.07E-03	3.38E-06	7.07E-03	6.89E-06	7.80E-06	8.47E-04	55185.6
2.02	2.36E+03	4.04	9.92E+03	6.05	2.44E+04	8.07	4.99E+04	9.95E-03	2.37E-05	7.07E-03	1.40E-06	7.07E-03	3.45E-06	7.14E-03	7.00E-06	7.93E-06	8.66E-04	56496.3
2.04	2.40E+03	4.07	1.01E+04	6.11	2.49E+04	8.15	5.11E+04	9.91E-03	2.42E-05	7.07E-03	1.43E-06	7.07E-03	3.53E-06	7.20E-03	7.10E-06	8.06E-06	8.86E-04	57833.5
2.05	2.45E+03	4.11	1.03E+04	6.16	2.55E+04	8.22	5.24E+04	9.87E-03	2.48E-05	7.07E-03	1.46E-06	7.07E-03	3.60E-06	7.26E-03	7.21E-06	8.19E-06	9.06E-04	59198
2.07	2.49E+03	4.15	1.05E+04	6.22	2.60E+04	8.29	5.37E+04	9.82E-03	2.54E-05	7.07E-03	1.49E-06	7.07E-03	3.68E-06	7.33E-03	7.32E-06	8.33E-06	9.26E-04	60590.4
2.09	2.53E+03	4.18	1.07E+04	6.27	2.65E+04	8.36	5.50E+04	9.78E-03	2.59E-05	7.07E-03	1.51E-06	7.07E-03	3.75E-06	7.39E-03	7.43E-06	8.47E-06	9.47E-04	62011.5
2.11	2.58E+03	4.22	1.09E+04	6.33	2.71E+04	8.44	5.63E+04	9.74E-03	2.65E-05	7.07E-03	1.54E-06	7.07E-03	3.83E-06	7.46E-03	7.55E-06	8.61E-06	9.69E-04	63462.1
2.13	2.63E+03	4.25	1.11E+04	6.38	2.76E+04	8.51	5.76E+04	9.70E-03	2.71E-05	7.07E-03	1.57E-06	7.07E-03	3.91E-06	7.52E-03	7.66E-06	8.75E-06	9.90E-04	64942.9
2.15	2.67E+03	4.29	1.13E+04	6.44	2.82E+04	8.58	5.90E+04	9.66E-03	2.77E-05	7.07E-03	1.60E-06	7.07E-03	3.99E-06	7.59E-03	7.78E-06	8.90E-06	1.01E-05	66454.9
2.16	2.72E+03	4.33	1.15E+04	6.49	2.88E+04	8.65	6.05E+04	9.61E-03	2.83E-05	7.07E-03	1.63E-06	7.07E-03	4.07E-06	7.65E-03	7.90E-06	9.04E-06	1.03E-05	67998.7
2.18	2.76E+03	4.36	1.17E+04	6.55	2.94E+04	8.73	6.19E+04	9.57E-03	2.89E-05	7.07E-03	1.66E-06	7.07E-03	4.15E-06	7.71E-03	8.03E-06	9.19E-06	1.06E-05	69575.4
2.20	2.81E+03	4.40	1.19E+04	6.60	3.00E+04	8.80	6.34E+04	9.53E-03	2.95E-05	7.07E-03	1.69E-06	7.07E-03	4.24E-06	7.78E-03	8.15E-06	9.34E-06	1.08E-05	71186
2.22	2.86E+03	4.44	1.22E+04	6.65	3.06E+04	8.87	6.49E+04	9.50E-03	3.01E-05	7.07E-03	1.72E-06	7.07E-03	4.32E-06	7.84E-03	8.28E-06	9.50E-06	1.10E-05	72831.4
2.24	2.91E+03	4.47	1.24E+04	6.71	3.12E+04	8.95	6.65E+04	9.46E-03	3.07E-05	7.07E-03	1.75E-06	7.07E-03	4.41E-06	7.91E-03	8.41E-06	9.66E-06	1.13E-05	74512.6
2.25	2.96E+03	4.51	1.26E+04	6.76	3.18E+04	9.02	6.81E+04	9.42E-03	3.14E-05	7.07E-03	1.78E-06	7.07E-03	4.50E-06	7.97E-03	8.54E-06	9.82E-06	1.15E-05	76230.9
2.27	3.00E+03	4.55	1.28E+04	6.82	3.24E+04	9.09	6.97E+04	9.38E-03	3.20E-05	7.07E-03	1.81E-06	7.07E-03	4.59E-06	8.04E-03	8.67E-06	9.98E-06	1.18E-05	77987.4
2.29	3.05E+03	4.58	1.30E+04	6.87	3.31E+04	9.16	7.14E+04	9.34E-03	3.27E-05	7.07E-03	1.84E-06	7.07E-03	4.68E-06	8.10E-03	8.81E-06	1.01E-07	1.21E-05	79783.3
2.31	3.10E+03	4.62	1.33E+04	6.93	3.37E+04	9.24	7.31E+04	9.31E-03	3.33E-05	7.07E-03	1.88E-06	7.07E-03	4.77E-06	8.16E-03	8.95E-06	1.03E-07	1.23E-05	81620.1
2.33	3.15E+03	4.65	1.35E+04	6.98	3.44E+04	9.31	7.48E+04	9.27E-03	3.40E-05	7.07E-03	1.91E-06	7.07E-03	4.86E-06	8.23E-03	9.09E-06	1.05E-07	1.26E-05	83499.3
2.35	3.20E+03	4.69	1.37E+04	7.04	3.50E+04	9.38	7.66E+04	9.23E-03	3.47E-05	7.07E-03	1.94E-06	7.07E-03	4.96E-06	8.29E-03	9.24E-06	1.07E-07	1.29E-05	85422.4
2.36	3.26E+03	4.73	1.40E+04	7.09	3.57E+04	9.45	7.85E+04	9.20E-03	3.54E-05	7.07E-03	1.98E-06	7.07E-03	5.05E-06	8.36E-03	9.39E-06	1.08E-07	1.31E-05	87391.3
2.38	3.31E+03	4.76	1.42E+04	7.15	3.64E+04	9.53	8.03E+04	9.16E-03	3.61E-05	7.07E-03	2.01E-06	7.07E-03	5.15E-06	8.42E-03	9.54E-06	1.10E-07	1.34E-05	89408
2.40	3.36E+03	4.80	1.44E+04	7.20	3.71E+04	9.60	8.23E+04	9.13E-03	3.68E-05	7.07E-03	2.04E-06	7.07E-03	5.25E-06	8.49E-03	9.70E-06	1.12E-07	1.37E-05	91475
2.42	3.41E+03	4.84	1.47E+04	7.25	3.78E+04	9.67	8.43E+04	9.09E-03	3.75E-05	7.07E-03	2.08E-06	7.07E-03	5.35E-06	8.55E-03	9.86E-06	1.14E-07	1.40E-05	93595
2.44	3.46E+03	4.87	1.49E+04	7.31	3.85E+04	9.75	8.63E+04	9.06E-03	3.82E-05	7.07E-03	2.11E-06	7.07E-03	5.45E-06	8.61E-03	1.00E-07	1.16E-07	1.43E-05	95771.5
2.45	3.52E+03	4.91	1.52E+04	7.36	3.93E+04	9.82	8.84E+04	9.03E-03	3.90E-05	7.07E-03	2.15E-06	7.07E-03	5.55E-06	8.68E-03	1.02E-07	1.18E-07	1.46E-05	98009.2
2.47	3.57E+03	4.95	1.54E+04	7.42	4.00E+04	9.89	9.06E+04	8.99E-03	3.97E-05	7.07E-03	2.18E-06	7.07E-03	5.66E-06	8.74E-03	1.04E-07	1.20E-07	1.50E-05	100314
2.49	3.62E+03	4.98	1.57E+04	7.47	4.08E+04	9.96	9.29E+04	8.96E-03	4.04E-05	7.07E-03	2.22E-06	7.07E-03	5.77E-06	8.81E-03	1.05E-07	1.22E-07	1.53E-05	102695
2.51	3.68E+03	5.02	1.59E+04	7.53	4.15E+04	10.04	9.52E+04	8.93E-03	4.12E-05	7.07E-03	2.25E-06	7.07E-03	5.88E-06	8.87E-03	1.07E-07	1.24E-07	1.56E-05	105165
2.53	3.73E+03	5.05	1.62E+04	7.58	4.23E+04	10.11	9.77E+04	8.90E-03	4.20E-05	7.07E-03	2.29E-06	7.07E-03	5.99E-06	8.94E-03	1.09E-07	1.27E-07	1.60E-05	107740
2.55	3.79E+03	5.09	1.65E+04	7.64	4.31E+04	10.18	1.00E+05	8.86E-03	4.27E-05	7.07E-03	2.33E-06	7.07E-03	6.10E-06	9.00E-03	1.11E-07	1.29E-07	1.64E-05	110418
2.56	3.84E+03	5.13	1.67E+04	7.69	4.39E+04	10.25	1.03E+05	8.83E-03	4.35E-05	7.07E-03	2.36E-06	7.07E-03	6.21E-06	9.06E-03	1.13E-07	1.31E-07	1.67E-05	113004
2.58	3.90E+03	5.16	1.70E+04	7.75	4.47E+04	10.33	1.04E+05	8.80E-03	4.43E-05	7.07E-03	2.40E-06	7.07E-03	6.33E-06	9.13E-03	1.14E-07	1.33E-07	1.70E-05	114600
2.60	3.96E+03	5.20	1.72E+04	7.80	4.56E+04	10.40	1.05E+05	8.77E-03	4.51E-05	7.07E-03	2.44E-06	7.07E-03	6.44E-06	9.19E-03	1.14E-07	1.34E-07	1.72E-05	116042
2.62	4.01E+03	5.24	1.75E+04	7.85	4.64E+04	10.47	1.08E+05	8.74E-03	4.59E-05	7.07E-03	2.48E-06	7.07E-03	6.56E-06	9.26E-03	1.16E-07	1.36E-07	1.76E-05	118885
2.64	4.07E+03	5.27	1.78E+04	7.91	4.73E+04	10.55	1.11E+05	8.71E-03	4.68E-05	7.07E-03	2.52E-06	7.07E-03	6.68E-06	9.32E-03	1.19E-07	1.39E-07	1.80E-05	121655
2.65	4.13E+03	5.31	1.81E+04	7.96	4.81E+04	10.62	1.14E+05	8.68E-03	4.76E-05	7.07E-03	2.56E-06	7.07E-03	6.81E-06	9.39E-03	1.21E-07	1.41E-07	1.84E-05	124679
2.67	4.19E+03	5.35	1.84E+04	8.02	4.90E+04	10.69	1.16E+05	8.65E-03	4.84E-05	7.07E-03	2.60E-06	7.09E-03	6.92E-06	9.45E-03	1.23E-07	1.44E-07	1.88E-05	127739
2.69	4.25E+03	5.38	1.86E+04	8.07	4.99E+04	10.76	1.19E+05	8.62E-03	4.93E-05	7.07E-03	2.64E-06	7.14E-03	7.00E-06	9.51E-03	1.26E-07	1.46E-07	1.92E-05	130847
2.71	4.31E+03	5.42	1.89E+04	8.13	5.08E+04	10.84	1.22E+05	8.59E-03	5.01E-05	7.07E-03	2.68E-06	7.18E-03	7.08E-06	9.58E-03	1.28E-07	1.49E-07	1.97E-05	134015
2.73	4.37E+03	5.45	1.92E+04	8.18	5.18E+04	10.91	1.26E+05	8.56E-03	5.10E-05	7.07E-03	2.72E-06	7.22E-03	7.16E-06	9.64E-03	1.30E-07	1.51E-07	2.01E-05	137253
2.75	4.43E+03	5.49	1.95E+04	8.24	5.27E+04	10.98	1.29E+05	8.54E-03	5.19E-05	7.07E-03	2.76E-06	7.28E-03	7.24E-06	9.71E-03	1.33E-07	1.54E-07	2.05E-05	140569
2.76	4.49E+03	5.53	1.98E+04	8.29	5.37E+04	11.05	1.32E+05	8.51E-03	5.28E-05	7.07E-03	2.80E-06	7.33E-03	7.32E-06	9.77E-03	1.35E-07	1.56E-07	2.10E-05	143970
2.78	4.55E+03	5.56	2.01E+04	8.35	5.46E+04	11.13	1.35E+05	8.48E-03	5.36E-05	7.07E-03	2.84E-06	7.38E-03	7.41E-06	9.84E-03	1.38E-07	1.59E-07	2.15E-05	147460
2.80	4.61E+03	5.60	2.04E+04	8.40	5.56E+04	11.20	1.39E+05	8.45E-03	5.45E-05	7.07E-03	2.88E-06	7.42E-03	7.49E-06	9.90E-03	1.40E-07	1.62E-07	2.19E-05	151047

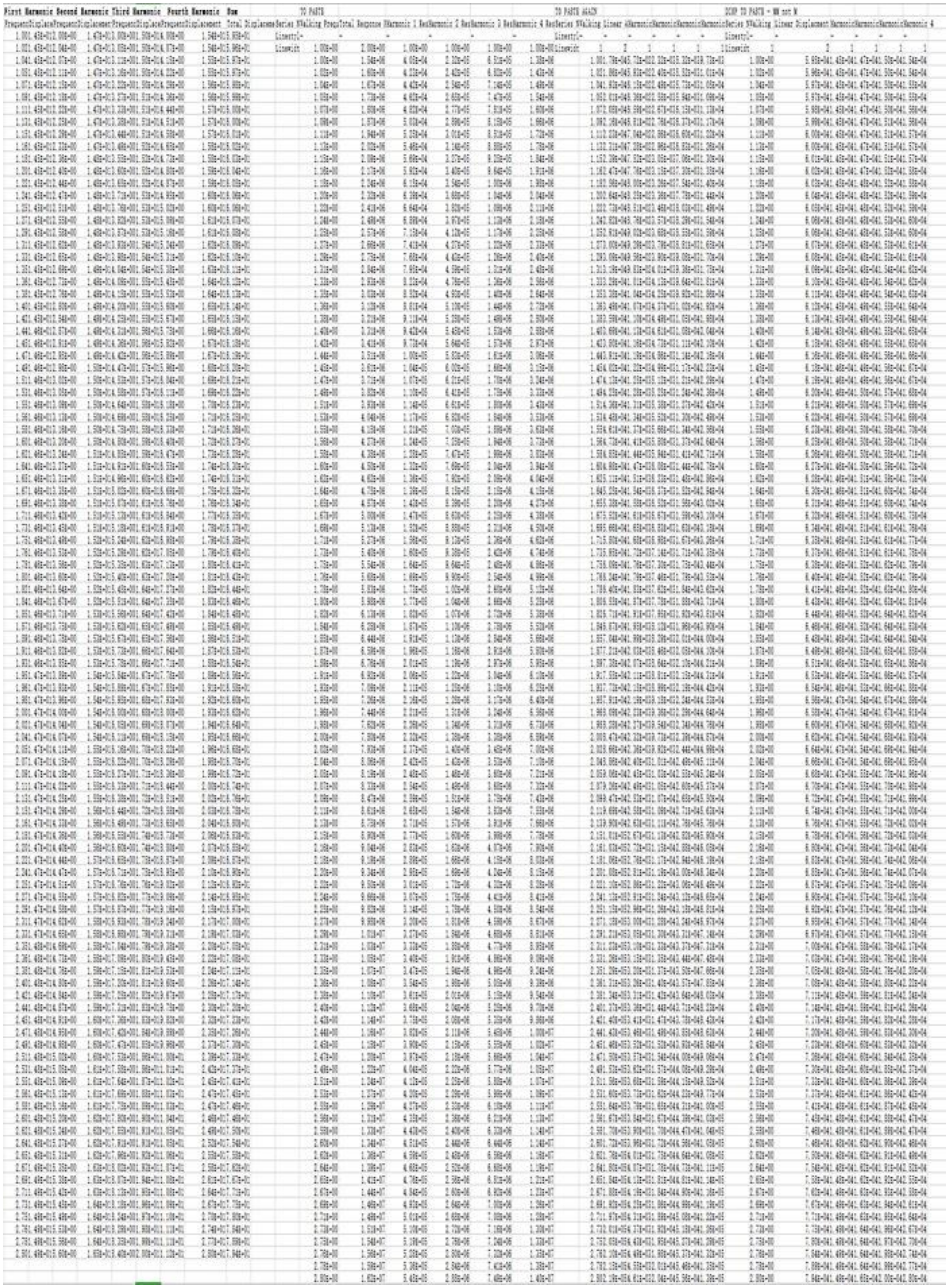
First Harmonic Second Harmonic Third Harmonic Fourth Harmonic Sum